Studies of the molecules form plasmodium falciparum that mediate pathogenesis

Mo, Min

2007

Mo, M. (2007). Studies of the molecules form plasmodium falciparum that mediate pathogenesis. Doctoral thesis, Nanyang Technological University, Singapore.

https://hdl.handle.net/10356/6566

https://doi.org/10.32657/10356/6566

Nanyang Technological University

NANYANG TECHNOLOGICAL UNIVERSITY

Studies of the molecules form Plasmodium falciparum that mediate pathogenesis

MO Min

School of Biological Sciences

2007

ACKNOWLEDGEMENTS

Firstly, I want to express my sincere and deep gratitude to my supervisor Dr. Julien Lescar for his expert guidance, encouragement and continual support during my Ph.D studies. Without his help, I cannot imagine how difficult it would be to successfully finish the Ph.D studies.

Next, I would like to express my special thanks to Dr. Peter Preiser (School of Biological Sciences, Nanyang Technological University) for providing the project of functional and structural analysis of adhesion molecules involving in malaria pathogenesis and giving me a great chance to learn knowledge about parasitology and protein biochemistry. I would also thank Dr. Panadda Boomserm (Institute of Molecular Biology and Genetics, Mahidol University, Thailand) for her wonderful collaboration on the project of Cry4Aa structure determination.

I would like to express my sincere gratitude to Mrs Lee Hooi Chen for her great efforts to help me on protein expression, purification and insect cell expression. With her continual encouragement and helpful discussion, I never felt frustrated even when the most difficult time came. I also want to express my deep thanks to all my labmates and friends in Dr. Lescar's and Dr. Preiser's lab, especially to Dr. Annie Gao, Dr. Masayo Kotaka, Dr.

Amy Ooi, Xu Ting, Fan Hui, Yap Tai Lieong, Mano Ravi, Kinsley and Jayasree Kaveri Iyer, for giving me innumerable fond memories of the years spent in the lab.

Last but not least, I want to express my deep thanks to my parents, sister and husband. They always stand by me and give me endless love and supports.

TABLE OF CONTENTS

SUMMARY

The cytoadherence and immune evasion properties of *Plasmodium falciparum* are primarily determined by the expression of members of a variant surface antigen family known as *Plasmodium falciparum* erythrocyte membrane protein-1 (PfEMP-1). PfEMP-1 proteins are encoded by *var* genes and contain multiple adhesive modules including the Duffy binding-like domain (DBL) and the cysteine-rich inter-domain region (CIDR). The interaction between CIDR1α and CD36 promotes adherence of parasitized erythrocytes to microvasculature of vital organs, such as heart, lung and central nervous system, leading to microvascular occlusion and organ failure. Based on sequence similarity divergence and ability to bind CD36, CIDR1α molecules can be divided into 2 classes: CD36 binding molecules and non CD36 binding molecules.

In this study, several CIDR1α domains of the *P. falciparum* clone 3D7, including both CD36 binding molecules and non CD36 binding molecules were expressed in *E. coli* in functional forms. According to circular dichroism analysis, the secondary structure of CIDR1α is predominantly α-helical. Using site-directed mutagenesis, truncation and domain swapping experiments, the CD36 binding region was mapped to the C-terminal region of the CIDR1α domain. Murine polyclonal antisera raised against this C-terminal region recognize the parasite surface-expressed PfEMP-1 and inhibit the interactions between CD36 and CIDR1α. In addition, this polyclonal

antisera show cross-reactive protection effects against several *P. falciparum* strains. The N-terminal region of CIDR1α may act as a scaffold to maintain the integrity of the whole structure. In conclusion, since the CD36 molecule is a critical receptor for the anchoring of parasitized erythrocytes to the microvascular endothelium, disruption of interactions between CD36 molecule and CIDR1α domain with small molecule compounds or by specific antibodies raisted against the C-terminal region of CIDR1α holds great promise for the future development of new therapeutics or vaccines against malaria.

PUBLICATION

Boonserm P., **Mo M.,** Angsuthanasombat C. and Lescar J.

Structure of the functional form of the mosquito larvicidal Cry4Aa toxin from Bacillus thuringiensis at a 2.8-angstrom resolution.

J Bacteriol. 2006 May;188(9):3391-401.

Mo M., Lee H.C., Preiser P. and Lescar J.

The Cysteine-rich inter-domain region CIDR1α of Plasmodium falciparum erythrocyte membrane protein 1 (PfEMP-1) binds to the CD36 receptor via its C-terminal domain.

Submitted

Mo M., Lee H.C., Annie G, Lescar J. and Preiser P.

Mapping the region of the CIDR1α domain responsible for binding to the CD36 receptor molecule.

Second Annual BioMalPar Conference on Biology and Pathology of the Malaria Parasite, 05 Apr. to 08 Apr., 2006, EMBL-Heidelberg, Germany

11th International Congress of Parasitology (ICOPA XI), 06 Aug. to 11 Aug. 2006, Glasgow, Scotland

Oral presentation

LIST OF TABLES

LIST OF FIGURES

GLOSSARY

Gametocyte: The sexual stage of malaria parasites. Male gametocytes (microgametocytes) and female gametocytes (macrogametocytes) are inside red blood cells (RBC) in the circulation. If they are ingested by a female *Anopheles* mosquito, they undergo sexual reproduction which starts the extrinsic (sporogonic) cycle of the parasite in the mosquito.

Giemsa staining: A classical method is used to differentiate DNA and/or cytoplasmic morphology of platelet, RBC, WBC and parasites.

Merozoite: A daughter-cell formed by asexual development in the life cycle of malaria parasites. Liver-stage and blood-stage malaria parasites develop into schizonts which contain many merozoites. When the schizonts are mature, they (and their host cells) rupture; the merozoites are released and infect RBCs.

Oocyst: A stage in the life cyle of malaria parasites, oocysts are rounded cysts located in the outer wall of the stomach of mosquitoes. Sporozoites develop inside the oocysts. When mature, the oocysts rupture and release the sporozoites, which then migrate into the mosquito's salivary glands, ready for injection into the human host.

Schizogony: Asexual reproductive phase of malaria parasites. In RBCs schizogony is development of a single trophozoite into numerous merozoites, in which DNA replicates multiple rounds.

Schizont: A developmental form of the malaria parasite that contains many merozoites. Schizonts are seen in the liver-stage and blood-stage parasites.

Sporozoite: Sporozoites are produced in the mosquito's oocyst and migrate to the mosquito's salivary glands. They can be inoculated into a human host when the mosquito takes a blood meal on the human. In the human, the sporozoites enter liver cells where they develop into the next stage of the malaria parasite life cycle (the liver stage or exo-erythrocytic stage).

Trophozoites: A developmental form during the blood stage of malaria parasites. After merozoites have invaded the RBC, they develop into trophozoites (sometimes, early trophozoites are called "rings" or "ring stage parasites"); trophozoites develop into schizonts.

Zygote: One of the two cells (female egg cell and male sperm cell) that, together, form the basis of fetal development. The DNA in each of these cells contains half of the information necessary to form a new individual.

ABBREVIATIONS

AMA-1: Apical Membrane Antigen 1

AP: Alkaline Phosphatase

ATS: Acidic Terminal Sequence

BFU-E: burst-forming unit-erythron

CD: Circular Dichroism

CFU-E: Colony-forming unit-erythron

CIDR: Cysteine-rich Interdomain Region

CM: Cerebral malaria

CSA: Chondroitin Sufate A

CSP: Circumsporozoite Protein

DAPI: 4', 6-Diamidino-2-phenylindole dihydrochloride

DARC: Duffy Antigen Receptor for Chemokines

DBPv: *Plasmodium vivax* Duffy-Binding Protein

DNA: Deoxyribonucleic Acid

DTT: Dithiothreitol

EBA-175: Erythrocyte Binding Antigen 175

EBL: Erythrocyte Binding-like protein

E. coli: Escherichia coli

EDTA: Ethylenediaminetetraacetic Acid

ELISA: Enzyme-Linked Immunosorbent Assay

FPLC: Fast Performance Liquid Chromatography

EPO: Erythropoietin

GPI: Glycosylphosphatidylinositol

GST: Glutathione S Transferase

HPLC: High Performance Liquid Chromatography

HRP: Horseradish Peroxidase

HS: Heparin Sulfate

ICAM-1: Intercellular Adhesion Molecule 1

IFA: Immunofluorescence Assay

IFNγ: Interferon-γ

IL: Interleukine

IPTG: Isopropyl-β-D-1-thiogalactoside

LB: Luria Broth

LTα: Lymphotoxinα

Kb: Kilobase

kDa: Kilodalton

MC: Malay Camp

NTS: N-terminal segment

Pf: *Plasmodium falciparum*

Pk: *Plasmodium knowlesi*

Pv: *Plasmodium vivax*

RHs: Reticulocyte binding protein homologues

Rifin: Repetitive Interspersed Family

PRBC: Parasitized Red Blood Cell

PfEMP-1: *Plasmodim falciparum* Erythrocyte Membrane Protein-1

PVM: Parasitophorous Vascular Membrane

MBP: Maltose-Binding Protein

MSP: Merozoite Surface protein

Ni-NTA: nickel-nitrilotriacetic acid

NMR: nuclear magnetic resonance

NO: Nitric oxide

OD: Optical Density

OPD: O-Phenylenediamine Dihydrochloride

PE: Parasitized erythrocyte

PBS: Phosphate Buffered Saline

PCR: Polymerase Chain Reaction

RAP: Rhoptry-associated Protein

RESA: Ring infected Erythrocyte Surface Antigen

RhopH: High molecular mass Rhoptry protein

RIMA: Ring Membrane Antigen

RMSD: Root-Mean-Square Deviation

SDS-PAGE: Sodium Dodecyl Sulphate-polyacrylamide gel electrophoresis

Stevor: Sub-telomeric Variable Open Reading frame

TNFα: Tumor Necrosis factor α

TSP: Thrombospondin

TRAP: Sporozoite protein Thrombospondin-related Adhesion Protein

Tris-HCl: Tris (hydroxymethyl) aminomethane hydrochloride

VCAM-1: Vascular Cell Adhesion Molecule-1

VSA: variant surface antigens

WHO: World health organization

CHAPTER 1: Introduction

1.1 Overview

Plasmodium is a protozoan, belongs to the phylum Apicomplexa, class *Haemosporidea*, order *Haemosporidia*, genus *Plasmodium*. There are many *Plasmodium* species that infect vertebrates, such as reptiles, birds, rodents, monkey and human. Four *Plasmodium* parasite species infect humans, namely, *Plasmodium vivax, Plasmodium ovale, Plasmodium malariae* and *Plasmodium falciparum*. Besides *Plasmodium*, the phylum Apicomplexa includes other human and veterinary parasites such as *Toxoplasma*, *Theileria* and *Babesia*. They all share common features including the presence of a specialized apical complex which is central to the invasion process (Cowman & Crabb, 2006). However, their life cycles are not completely similar. *Toxoplasma, Elimeria* and *Cryptosporidium* are transmitted directly between vertebrate hosts; while *Plasmodium* needs an arthropod vector, a female *Anopheles* mosquito, to transmit the parasite to a vertebrate host during blood feeding (Cowman & Crabb, 2006).

In humans, the most severe form of malaria is caused by *Plasmodium falciparum*, which infects over 300 million people all over the world and causes more than 2 million deaths each year (Snow *et al*., 2005). Although chemotherapeutic agents have been developed in the past 20 years to cure malaria infections, malaria remains a major pediatric killer in many parts of sub-Saharan Africa

and South Asia. A greater understanding of the host-parasite interaction would undoubtedly assist the development of new treatments and vaccines with a view to ensure a long-term sustainable reduction of the global burden caused by malaria.

In this introduction, the life cycle of the *Plasmodium* parasite and the pathology of severe malaria will first be described, followed by a discussion of invasion of erythrocyte by the parasite. Subsequently, the ultrastructure of *P. falciparum* merozoite, molecules involved in erythrocyte invasion and the sequestration process which is important pathogenicity will be described. Molecules encoded by *var* gene involved in cytoadherence, and *Plasmodium falciparum* erythrocyte protein 1 (PfEMP-1) will be discussed. Finally, the interactions between CD36 and Cysteine-rich interdomain region 1α (CIDR1α) domain will be reviewed.

1.2 Life cycle of the malaria parasites

The life cycle of the malaria parasite involves two hosts: the *Anopheles* mosquito and a vertebrate host.

When the *Anopheles* mosquito feeds on a vertebrate host, it releases sporozoites into the bloodstream (**Figure 1. 1** (1)). The sporozoites then travel to the liver within 2 min (Shin *et al.*, 1982). When they reach the liver sinusoids, sporozoites exit the circulation and enter the liver parenchyma to infect hepatocytes. Sporozoites breach the plasma membrane of the hepatocytes, traverse through its cytosol and leave by wounding the membrane again (Mota *et al.*,

2001). This process probably involves lipases, proteases or pore-forming proteins (Mota and Rodriguez, 2004). Sporozoites would migrate through several host cells before finally invading a hepatocyte leading to the formation of a vacuole. This migration process would activate sporozoites for infection and increase the susceptibility of host hepatocytes (Mota *et al*., 2002). Upon invasion in hepatocytes, sporozoites undergo a process known as pre-erythrocytic schizogony. During this process, sporozoites will develop and multiply into merozoites (**Figure 1. 1** (2)-(3)). In addition, for *Plasmodium vivax* and *Plamodium ovale*, the sporozoites will differentiate into merozoites as well as hypnozoites. The hypnozoite can remain dormant in hepatocytes for weeks to years. At the end of the pre-erythrocyte stage, the envelope of the cell containing the schizont ruptures and releases 10,000 to 30,000 merozoites into the surrounding tissues, as well as into the blood circulation, with the majority of merozoites invading the red blood cells (RBCs) in the liver sinusoids (**Figure 1. 1** (4)).

The merozoite which invades RBCs develops into trophozoites. During this process, they feed on hemoglobin from erythrocyte by pinocytosis into the cytostome, a peripheral tubular structure of RBC. Many small tubular vesicles containing hemoglobin fuse to form the acidic food vacuole (Yayon *et al*., 1984). The hemoglobin inside the food vacuole is oxidized to methemoglobin in the acidic environment PH and is subsequently hydrolyzed by aspartic protease and cysteine proteases into free heme and small peptides (Eggleson *et al*., 1999).

These peptides are further hydrolyzed to amino acids by cytosolic exopeptidase and the released amino acids are used by the parasite for their own protein synthesis (Sherman, 1998). Since free heme is a lipophilic molecule causing changes in membrane permeability and lipid peroxidation of the parasite membrane (Ryter and Tyrrell, 2000), the malaria parasite is equipped with a unique heme detoxification system to produce hemozoin (Ginsburg *et al.*, 1998; Sherman, 1998). Trophozoite lysate promotes polymerization of heme and produces hemozoin, a process mediated by histidine rich protein II (Sullivan *et al.*, 1996), linoleic acid and phospholipids etc. (Fitch *et al.*, 2000; Dorn *et al.*, 1998). The accumulation of digested hemozoin is seen as dark granules inside the RBCs by Giemsa staining. After a period of growth, the trophozoite undergoes multiple rounds of asexual division called erythrocytic schizogony. The nucleus divides 3 to 5 times, followed by the division of cytoplasm forming schizonts. When the process of schizogony is completed, the RBC bursts and releases the merozoites into the blood stream (**Figure 1. 1** (5)-(6)). Repetition of the asexual blood-stage leads to a progressive increase of parasitaemia until the process is slowed down by the immune response of the host.

During the erythrocytic schizogony stage, some of the parasites differentiate into gametocytes corresponding to a sexual erythrocytic stage (**Figure 1. 1** (7)). The microgametocyte (male) and macrogametocyte (female) are ingested by an *Anopheles* mosquito during a blood meal (**Figure 1. 1** (8)). The development and

multiplication in the mosquito are called sporogonic cycle. In the mosquito's gut, the microgametocyte undergoes three rounds of nuclear replication. These eight nuclei then become associated with flagella that emerge from the body of the microgametocyte. This process is called exflagellation. The macrogametocyte undergoes the maturation into macrogametes. Exflagellation occurs spontaneously when infected blood is exposed to air. The highly mobile microgametes will fuse with the macrogametes and generate zygotes (**Figure 1. 1** (9)). The zygotes which become motile and elongated are called ookinetes (**Figure 1. 1** (10)). The ookinetes invade the midgut wall of the mosquito and develop into oocysts (**Figure 1. 1** (11)). The oocysts grow, rupture and release motile sporozoites, which then enters into the mosquito's salivary glands (**Figure 1. 1** (12)). After inoculation of sporozoites into a new vertebrate host, the parasites complete one life cycle (**Figure 1. 1**).

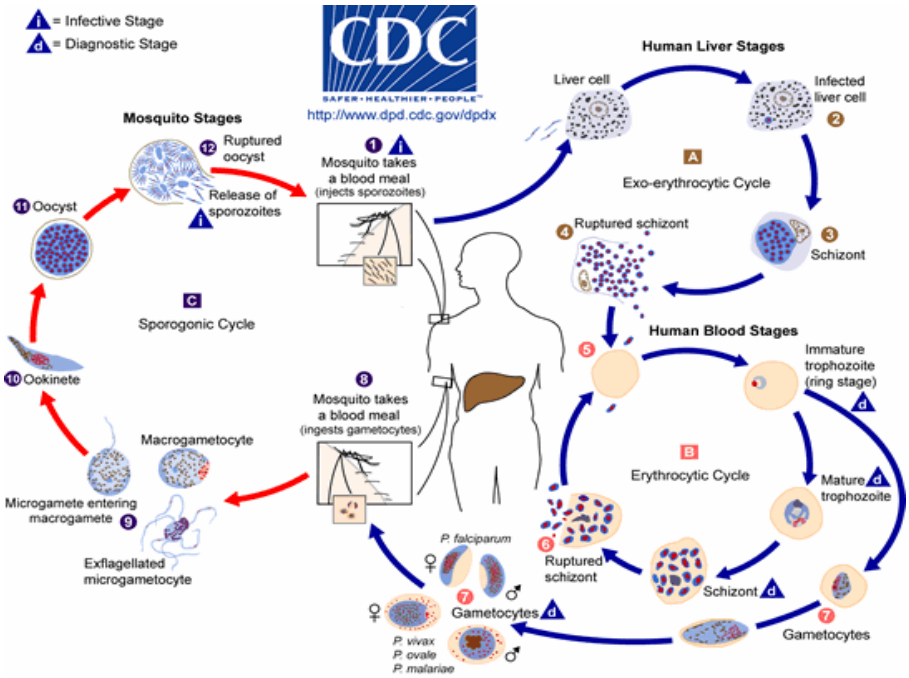

Figure 1. 1. Life cycle of the parasite *plasmodium*. Adapted from **http://www.dpd.cdc.gov/dpdx**.

1.3 Pathology of human malaria

In human, most of the severe and fatal malaria-related illnesses are caused by *P. falciparum*, although *P. vivax* and *P. malariae* infections can also have severe consequences, affecting the spleen, liver and kidney. Following transmission via the *anopheles* mosquito, sporozoites injected by the mosquito into the blood-stream immediately invade the liver, where they undergo an initial pre-erythrocytic or exo-erythrocytic cycle. Pathological processes in malaria are the result of the erythrocytic cycle. After developing in hepatocytes for 7 to 10 days, schizonts rupture, releasing merozoites which invade erythrocytes. In the blood circulation, they develop

from a ring form to trophozoites and finally to multisegmented schizonts. For *P. falciparum*, this process results in altering membrane transport mechanisms; developing of electron-dense protuberances or knobs beneath the surface membrane of RBC; expression of variant surface neoantigens and rosetting properties which result in sequestration of erythrocytes containing late trophozoites and schizonts in deep vascular beds.

Other effects are related to the immunological response of the host to parasite antigens and alterations of the membrane of RBC surface. These include stimulation of the reticulo-endothelial system, changes in regional blood flow and vascular endothelium, systemic complications of altered biochemistry, anemia, tissue and organ hypoxia and a systemic inflammatory response characterized by the release of cytokines and interleukins (Day *et al.*, 1999).

Sympotoms of severe malaria includes severe anemia, respiratory distress, cerebral and placental malaria, jaundice, renal failure, shock, acidosis, metabolic and haemostatic abnormalities. Among them, cerebral malaria, placental malaria, severe anemia and respiratory distress have a potential fatal outcome. Here we focus on cerebral malaria, placental malaria and severe anemia.

1.3.1 Cerebral malaria

Cerebral malaria (CM) is used to describe a syndrome consisting of coma not attributable to convulsions, hypoglycemia or meningitis in a patient with parasitemia (Newton *et al.*, 1998).

Cerebral involvement is confined to *P. falciparum* infection. The main clinical features of CM include metabolic acidosis (English *et al.*, 1996a), dehydration (English *et al.*, 1996c), convulsion and coma (Crawley *et al.*, 1996). Mutiple pathogenic mechanisms have been suggested but none have been established. It has been demonstrated that cytoadherence of parasitized erythrocytes to the endothelium of cerebral venules results in the sequestration and tight packing of infected cells in the vessels (Dondorp *et al.*, 2000), providing the evidence that not only parasitized RBC (PRBC) and clumps of uninfected RBC occlude the small blood vessels, platelets and other fibrillar material present in the affected blood brain vessels (Grau *et al.*, 2003). In addition, intracytoplasmic breakdown of hemoglobin by the parasite causes accumulation of intraerythrocytic pigment globules (Taylor *et al.*, 2004). Pigment deposition in the brain is often marked, with pigment granules bound to ghosted erythrocyte membranes (Pongponratn *et al.*, 1985; Lackner *et al.*, 2006). The direct consequence of sequestration is the systemic induction of lymphotoxin α (LTα) (Engwerda *et al.*, 2002) and tumor necrosis factor α (TNFα) by macrophages (Grau *et al.*, 1989; Kwiatkowski *et al.*, 1990; Brown *et al.*, 1999). These cytokines were suggested to be involved in CM pathogenesis. However, in many cases of CM in children, coma seems to be a response to metabolic stress rather than primary microvascular occlusion (English *et al.*, 1996b). In severe malaria, there may be significant reduction in the deformability of uninfected RBCs

(Miller *et al*., 1971; Dondorp *et al*., 2000). Although the pathogenesis of this abnormality is not clear, it would be involved in compromising blood flow, leading to a decrease in the supply of oxygen and other nutrients to the brain, and causes acidosis (Miller *et al*., 2002a). Nitric oxide (NO) production was also proposed to show pathogenic effects in cerebral malaria, providing that increased inducible NOS (the NO metabolites) expression and makers of NO production in severe malaria (Clark *et al*., 2003).

The adhesion of PRBCs has been investigated *in vivo*, and it is now clearly shown that this adhesion is due to specific receptor-mediated events between parasite ligands which are expressed on the infected erythrocyte surface and host endothelial adhesion molecules (Baruch *et al*., 1995; Chen *et al*., 1998; Bian *et al*., 2000). *Plasmodium falciparum* erythrocyte membrane protein 1 (PfEMP-1) is an important and well studied cytoadherence protein expressed by PRBC that mediates this adhesion process (Baruch *et al*., 1995).

1.3.2 Placental malaria

During pregnancy, women become particularly susceptible to *P. falciparum* infection. The infection has adverse effects on both mother and unborn child, causing maternal anaemia and low birthweight babies (Brabin *et al*., 1983; Mcgregor *et al*., 1983). Sequestration of mature stage of PRBCs in the placental blood spaces is responsible for placental malaria (Fried *et al*., 1998; Ricke *et al*., 2000; Duffy and Fried, 2003). Sequestration allows these

parasites to grow and multiply, thus avoiding spleen-mediated clearance mechanisms from the host. However, it also leads to an inflammatory response (Suguitan *et al.*, 2003) and deposition of fibrinoid material in the host placenta (Walter *et al.*, 1982), which may reduce placental blood flow (Dorman *et al.*, 2002), causing impaired fetal growth and prematurity (Menendez *et al.*, 2000b).

Sequestration is mediated by DBLγ domain of PfEMP-1 and CSA in the placenta (Buffet *et al.*, 1999; Reeder *et al.*, 1999) (See below).

1.3.3 Severe anemia

World health organization (WHO) has defined severe malarial anemia as a hemoglobin concentration less than 50g/l or a hematocrit less than 0.15 in the presence of a *P. falciparum* parasitaemia more than 10 000 parasites/µl, with a normocytic blood film (Warrell *et al.*, 1990). The anemia provoked by malaria is multifactorial, involving both the destruction of RBC and decreased production of RBC (Phillips and Pasvol, 1992; El Hassan *et al.*, 1997; Menendez *et al.*, 2000a).

Possible mechanisms responsible for increased RBC destruction include rupture of PRBC, phagocytosis of PRBC and unparasitized RBC, hypersplenism and antoimmune hemolysis (Davis *et al.*, 1990; Phillips and Pasvol, 1992; Angus *et al.*, 1997; Dondorp *et al.*, 1999; Kai *et al.*, 1999;). It has been shown that the severity of early anemia in acute malaria correlates with density of parasitemia and

schizontemia. Rupture of PRBCs, in circulation or sequestered in deep vasculature, is the direct reason for anemia (Warrell *et al*., 1990; Phillips and Pasvol, 1992). Proliferation and hyperactivity of macrophages in the reticuloendothelial system result in increased phagocytosis of PRBC and unparasitized RBC. Reduced deformability of RBC and membrane binding of parasite components also activate macrophages (Davis *et al*., 1990; Dondorp *et al*., 1999). The spleen is essential for the clearance of malarial parasitemia because it filters infected RBC from the circulation. In case of severe anemia, the spleen pools parasitized and unparasitized RBCs from circulation, hemolyzes them and expands the plasma volume (Augus *et al*., 1997). Deposition of immunoglobulin and complement component on the surface of unparasitized RBCs causes antoimmune hemolysis (Kai *et al*., 1999).

Possible mechanisms responsible for decreased RBC production include inflammation-induced erythroid hypoplasia, suppression of erythropoietin (EPO) synthesis, dyserythropoiesis, imbalance in cytokine ratio and concomitant infections (Phillips *et al*., 1986; Clark and Chaudhri, 1988; Kurtzhal *et al*., 1998; Warrell *et al*., 1990; El Hassan *et al*., 1997). During the development of acute malaria, the release of reticulocytes is delayed, indicating a transient suppression of the response of EPO (Phillips *et al*., 1986; Warrell *et al*., 1990). This effect is probably mediated by an autologous serum factor which suppresses the growth of early precursors of RBC, such as burst-forming unit-erythron (BFU-E) and the colony-forming unit-

erythron (CFU-E) (Jootar *et al*., 1993). EPO synthesis is also suppressed in some adult individuals of Thai and Sudanese origin, probably due to the effects of TNF (Burgmann *et al*., 1996; El Hassan *et al*., 1997; Clark and Chaudhri, 1988). Dyserythropoiesis is mainly observed in individuals with recurrent *falciparum* infections (Phillips and Pasvol, 1992). Serum TNF, interleukin 10 (IL-10) and interferon γ (IFNγ) levels are all increased in malaria patients, and their concentrations generally correlate directly with the severity of disease (Warrel *et al*., 1990; Othoro *et al*., 1999; McGuire *et al*., 1999). Infection by *P. falciparum* suppresses the host immune system and secondary infections are very common (Warrell *et al*., 1990).

Due to the complex pathophysiology of malarial anemia, there is currently no effective management and preventive tools.

1.4 Parasite invasion process

Erythrocyte invasion by malaria parasites requires specific molecular interactions between merozoites and receptors at the surface of RBCs. Several molecules implicated in the invasion process have been identified in the rhoptry, micronemes and dense granules of merozoites. These secretory organelles are collectively known as apical organelles because of their localization at the apical end of the parasite. The invasion process includes: primary contact (A), apical reorientation, irreversible attachment and junction formation (B), movement of junction powered by the parasite's

actin-myosin motor (C), shedding of merozoite coat surface (D), and closure of the parasitophorous vacuole membrane (PVM) and erythrocyte membrane (E) (**Figure 1. 2**). The initial contact between the merozoite and erythrocyte is a crucial step, because the parasite has to distinguish erythrocytes from other cell types for invasion. The initial contact appears to be host-cell specific since *Plasmodium knowlesi* merozoites attach only to erythrocytes from susceptible hosts like rhesus/human, but not to erythrocytes from non-susceptible hosts like guinea pig/chicken (Miller *et al*., 1979). Recognition and primary adherence occur at relatively long distance, and are of low affinity and reversible (Bannister & Dluzewski, 1990). Following primary attachment, reorientation ensues, whereby the erythrocyte surface wraps around the merozoite to juxtapose the apical end of the merozoite with the erythrocyte membrane, thus facilitating close interaction of the molecules within the apical organelles with the membrane. Once the apical prominence of the merozoite is apposed directly towards the erythrocyte membrane, a junction is formed between the invading merozoite and the erythrocyte membrane. The junction is characterized by an increased electron-dense thickness under the erythrocyte membrane at the site of contact between the merozoite and the erythrocyte (Aikawa *et al*., 1978; Miller *et al*., 1979). This process is an irreversible step that commits the parasite to invasion. After the tight junction is formed between the parasite and the host membrane, the junction moves to the posterior end of the merozoite powered by the parasite actin-

myosin motor (Keeley & Soldati, 2004). This is a proteolytic event involving shedding of the coating covering the merozoite surface by serine proteases (Harris *et al.*, 2005). As the parasite pushes its way into the host cell, it creates a parasitophorous vacuole (PV) to seal itself from the host-cell cytoplasm and form an environment hospitable for its development. Once the parasite has completed its entry, the tight junction will disappear and the respective parasitophorous vacuole membrane (PVM) and the host erythrocyte membrane will fuse and separate, thus completing the entry process.

Upon invasion of the host cell, the parasites are enclosed in a PV, in which they undergo growth from ring to trophozoite stage followed by asexual division to produce daughter meroites. Newly formed merozoits in the schizont must egress from infected erythrocytes to initiate new invasion. This process involves the disruption of the PV and the host-cell membrane. The egression of *P. falciparum* involves a sudden increase in the intracellular pressure during the late phase of the blood-stage cycle. These biochemical changes that destabilize the infected cell cytoskeleton combine to promote an explosive event which effectively disperses the non-motile merozoites (Glushakova *et al.*, 2005). Salmon *et al.* have proposed a model for the process of the rupture. In this model, merozoites enclosed within the PVM first exit from the host erythrocyte and then rapidly escape from the PVM by a proteolysis-dependent mechanism (Salmon *et al.*, 2001). Candidate proteases include members of the serine repeat antigen (SERA) family that

localize to the parasitophorous vacuole (Hodder *et al.*, 2003; Miller *et al.*, 2002b). However, recent studies by Cowman *et al.* demonstrated that merozoite egress from infected erythrocytes involves a primary rupture of the PVM followed by a secondary rupture of the erythrocyte plasma membrane (Wickham *et al.*, 2003).

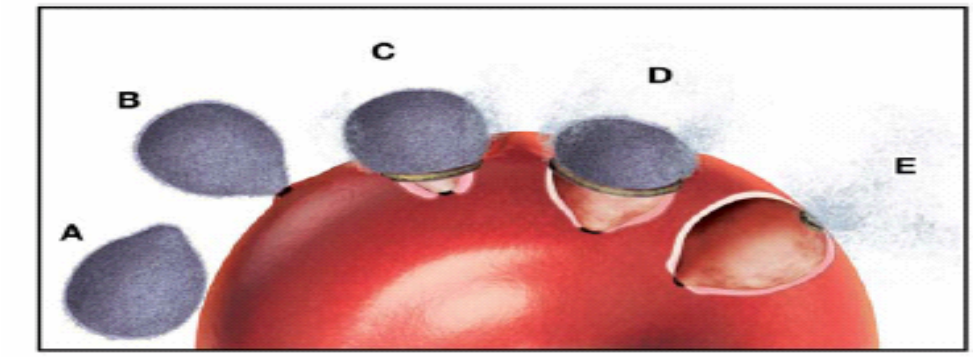

Figure 1. 2. The invasion process of *Plasmodium* parasites. The invasion process includes several steps: primary contact (A), apical reorientation, irreversible attachment and junction formation (B), movement of junction powered by parasite's actin-myosin motor (C), shedding of merozoite coat surface (D), and closure of the PVM and erythrocyte membrane (E) (adapted from Cowman & Crabb, 2006).

1.5 Ultrastructure of the apical organelles of merozoite

Apicomplexan parasites share a variety of morphological traits that are considered specific for this phylum, including an elongated shape and a conspicuous specialization of the apical region (Aikawa *et al.*, 1971). They all have a collection of unique organelles termed the apical complex which includes rhoptries, the micronemes, the

apical polar ring and the dense granules (**Figure 1. 3**). Rhoptries and micronemes are unique secretary organelles that generally contain molecules required for motility, adhesion and invasion to host cells as well as establishment of the PV (Dubremetz *et al.*, 1993; Carruthers & Sibley, 1997; Carruthers *et al.*, 1999). The apical polar ring is a hallmark organelle of all members of the Apicomplexa (Russell & Burns, 1984; Nichols & Chiappino, 1987). Experiments in *Toxoplasma gondii* indicate that the micronemes are expelled first and occur with initial contact between the parasite and host (Carruthers and Sibley, 1997). Microneme proteins are presumably important for primary contact and junction formation. The rhoptries are discharged immediately after the micronemes and the release of their contents correlate with the formation of the PV (Sam-Yellowe, 1996; Carruthers and Sibley, 1997). Dense granule contents are released after the parasite has completed its entry, and therefore, are usually implicated in the modification of the host cell, such as making erythrocyte membrane more permeable to small molecular weight metabolites to benefit an actively growing parasite (Ginsburg, 1994). Besides apical complex, there is a group of glycosylphosphatidylinositol (GPI) anchored membrane proteins located on the surface of the merozoite.

1.5.1 GPI-anchored surface proteins

The surface coat of merozoites is largely comprised of GPI anchored membrane proteins and their associated parners (Holder *et*

al., 1994). This group of proteins is presumedly involved in ealy recoginition and attachment. The merozoite surface proteins family (MSPs) is involved in the initial interaction of the parasite with the RBC (Holder *et al*., 1994; Carruthers *et al*., 1999). MSP-1, 2, 4, 5, 8 and 10 are anchored on the membrane via a GPI membrane anchor (Marshall *et al*., 1997, 1998; Black *et al*., 2001, 2003), while other MSPs such as MSP-3, MSP-6, MSP-7 and MSP-9 are soluble and are partially associated with the merozoite surface (Stahl *et al*., 1986; Weber *et al*., 1988b; McColl and Anders, 1997; Trucco *et al*., 2001). MSP-1 was the first *Plasmodium* MSP to be discovered and is the most well characterized member of the MSP family. Evidence showing the involvement of MSP-1 in erythrocyte invasion includes its uniform distribution over the merozoite surface and the observation that antibodies against MSP-1 inhibit invasion (Holder *et al*., 1994). MSP-1 undergoes extensive proteolytic process during late schizogony and after merozoite release (Holder and Freeman, 1982, 1984; Freeman and Holder, 1983; David *et al*., 1984). The molecule is cleaved into four fragments (N-terminal 83KDa fragment, central region 30kDa and 38kDa fragments and C-terminal 42kDa fragment in *P. falciparum*) that remain bound on the merozoite surface (Holder *et al*., 1987). In the final proteolytic step, the 42kDa fragment is cleaved into a 33kDa soluble fragment, and a 19kDa fragment which remains attached to the merozoite surface after invasion (Blackman *et al*., 1991). It was demonstrated that MSP-1 has a crucial role in erythrocyte invasion as: antibodies against this

19kDa fragment block erythrocyte invasion *in vitro* and immunization with the recombinant 19kDa protein in mice and monkeys elicits protection against parasite challenge (Daly and Long, 1993; Ling *et al*., 1994; Kumar *et al*., 1995).

1.5.2 Rhoptries

Rhoptries are pear-like membrane-bound vesicles occupying the apical end of the merozoite. Electron microscopy shows that each rhoptry consists of two distinct parts: an electron-dense rounded basal bulb and a less dense tapering shape rhoptry duct that ends beneath the plasma membrane covering the apical prominence (Bannister and Dluzewski, 1990; Bannister *et al.*, 2000). In *P. falciparum*, the basal bulb is composed of homogenously packed granules or fibrils about 5 nm long, while the apical part is filled with fibers or granules. Their overall dimension is about 550 nm long and 250 nm in diameter (Bannister *et al.*, 2000).

For *Plasmodium* and *Toxoplasma*, the rhoptries appear to be formed initially as small vesicles which grow bigger, probably via a simple Golgi body generated by vesicular budding from the nuclear envelope (Langreth *et al.*, 1978; Bannister *et al.*, 2000).

Many proteins studied so far are located in the basal bulb or duct of rhoptries. For example, the rhoptry-associated protein (RAP1/2/3) complex is situated in the bulb (Crewther *et al.*, 1990), while high molecular mass rhoptry protein 1/2/3 (RhopH1/2/3) is in the duct (Roger *et al.*, 1988; Sam-Yellowe *et al.*, 1995). The

membrane surrounding the rhoptry is a typical bilayer membrane, containing a substantial number of embedded particles (Bannister *et al.*, 2000).

When rhoptries discharge their contents, the tips of the ducts fuse with each other and with the merozoite plasma membrane, and the rhoptries become irregular in shape as they collapse (Ailawa *et al.*, 1978). It has been demonstrated that in *P. knowlesi*, the rhoptry content is converted from a granular to a lamellar form during RBC invasion (Bannister & Mitchell, 1989). Supposing that the total lamellar contents of a merozoite are transformed into a membranous configuration, these would be sufficient to create a vacuole large enough to contain the invading merozoite within an infected RBC.

The proteins inside rhoptry could play a major role in the invasion process (Sidduqui *et al.*, 1987; Ridley *et al.*, 1990). The extraction from rhoptries often requires ionic detergents, suggesting they reside in a highly membranous environment (Etzion *et al.*, 1991). There are three types of proteins that reside in rhoptry: a low molecular weight complex, a high molecular weight complex and reticulocyte binding protein homologues (RHs). RAP belongs to the low molecular weight complex which includes RAP-1 (about 80kDa), RAP-2 (42kDa) and RAP-3 (37kDa) (Crewther *et al.*, 1990). However, these RAP proteins do not play essential roles for RBC invasion because mistargeting of RAP-1 or RAP-2 did not affect the invasion phenotype of merozoites *in vitro* (Baldi *et al.*, 2000). RhopHs are situated in the rhoptry duct and bind to human RBCs

(Sam-Yellowe & Perkins, 1991). Members of the RHs are found in all *Plasmodium spp*. and are thought to play an important role in parasite virulence, host cell selection and possibly immune evasion (Preiser *et al*., 1999; Carlton *et al*., 2002). To date, six RH members have been identified in *P. falciparum*, PfRH1 (Rayner *et al*., 2001), PfRH2a&2b (Rayner *et al*., 2000; Triglia *et al*., 2001), PfRH3 (Pseudogene) (Taylor *et al*., 2001), PfRH4 (Kaneko *et al*., 2002) and PfRH5 (Cowman and Crabb, 2006). PfRH1 is involved in erythrocyte binding and plays a role in erythrocyte invasion in a neuraminidase sensitive, trypsin and chymotrypsin resistant manner (Rayner *et al*., 2001). Although no erythrocyte-binding activity of PfRH2b has been demonstrated, it can mediate invasion through a neuraminidase and trypsin resistant but chymotrypsin sensitive manner (Duraisingh *et al*., 2003b). PfRH4 binds to a uncharacterized neuraminidase and chymotrypsin resistant receptor, but its erythrocyte-binding activity has not been shown (Stubbs *et al*., 2005). The functions of PfRH2a and PfRH5 are not yet known.

1.5.3 Micronemes

In *P. falciparum,* the micronemes are fusiform sacs about 120 nm long attached at one end to the rhoptry duct and fan out into the apical cytoplasm of the merozoite (Bannister *et al*., 1989). They vanish assumingly by releasing their contents into the rhoptry duct during invasion process (Bannister *et al*., 1989). Structural evidence

suggests that micronemes are formed by vesicular budding from the Golgi apparatus like other apical organelles (Ward *et al.*, 1994).

AMA-1 is presumably responsible for apical reorientation (Mitchell *et al.*, 2004). This protein is a Type I integral membrane protein, with conserved C-terminal cytoplasmic and ecto-domains (Hodder *et al.*, 1996). AMA-1 is retained in the microneme organelles after synthesis but transitorily translocates to the rhoptry neck of the merozoite (Healer *et al.*, 2002). AMA-1 is required to establish the apical interaction through parasite adhesions located initially at the neck of the rhoptries and in the micronemes. This interaction is the key link between the weak primary contact involving MSP and the irreversible tight associations formed with microneme proteins (Cowman & Crabb, 2006).

The erythrocyte binding protein/ligand (EBLs) family involved in invasion is present in micronemes. EBL homolog include the Duffy binding protein (DBP) of *P. vivax* and *P. knowlesi* (Chitnis and Miller, 1994), *P. falciparum* EBA-175 (Sim *et al.*, 1994; Camus *et al.*, 1985), EBL-1, EBA-140/BAEBL, PEBEL, EBA-181/JSEBL and MAEBL (Adams *et al.*, 1992; Adams *et al.*, 2001; Blair *et al.*, 2002). Like DBP from *P. vivax* and *P. knowlesi*, these proteins share a similar cysteine-rich binding domain and thus belong to the Duffy-binding-like (DBL) superfamily (Adams *et al.*, 2001). Initial attachment and apical reorientation can occur normally when *P. vivax* or *P. knowlesi* merozoites interact with Duffy-negative erythrocytes, however, the junction can not be formed in the absence

of the Duffy blood group antigen (Miller *et al.*, 1979; Hans *et al.*, 2005). Hence, invasion of human erythrocytes by *P. vivax* or *P. knowlesi* is completely dependent on the presence of the Duffy blood group antigen at the surface of erythrocytes and its interaction with the parasite Duffy-binding protein. The erythrocyte-binding domain of *P. vivax* lies within region II, a conserved N-terminal cysteine-rich region (Chitnis and Miller, 1994; Chitnis *et al.*, 1996). EBA-175 was the first identified erythrocyte binding protein in *P. falciparum* (Camus and Hadley, 1985). It mediates the invasion of erythrocyte in a glycophorin-A dependent manner (Sim *et al.*, 1994; Camus *et al.*, 1985). The binding specificity of EBA-175 is not only determined by the presence of sialic acid residues but also by the amino acid sequence of glycophorin A (Sim *et al.*, 1994). However, targeted disruption of EBA-175 in the parasite clone W2mef, whose invasion is sialic acid-dependent, was found to associate with a switch to a sialic acid-independent pathway of invasion (Reed *et al.*, 2000; Duraisingh *et al.*, 2003a). EBL-1, EBA-140/BAEBL, PEBEL and EBA-181/JSEBL are paralogues of EBA-175 in *P. falcuparum* genome (Adams *et al.*, 2001). Both BAEBL and JESEBL are involved in erythrocyte binding, but no switch in invasion pathway has yet been demonstrated (Adams *et al.*, 2001; Mayer *et al.*, 2001, 2004; Gilberger *et al.*, 2003b).

1.5.4 Dense granules

In *P. knowlesi* and *P. falciparum*, the dense granules are spheroidal membranous vesicles of about 80 nm in diameter (Torii *et al.*, 1989; Bannister & Mitchell, 1989; Aikawa *et al.*, 1990). They have densely granular interiors and are situated between the rhoptries and the merozoite nucleus. After invasion of RBCs, the dense granules move to the merozoite surface and release their contents by exocytosis from the parent plasma membrane into the PV (Torii *et al.*, 1989; Bannister *et al.*, 1990). Electron microscopic studies show that the dense granules play a role subsequent to the entry of the merozoite into the erythrocyte (Bannister *et al.*, 1975). Different dense granule proteins, such as ring infected erythrocyte surface antigen (RESA) (Aikawa *et al.*, 1990; Culvenor *et al.*, 1991), ring membrane antigen (RIMA) (Trager *et al.*, 1992) and subtilisin-like proteins (Blackman *et al.*, 1998) locate to different regions and at least one dense granule protein is released during or after erythrocyte invasion (Culvenor *et al.*, 1991; Trager *et al.*, 1992; Blackman *et al.*, 1998).

RESA originates from the dense granule of the merozoite and is released after merozoite invasion in localized areas of the PV space, before passing into the cytosol of newly invaded RBCs (Aikawa *et al.*, 1990; Culvenor *et al.*, 1991). Within the RBC cytosol, RESA associates with spectrin and can protect spectrins against heat-induced conformational changes (Foley *et al.*, 1991). RESA is probably not involved in the initial merozoite invasion steps but has

function after invasion, presumably by modifying the cytoskeleton to facilitate survival of RRBC in the peripheral circulation (Culvenor *et al.*, 1991). RIMA is a 14kDa protein detected in the late schizonts and free merozoites stage. Its detailed function is still unknown.

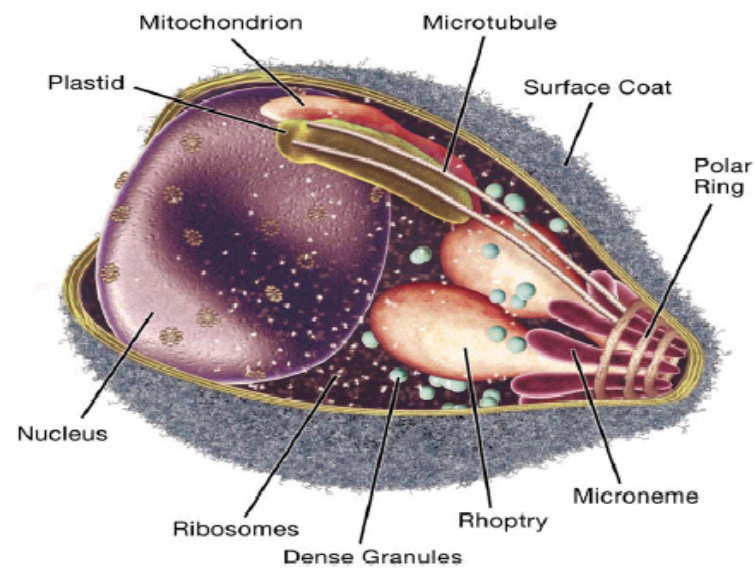

Figure 1. 3. Ultrastructure of apical organelles of *P. falciparum* merozoite (adapted from Cowman & Crabb, 2006).

1.5.5 Structures of erythrocyte invasion molecules

So far, only a few structures of erythrocyte invasion molecules have been solved. They include AMA-1 (Pizarro *et al.*, 2005; Bai *et al.*, 2005), EBA-175 (Tolia *et al.*, 2005), and *P. knowlesi* DBL domain (Singh *et al.*, 2006).

AMA-1 is a classical type 1 membrane protein composed of three domains: a N-terminal domain I, a central domain II and a C-

terminal domain III (**Figure 1. 4**) (Bai *et al.*, 2005; Pizarro *et al.*, 2005). Structural studies show that domains I and II possess a PAN fold possibly involved in receptor binding (Pizarro *et al.*, 2005). The characteristics of a PAN fold include a conserved core of disulphide bridges and secondary structure elements (Toedai *et al.*, 1999). The PAN fold is found in proteins with diverse adhesion function, binding to protein or carbohydrate receptors. The AMA-1 structure of *P. falciparum* also showed that the accumulation of polymorphic residues at a deep, highly structurally conserved groove, results from selection pressure by the host immune system (Bai *et al.*, 2005).

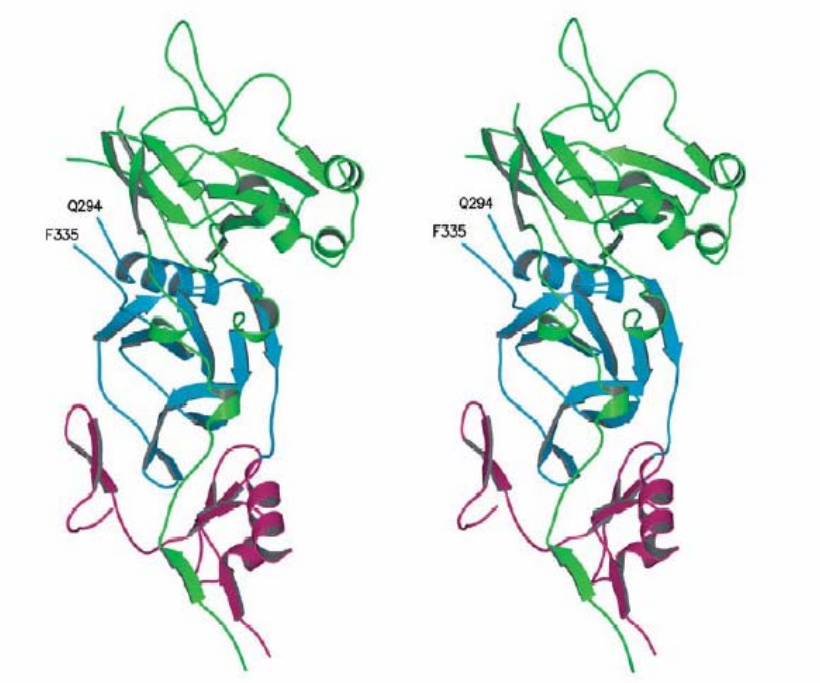

Figure 1. 4. A stereo view of the ectoplasmic region of AMA-1 in ribbon representation showing domain I (green), domain II (blue) and domain III (magenta). Residues Gln^{294} and Phe^{335} indicate the limits of disordered loop from domain II (adapted from Pizarro *et al.*, 2005).

The first DBL structure solved was EBA-175 region II (RII) which consists of two DBL domains—F1 and F2. F1 and F2 are homologous to the Duffy binding protein (DBP) of *P. vivax* and *P. knowlesi*. The 2.3Å resolution structure shows a dimer, with extensive interactions between elongated monomers (Tolia *et al.*, 2005). The overall structure reveals an elongated molecule, composed primarily of α-helices, with two antiparallel β hairpins and several bound sulfate molecules (Tolia *et al.*, 2005) (**Figure 1. 5**). Glycophorin A is an erythrocyte transmembrane dimer with two heavily glycosylated extracellular domains per dimer (MacKenzie *et al.*, 1997). Binding between EBA-175 RII and glycophorin A involves sialic acids on the mucin domain of glycophorin A (Camus and Hadley, 1985; Adams *et al.*, 1992; Sim *et al.*, 1990). In order to locate the receptor binding surfaces and to study the binding of EBA-175 RII to glycophorin A, RII was co-crystallized with the α-2,3-sialyllactose. This glycan contains the essential component Neu5Ac(α2,3)-Gal of the Glycophorin A glycan moiety responsible for binding, thus the structure may mimic the binding between Glycophorin A and EBA-175 region II *in vivo*. Six glycan binding sites were observed in the RII dimer interface. Four of them are inside the F1-F2 channel, and the other two are exposed on the surface and were separated from the channel by the β fingers (**Figure 1. 5**).

Based on the solved EBA-175 RII structure, they proposed a model for erythrocyte binding during the invasion process. Ligand-

receptor interaction at the erythrocyte surface might trigger RII dimerization via the dimeric glycophorin A extracellular domain. Following this event, signaling within the merozoite might be triggered through the cytoplasmic domain of the EBA175 protein, which is essential for invasion but not for protein trafficking (Gilberger *et al*., 2003a). However, recent studies using EBA-GFP chimeric proteins demonstrated that the conserved cysteine-rich region in the ectodomain of EBA is necessary for correct protein trafficking to the micronemes, and not the cytoplasmic tail nor the transmembrane region (Treeck *et al*., 2006).

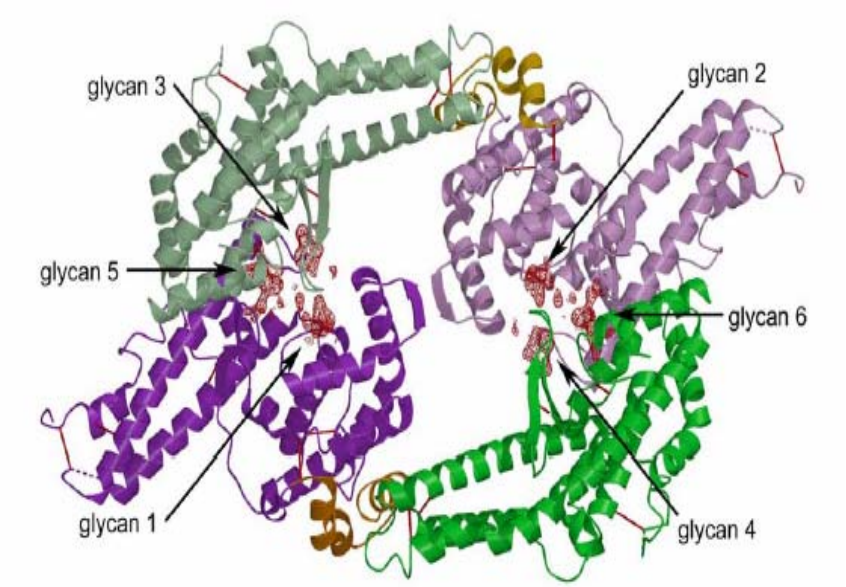

Figure 1. 5. Crystal structure of EBA-175 RII with sialyllactose. Ribbon diagram of RII with the position of six glycans. F1 domains are colored green or light green; F2 domains are purple or light purple and the linker regions are gold or light gold (adapted from Tolia *et al.,* 2005).

Another DBL domain recently solved is the Duffy-binding-protein of *P. knowlesi* (Pkα-DBL), which invades human erythrocyte exclusively through the host Duffy antigen receptor for chemokines (DARC). The Pkα-DBL protein is homologous to the two DBLs of EBA-175. The overall fold of the Pkα-DBL is monomer composed of α-helics. It has a boomerang-shape spread over three distinct subdomains (Singh *et al.*, 2006). All 12 conserved cysteines of Pkα-DBL are involved in intradomain disulfide bridges, which are identical to that of F1 and F2 DBL domains of EBA-175, except for an additional disulfide bridge in F2. Pkα-DBL can be divided into three subdomains: a random-coil stretch of residues 15-52 constitutes sub-domain 1, residues 64-180 make up sub-domain 2 (α1-α6), and sub-domain 3 extends from residues 186-307 (α7-α12) (**Figure 1. 7**). It has no inter-subdomain disulphide bridges, and the three sub-domains remain connected through hydrophobic surfaces and flexible linkers (**Figure 1. 7**).

The structure of Pkα-DBL provides insight into the molecular basis for receptor recognition and immune evasion employed by the malaria parasites. Singh *et al*. proposed a "just-in-time" model for immune evasion. Based on their analysis the highly polymorphic residues cluster on the opposite side of sub-domain 2. Secretion of DBP from micronemes is probably followed by rapid DARC engagement, burying the binding site residues and enabling immune response evasion. The DARC-recognition site and clusters of

polymorphic residues lie on opposite sides, thus the residues under the strongest immune selective pressure are those that remain exposed on the protein surface opposite the receptor binding domain (Adams *et al.*, 1990; VanBuskirk *et al.*, 2004). According to this model, the polymorphism is predominantly manifested on the opposite surface of the residues under immune attack (**Figure 1. 8**) (Singh *et al.*, 2006). However, it has been shown that *P. vivax* DBP polymorphisms are widely dispersed over the DBP domain (Baum *et al.*, 2003; Cole-Tibuan and King, 2003; Ampudia *et al.*, 1996; Xainli *et al.*, 2000; Kho *et al.*, 2001). Therefore, some polymorphisms distal to the proposed binding site might represent residues under weaker immune selective pressure or possible alter affinity to DARC at other residues of the minimal 35 amino acid receptor in a way that enhances invasion efficiency (McHenry and Adams, 2006). Co-crystallization of the DBL domain with its receptor is now required to clarify the process of erythrocyte invasion and mechanisms for immune evasion employed by parasite merozoites.

Despite an overall structural conservation between F1-F2 and Pkα DBL, their oligomeric states significantly differ. EBA-175 RII F1-F2 shows concentration-dependent dimerization, whereas Pkα DBL is monomeric in nature (Singh *et al.*, 2006). These two proteins bind to different substrates (EBA-175 binds to glycophorin A, while Pkα DBL binds to DARC), implying they have distinct binding sites for different interactions and the binding involved dimerization. In EBA-175 RII, the dimerization was shown to be critical for binding

to glycophorin A on erythrocytes. The glycan binding sites were mapped to a dimer interface formed by the interaction of two different RII monomers that assembled in an anti-parallel fashion. Mutants which disrupted the salt bridge or water-mediated interaction between the two monomers of EBA-175 showed reduced binding activities to erythrocytes (Tolia *et al*., 2005). In contrast, the proposed Pkα-DBL interaction with DARC does not appear to require dimerization as shown by site-directed mutagenesis (Singh *et al*., 2006) and the region involved in dimerization in EBA-175 RII is missing in Pkα-DBL. Overall, these comparisons suggest that a single binding site will not be sufficient to explain all DBL interactions with their varied receptors. More studies focusing on individual DBL structures are still needed to to further understand strategies of parasite invasion.

It has been suggested that despite the extent of sequence diversity in DBL domains, they may share a common fold due to the presence of conserved cysteines (Smith *et al*., 2000b). Biochemical and molecular studies have shown that the binding residues of DBL domains lie in the central regions. The central regions of DBPv, DBPk, EBA-175 F2, DBLα domain of strain R29 and DBLγ domain of strain FCR3 retain their binding ability when expressed on their own, suggesting that they constitute a functional module that folds independently and similarly (Mayor *et al*., 2005). Thus, the structures of EBA-175 RII and Pkα-DBL provide good models for

these DBL-containing proteins and predictions about the DBL-dependent pathways of invasion.

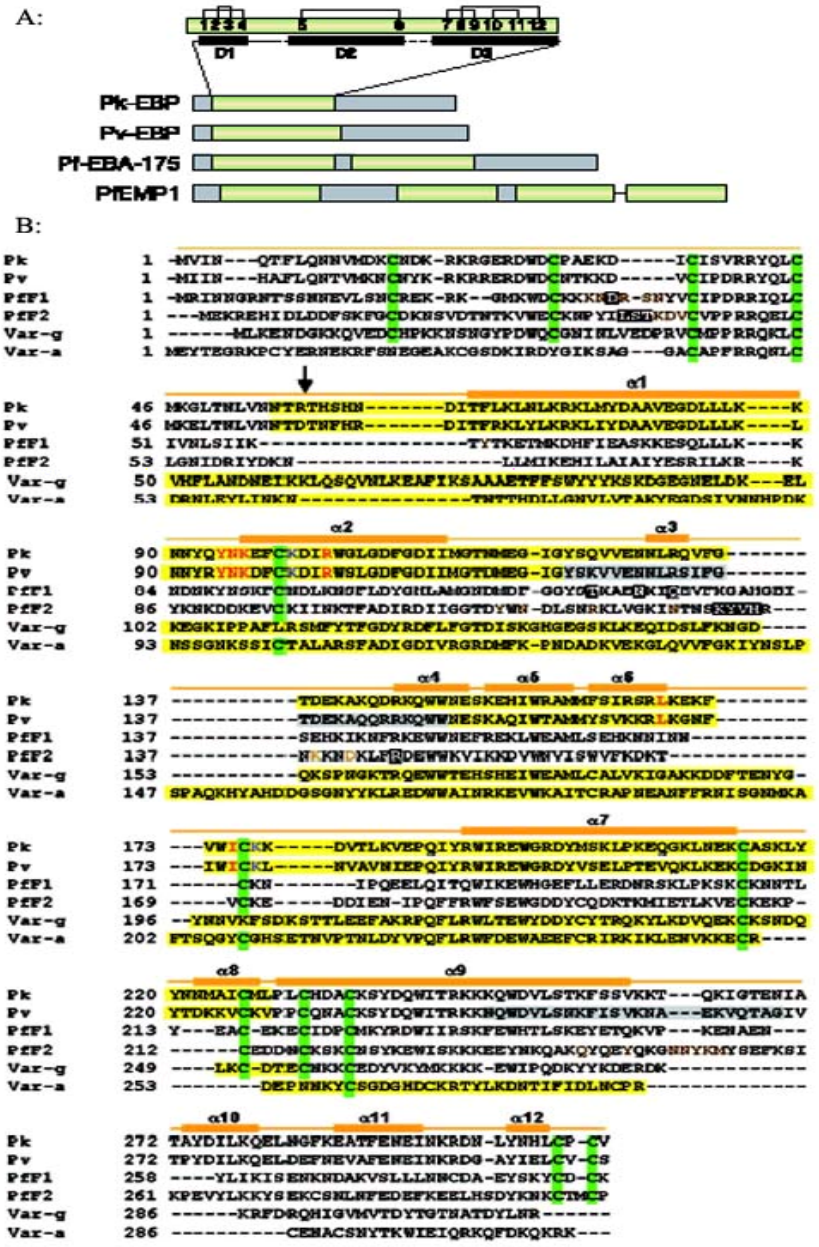

Figure 1. 6. Sequence alignment of homologous DBLs from three EBPs and two PfEMP-1 proteins. Panel A shows the disulphide bonds present in subdomains 1, 2 and 3 of Pkα-DBL. Homologs of

Pkα-DBL (green boxes) are present in many EBP (Pv-DBL and EBA-175) and PfEMP-1 proteins. Panel B shows the sequence alignment of DBL homologs (Pkα-DBL, Pv-DBL, EBA-175 and two PfEMP-1 proteins). Secondary structure elements of Pkα-DBL/Pv-DBL are shown in orange, the minimal receptor-binding region is shown in yellow, and conserved cysteine residues in green. The proteolytic site on Pkα-DBL is indicated by an arrow. Pv-DBL clusters of polymorphic residues are shown in grey, mutations that affect DARC recognition are shown in red, contact residues between F1-F2 and sialic acid are shown in brown, and F1-F2 dimerization elements are boxed (adapted from Singh *et al.*, 2006).

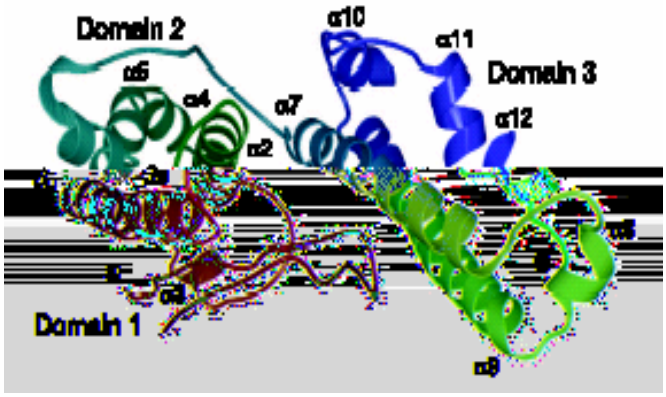

Figure 1. 7. Structure of Pkα DBL. The structure has a compact, flat architecture. The three sub-domains of PkαDBL are sub-domain 1 (residues 15-52), sub-domain 2 (residues 64-180) and sub-domain 3 (residues 186-307) (adapted from Singh *et al.*, 2006).

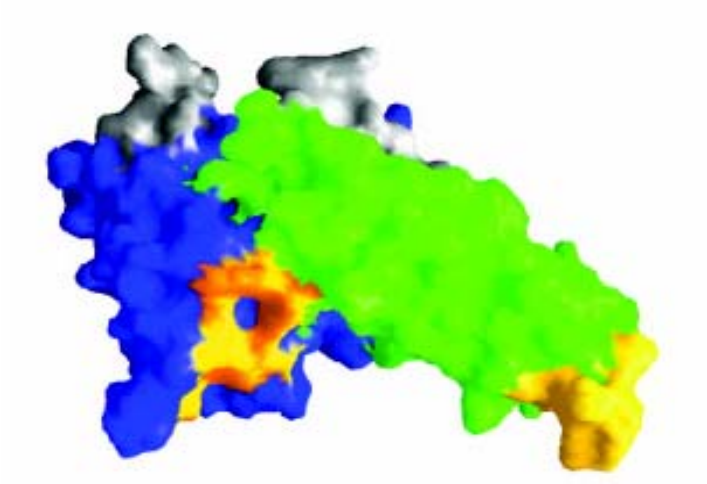

Figure 1. 8. Model of Pkα DBL and erythrocyte interaction. The molecular surface shows polymorphic residues (grey) on the Pv DBL molecule and the DARC-recognition site (orange). Sub-domain 1, 2 (blue) and 3 (green) are shown (adapted from Singh *et al.*, 2006).

1.6 Molecular basis of RBCs sequestration in malaria

Post-mortem examinations of people who have died from *P. falciparum* infections show accumulation of PRBCs within the small vessels of many tissues, including brain, lung, placenta etc. (Walter *et al.*, 1982; McPherson *et al.*, 1985; Oo *et al.*, 1987). Microvascular sequestration is a main cause of mortality in severe malaria cases. Sequestration is mediated by a process called cytoadherence, which refers to the unique ability of parasites to adhere to capillary and postcapillary venular endothelium during the second half of the 48-hours life cycle (MacPherson *et al.*, 1985). Cytoadherence may confer several survival advantages to the parasites: 1) Deep tissue microvasculature places the PRBC in a parasite-favoring

microaerophillic environment, thereby promoting more rapid asexual multiplication. 2) PRBCs are shielded by roseting, which is the adhesion of uninfected RBCs to infected RBCs. 3) Adhesion to endothelium allows parasites at trophozoite and schizont stages to escape clearance by the spleen (Miller *et al.*, 2002a; Sherman *et al.*, 2003). This clearance is mediated by recognition of their deformability and opsonization with antibodies and/or complement components (Cranston *et al.*, 1984; Looareesuwan *et al.*, 1987; Ho *et al.*, 1990). Studies have indentified several PfEMP-1 receptors at the endothelial surface: thrombospondin (TSP) (Roberts *et al.*, 1985), Heparin sulfate (HS) (Rowe *et al.*, 1997), complement receptor 1 (CR1) (Mayor *et al.*, 2005), CD36 (Barnwell *et al.*, 1989), intercellular adhesion molecule-1 (ICAM-1) (Berendt *et al.*, 1989), vascular cell adhesion molecule-1 (VCAM-1) (Ockenhouse *et al.*, 1992) and chondroitin sulfate A (CSA) (Rogerson *et al.*, 1997). Each of these receptors interacts with specific domain(s) of PfEMP-1 (see below).

1.6.1 PfEMP-1 and *var* genes in *P. falciparum* clone 3D7

PfEMP-1 is an important virulence factor encoded by a family of about 60 *var* genes which is used by the parasite to interact with the human host. The PfEMP-1 protein is exported to the surface of infected RBCs where it mediates adherence to host endothelial receptors, resulting in the sequestration of infected cells in a variety of organs (Keyes *et al.*, 2001). These adherence properties are

important virulence factors that contribute to the development of severe disease. These proteins are also targets of the host protective antibody response (Bull *et al.*, 1998), but transcriptional switching between *var* genes permits antigenic variation and immune evasion, facilitating chronic infection transmission by malaria.

In 2002, the first complete genome of *P. falciparum* clone 3D7 was sequenced and reported. Analysis of its chromosome structure, gene content and functional classification of its proteins will help us to better understand the features of the parasitology.

The 22.8-megabase nuclear genome of *P. falciparum* (clone 3D7) consists of 14 chromosomes varying in size from 0.643 to 3.29 megabase, encodes about 5,268 genes, most of them being (A+T)-rich (80.6%) sequences (Gardner *et al.*, 2002). Of the 5,268 predicted proteins, about 60% do not have sufficient similarity to proteins in other organisms to be assigned a function. Thus almost two-thirds of the sequences appear to be unique to this organism, a proportion much higher than in other eukaryotes. This may reflect the greater evolutionary distance between *Plasmodium* and other eukaryotes that have been sequenced (Gardner *et al.*, 2002). Compared to the genomes of eukaryotic microbes, the genome of *P. falciparum* encodes fewer enzymes and transporters, but a large proportion of genes are devoted to immune evasion and host-parasite interactions (Gardner *et al.*, 2002). At least 1.3% of *P. falciparum* genes are involved in cell-cell adhesion or the invasion of host cells

and about 3.9% are involved in the evasion of the host immune system (Gardner *et al.*, 2002).

In common with other organisms, highly variable gene families are clustered within the telomeres. *P. falciparum* contains three such families termed *var*, *rif* and *stevor*, which encode proteins known as PfEMP-1, repetitive interspersed family (rifin) and sub-telomeric variable open reading frame (stevor), repectively (Leech *et al.*, 1984; Weber *et al.*, 1988a; Cheng *et al.*, 1998; Kyes *et al.*, 1999). The 3D7 genome contains 59 *var*, 149 *rif* and 28 *stevor* genes, but for each family there are a number of pseudogenes and gene truncations (Gardner *et al.*, 2002). Rifins are expressed on the surface of infected RBCs and suggested to undergo antigenic variation (Keyes *et al.*, 2001). Proteins encoded by *stevor* genes show sequence similarity to rifins, but they are less polymorphic than the rifins (Cheng, *et al.*, 1998). The distinct location of stevor in Maurer's clefts, unique membranous structures located in the cytoplasm of infected erythrocytes, indicates it might involve sorting and assembly of proteins destined for the surface of infected erythrocyte (Kaviratne *et al.*, 2002).

Var genes consist of two exons, one is between 3.5 and 9.0 Kb in length, polymorphic and encodes an extracellular region of the protein; the other is between 1.0 and 1.5 Kb in length, encodes a conserved cytoplasmic tail that contains acidic amino-acid residues (Gardner *et al.*, 2002). The *var* genes are made up of three recognizable domains known as Duffy-binding like (DBL); Cysteine-

rich interdomain region (CIDR) and constant2 (C2) domains (Peterson *et al*., 1995; Baruch *et al*., 1997; Smith *et al*, 2001). These domains can be further assigned to several sub-classes: α to ε and X for DBL domains and α to γ CIDR domains. Based on the different combinations of DBL and CIDR subdomains, *var* genes can be classified into 16 types. The most common type is type 1, with 38 genes in this category, consisting of DBLα, CIDR1α, DBL and CIDRβ/γ followed by the acidic terminal sequence (ATS). A total of 58 *var* genes commence with a DBLα domain, and in 51 cases this is followed by CIDR1α, and in 46 *var* genes the last domain is CIDR β/γ. The highly conserved type 1 *var* gene combination indicates functional relevance. However, the rest of *var* genes are more diverse than type 1. Four *var* genes are atypical with the first exon consisting solely of DBL domains (type 3 and 13) (Gardner *et al*., 2002). Reasons for the diversity of arrangement among these different domains are still unknown.

1.6.1.1 Semi-conserved head structure

The DBLα domain and CIDRα form a tandem unit known as the PfEMP-1 protein semi-conserved head (Su *et al*., 1995; Chen *et al*., 2000). Based on sequence classification, distinct PfEMP-1 head structures were defined. Studies by Robinson *et al*. (2003) grouped the CIDR domains into three major types α, β, γ and α1 subtypes using the neighbour-joining method. The "FCRvar CSA-like" sequence, which is a non CD36-binding sequence, was designated as

a CIDRα1 subtype (Robinson *et al.*, 2003). The majority of PfEMP-1 proteins have "type 1" head structure consisting of a DBLα and CIDR1α domain. A subset of PfEMP-1 proteins have a type 2 head structure with a CIDRα1 or CIDRγ domain and of DBLα1 domain (Robinson *et al.*, 2003) (**Figure 1. 9**). In the 3D7 genome, 38 out of 59 predicted PfEMP-1 proteins share the same common type domain architecture (NTS-DBL1α-CIDR1α-DBL2δ-CIDR2β/γ-ATS), which contains the type 1 head structure. The remaining PfEMP-1 proteins in the 3D7 clone are larger and can be devided architecturally into 13 different binding regions, based on the domain composition (Gardner *et al.*, 2002). Thus, the head structure is another criterion for classifying PfEMP-1 proteins. The semiconserved head structure mediates binding to multiple host receptors, such as heparin sulfate (HS)-like glycosaminoglycan (GAG), CR1, blood group A antigen and CD36 (Chen *et al.*, 2000; Rowe *et al.*, 2000; Mayor *et al.*, 2005). Among them, DBL1α is involved in binding HS-like GAG, CR1 and blood group A (Chen *et al.*, 2000; Rowe *et al.*, 2000; Mayor *et al.*, 2005); while CIDR1α binds to CD36 (Baruch *et al.*, 1997; Chen *et al.*, 2000) (**Table 1. 1**).

PfEMP1 domains	receptor	binding region within the domain	reference
DBLα	CR1	C5-C12 (R29 strain)	Mayor *et al.*, 2005
DBLα	HS/heparin	Not known	Barragan *et al.*, 2000
CIDR1α	CD36	179 amino acids (MC strain)	Baruch *et al.*, 1997
DBLβC2	ICAM-1	Not known	Smith *et al.*, 2000a
DBLγ	CSA	67 amino acids (FCR3 strain)	Gamain *et al.*, 2004

Table 1. 1. Interaction between PfEMP-1 receptors and attachment molecules. CIDR1α from strain MC binds CD36 through 179 amino acids of strain MC. The central region cysteine 5 to cysteine 12 of DBLα from *P. falciparum* strain R29 binds CR1. The central 67 amino acids residue of DBLγ from strain FCR3 binds CSA. Binding regions within the domain of DBLα to HS and DBLβC2 to ICAM-1 are unknown.

1.6.1.2 DBL sequence

The arrangement of five DBL types with three CIDR types is not random. Three domain pairings were observed at high frequency (Smith *et al.*, 2000b; Gardner *et al.*, 2002). The first domain pair associates DBL1α with CIDR1α at the amino terminus, refered as head structure, and has been discussed in the previous section. Another domain pair is DBLδ and CIDRβ/γ. This tandem domain pair frequently precedes the transmembrane region (70% of the total

20 analyzed PfEMP-1s), in which case the CIDR domain is universally of the β type (Smith *et al.*, 2000b). The function of this domain tandem is still unknown.

The third tandem domain combination is the pairing of DBLβ and C2 domains. It has been found 13 out of 59 PfEMP-1 proteins contain DBL2βC2 tanden arrangement (Gardner *et al.*, 2002). This DBL2βC2 domain was shown to mediate binding with ICAM-1 (Smith *et al.*, 2000a) (**Table 1. 1**). ICAM-1 is a glycoprotein that acts as a ligand for the leukocyte integrin lymphocyte function-associated antigen-1 (LFA-1) and plays a central role in the generation of an immune response (Rothlein *et al.*, 1986). It is distributed widely on venular endothelium, where it is crucial for neutrophil adhesion before the transmigration of these cells into an inflammatory focus (Smith *et al.*, 1988). ICAM-1 expression on endothelial cells can be upregulated by the proinflammatory cytokines TNF-α, IL-1, and interferon-γ (IFN-γ) (Pober *et al.*, 1987). Since the binding between DBLβC2 and ICAM-1 is relatively weak and cannot trigger massive sequestration by itself, it has been proposed that binding to ICAM-1 and CD36 synergize to allow static adhesion of *P. falciparum*-infected erythrocytes to host endothelium under flow conditions (Cooke *et al.*, 1994; Yipp *et al.*, 2000). However, recent studies showed CIDR1α domain is not critical for DBL2β domain binding to ICAM-1 molecule in strain JDP8 (Chattopadhyay *et al.*, 2004). The interactions between these two domains still need further evaluation.

Both the DBL3γ domain of var1CSA (from the CSA-binding strain FCR3CSA), and DBL2γ domain of CS2var (from the CS2 strain) bind CSA (Buffet *et al.*, 1999; Reeder *et al.*, 1999; Reeder *et al.*, 2000). In both cases, the domain of PfEMP-1 that mediates specific binding to CSA *in vitro* was a DBLγ type domain. Antibodies raised against each of these two DBLγ domains showed specific inhibitory effects of parasitized erythrocyte (PE) adhesion to CSA (Buffet *et al.*, 1999; Reeder *et al.*, 1999). Moreover, recombinant DBLγ proteins are able to elicit antibodies reactive to CSA-binding parasite isolates from different endemic regions, demonstrating that the epitopes of this domain are well conserved among different CSA-binding parasite isolates (Costa *et al.*, 2003). In the strain FCR3-CSA, the minimal CSA binding region of the DBLγ domain has been localized to a central 67-residue fragment (Gamain *et al.*, 2004) (**Table 1. 1**).

Recently, another DBL type-DBL3x of var2CSA from strain 3D7 was shown to bind CSA (Bir *et al.*, 2006). Since anti-DBL3γ sera cross-reacted with the DBL3x domain of var2CSA and blocked the binding of DBL3x to CSA, DBL3γ and DBL3x must share common B-cell epitopes (Bir *et al.*, 2006). Thus these epitopes may serve as targets for raising protective antibodies and form the basis for development of a vaccine against placental malaria as PRBCs isolated from the placeta predominantly bind CSA (Fried *et al.*, 1998; Ricke *et al.*, 2000; Duffy and Fried, 2003).

1.6.1.3 CIDR sequence

Within the PfEMP-1 family of the *P. falciparum* clone 3D7, CIDR1α type sequences bind to CD36, whereas CIDRβ and CIDRγ type sequences do not (**Figure 1. 9**). CIDR1α-type sequences are uniquely localized to the PfEMP-1 head structure, a position that may favor their interaction with CD36. In contrast, CIDRβ or CIDRγ type sequences do not bind CD36 and are more typically located within the second DBL/CIDR tandem (Robinson *et al.*, 2003). Futhermore, almost all CIDRα1 subtype, which supposedly do not bind CD36, are paired downstream with particular DBL sequences, named DBL1α subtype and shared distinct amino acid feature with CIDR1α type (Robinson *et al.*, 2003). Thus different CIDR sequence types, domain combinations as well as domain location may contribute to CD36-binding activity. In terms of the head structure, all PfEMP-1 proteins containing a type 1 head structure bind CD36, while none with a type 2 head structure do (Robinson *et al.*, 2003).

Previously, PRBCs isolated from the placenta bind CSA but not CD36, whereas peripheral PRBCs from non-pregnant women prodominently bind CD36 (Fried and Duffy, 1996; Scherf *et al.*, 2001; Flick *et al.*, 2001). PfEMP-1 proteins from CSA-binding parasites have a combination of a CSA-binding DBLγ domain and a non-CD36-binding CIDRα (Buffet *et al.*, 1999; Gamain *et al.*, 2001), suggesting these two domains may solely dictate determine the individual PfEMP-1 binding phenotype.

In addition to CD36, the CIDR1α domain from strain FCRS1.2 can also bind other receptors such as IgM and CD31 (Chen *et al.*, 2000). However, this is not the case for all parasites. So far, most of CIDR1α domains from non-pregnant women bind CD36 (**Table 1. 1**). I have focused my work on the interactions between CIDR1α and CD36 in this study.

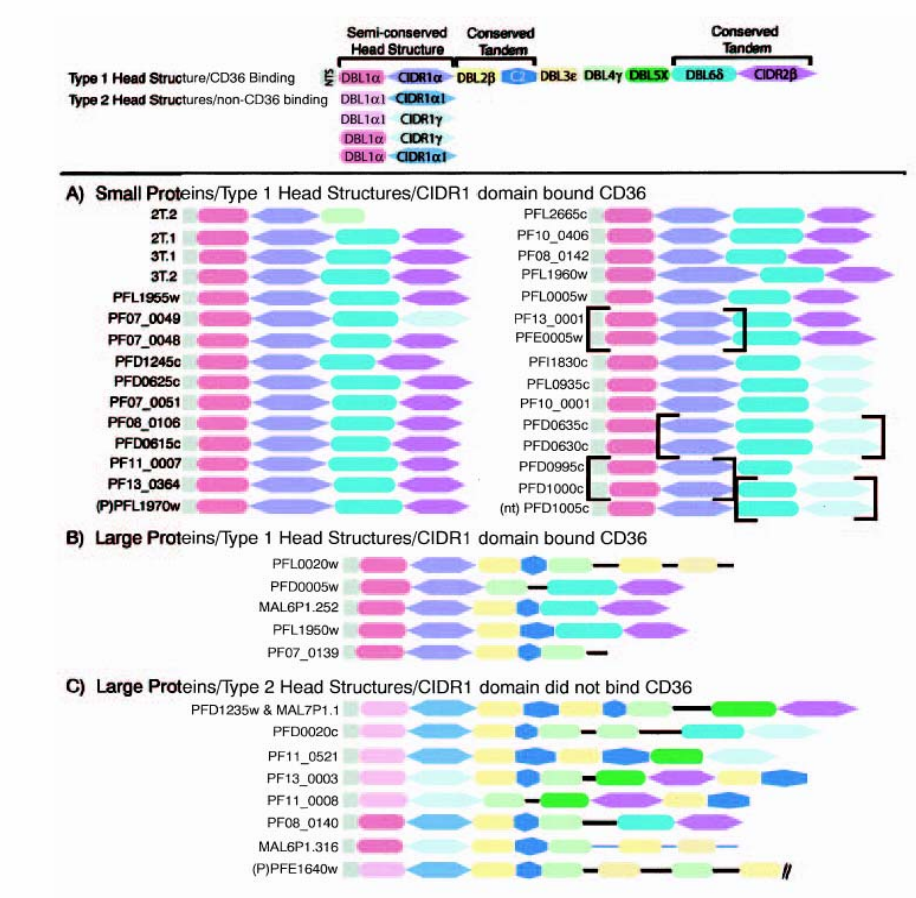

Figure 1. 9. Classification of PfEMP-1 binding regions from the *P. falciparum* clone 3D7 by head structure, domain composition and CD36-binding ability (adapted from Robinson *et al.*, 2003).

1.6.1.3.1 CD36 structure and function

CD36 (also called GPIIIb, GPIV and GP88) is a 88 kDa cell surface class B scavenger receptor found on the surface of several cell types including platelets, monocytes, dendritic cells and microvascular endothelial cells. It is believed to have two short intracellular domains and a large extracellular domain, and is highly N-glycosylated (with ten potential glycosylation sites). A hydrophobic region spans residues 184 to 204, which can contact the membrane, or form a hydrophobic pocket (**Figure 1. 10**) (Serghides *et al*., 2003). CD36 has been implicated in many diverse biological processes including angiogenesis, phagocytosis, lipid and glucose metabolism, and inflammation. CD36 is preferentially found within lipid rafts, which can facilitate its interaction with receptors, signaling and adaptor molecules. The CD36 receptor transports oxidized lipids and long chain fatty acids (Ibrahimi *et al*., 1996; Febbraio *et al*., 1999). It is also a phagocytic receptor for apoptotic cells (Stern *et al*., 1996) and a thrombospondin receptor (Asch *et al.,* 1993).

Under flow conditions, PEs appear to tether and roll on receptors such as ICAM-1, VCAM-1 and P-selectin, but adhere strongly to the CD36 molecule (Udomsangpetch *et al*., 1997; Ho & White, 1999). CD36 might provide a stable and long-lasting anchor for PRBCs to bind to the endothelial cells that line the postcapillary venules. Most of natural isolates of *P. falciparum* from non-pregnant malaria patients bind to CD36, whereas adherence to other receptors

is variable (Udomsangpetch *et al.*, 1997). Although CD36 is not linked to severe malaria diseases such as cerebral malaria (Cortes *et al.*, 2005), adherence to CD36 is thought to contribute significantly to malaria pathogenesis and adverse clinical outcomes. As a result, the development of therapeutics to inhibit or reverse this interaction would provide possible cures/vaccines for malaria (Cooke *et al.*, 1998). Using peptide mapping, various regions of CD36, including residues 155-183 (Daviet *et al.*, 1995) and 139-184 (Baruch *et al.*, 1999) have been implicated in cytoadherence. Both of the regions found are within an immunodominant and hydrophobic extracellular region of CD36 (Asch *et al.*, 1993).

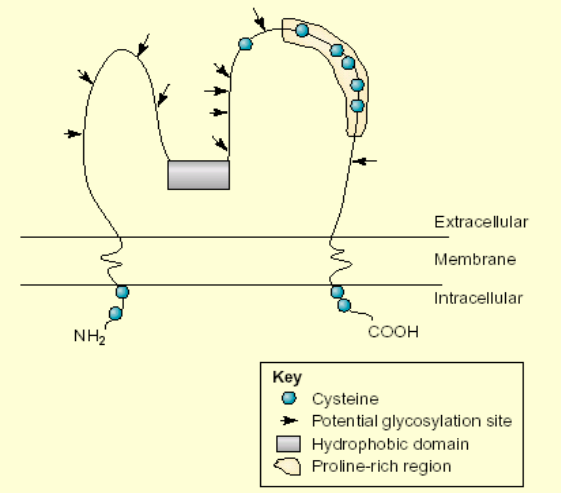

Figure 1. 10. Predicted topology of CD36 in the plasma membrane: having a 'hairpin-like' structure with α-helices at the N- and C-termini projecting through the membrane and a larger extracellular loop. It is highly N-glycosylated (ten potential glycosylation sites)and cysteine-rich (10 cysteines) (adapted from Serghides *et al.*, 2003).

1.6.1.3.2 Mapping the minimal CD36 binding domain of CIDR1α

Baruch *et al*. demonstrated that a 179-amino-acid fragment spanning residues 576 to 755 of the Malayan Camp (MC) PfEMP-1 protein, mediates PRBC adherence to CD36 (Baruch *et al*., 1997). This region corresponding to CIDR1α domain and includes seven cysteines and several conserved motifs including: the five cysteines within cysteine rich motif 1 (CRM1) (CX8CX3CX3CXC), LEX(V/L)LXKXXLL, GX4IX(H/R)XX(L/M)LXXE and TTIDKXLXHE (**Figure 1. 11**). Further studies using the strain FVO extending this region upstream (M1 region) or downstream (M3 region) confirmed the importance of this domain for binding CD36. Chimeric proteins were also produced exchanging regions of the MC CIDR1α that binds CD36 with the FCR3-CSA CIDR1α that does not bind CD36 (**Figure 1. 12**). However, none of these chimeras modified the binding properties of the MC and FCR3-CSA CIDR1α. Chimeras consisting of the MC r179 region flanked by the M1 and M3 of FCR3-CSA readily bound to CD36. In contrast, the region corresponding to r179 region in FCR3-CSA did not bind CD36 even when bordered by the M1 and M3 regions of MC (Gamain *et al*., 2001). Antibodies to the r179 glutathione-S-transferase (GST) fusion protein of the MC and the ItG (ItG/FVO type) strains agglutinated and blocked adherence of PRBCs to CD36 (Baruch *et al*., 1997). This demonstrated that the region r179 is responsible for binding CD36, but the minimal binding region has not been mapped yet.

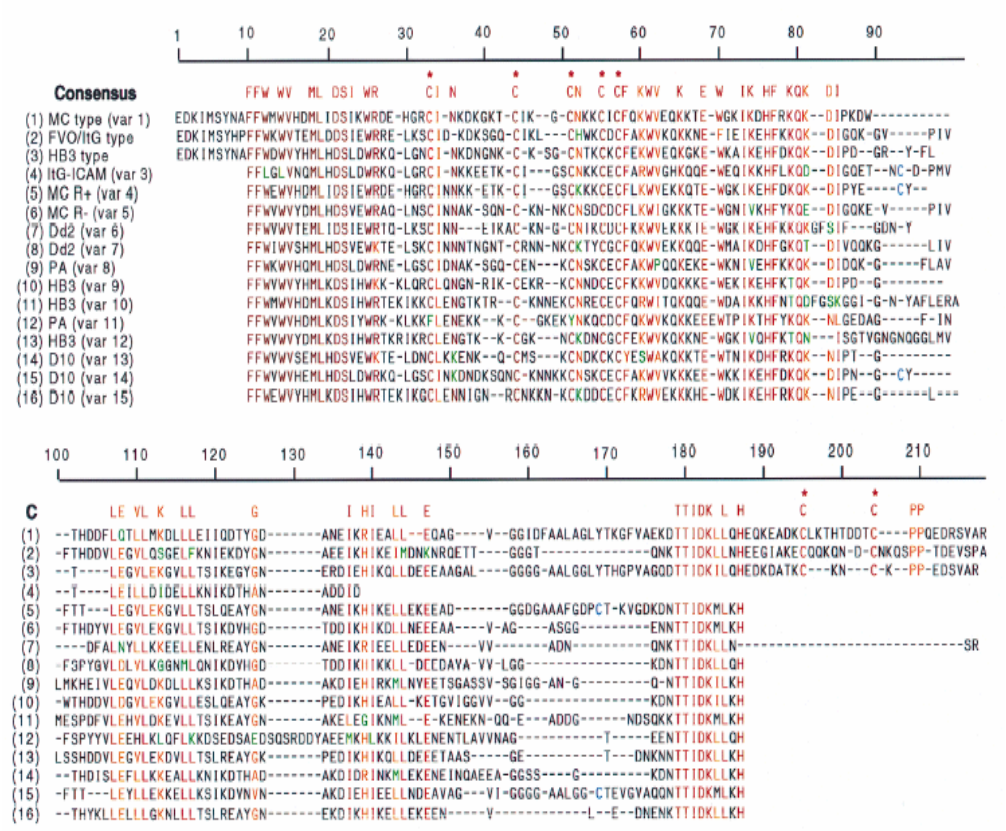

Figure 1. 11. Alignment of the predicted amino acid sequence of the CD36 binding domain from different *var* genes. The emerging consensus sequence of conserved amino acids is depicted on the top of the alignment. Highly conserved amino acids are indicated in red, conserved substitutions are indicated in orange and non conserved substitutions in green. The conserved cysteine residues are marked by asterisks and additional cysteine residues in blue (adapted from Baruch *et al*., 1997).

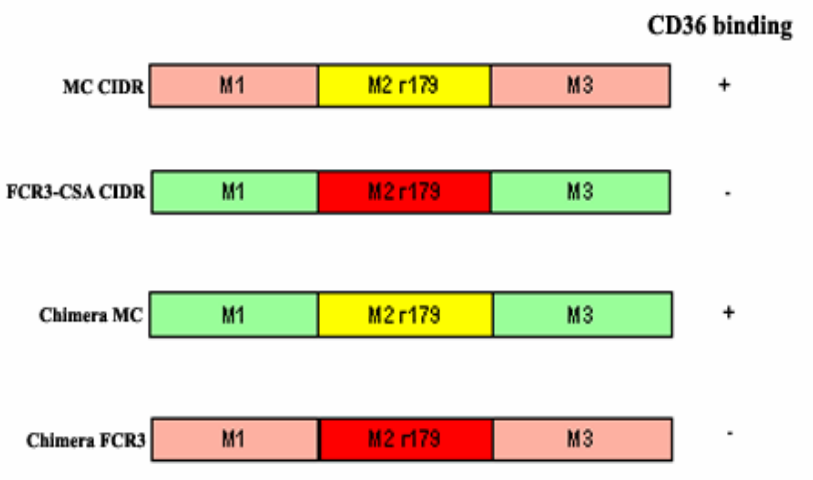

Figure 1. 12. Schematic representation and binding properties of the MC and FCR3-CSA CIDR1α chimeras. The CD36-binding domain extends upstream (M1 region) or downstream (M3 region) of r179 region (M2 region) in both MC strain and FCR3-CSA strain. Exchanging regions between MC strain and FCR3-CSA strain results in 2 new chimeric proteins. The wild type MC CIDR1α M1-M3 region and chimera MC protein bind CD36, while FCR3-CSA and chimera FCR3 protein does not.

1.6.1.3.3 CD36 peptides block cytoadherence of MC r179 of PfEMP-1

After the identification of the domain of PfEMP-1 which binds CD36, Baruch *et al*. mapped the CIDR1α binding domain to the amino acid 139-184 of CD36, pinpointing the 146-164 and the 145-171 regions (Baruch *et al.*, 1999). Three independent experiments were used to assess the ability of different peptides derived from CD36 to block the PRBCs or PfEMP-1 interaction with CD36. (1)

Peptide inhibition of binding of ^{125}I-PfEMP-1 to CD36; (2) Peptide inhibiting the binding of r179 to CD36; and (3) Peptides blockage of PRBC adherence to immobilized CD36. These experiments identified several peptides from CD36, encoding residues 139-155, 146-171, 145-171 and 156-184 that can disrupt MC r179 binding to CD36 in two different assays. These peptides had no effect on binding to ICAM-1, indicating that the inhibition is specific for CD36. Although the peptide encoding residues 139-155 was active, it displayed a much lower inhibition activity compared to the other three peptides, demonstrating that the CD36 binding domain for PfEMP-1 and PEs is located in residues 139-184, with residues 145-171 (ASHIYQNQFVQMILNSLINKSKSSMFQ) and residue 146-164 (SHIYQNQFVQMILNSLINK) playing important roles for the interaction (Baruch *et al*., 1999). Due to the poor solubility of the peptide 146-164, the application in PE adhesion assay was limited, hampering the definition of minimal binding domain. Four different *P. faciparum* strains which adhere to host receptor CD36, namely MC-R+, FCR3-C5, ItG2-ICAM and A4ultra, were used for peptide inhibition assay. These peptides inhibited the PE/PfEMP-1 interaction with CD36 of the 3 different strains, known to express different CIDR1α sequences (strain MC-R+, FCR3-C5 and A4ultra) (Baruch *et al*., 1997; Smith *et al*., 1998). Thus regardless of the variation in CIDR sequences, erythrocytes infected with CD36-binding strains are able to recognize the same region of CD36.

1.6.1.3.4 Mutagenesis studies of CIDR1α domain

Having determined the CD36 binding domain of PfEMP-1 from the MC strain, several studies tried to define the minimal region(s) or amino acids within CIDR1α which are directly involved in CD36-binding. Parasites isolated from human placenta can bind CSA and hyaluronic acid but not to CD36 (Fried *et al.*, 1996; Beeson *et al.*, 2000). This dichotomy between parasite adhesion to CD36 and to CSA may provide some clues to understand the CIDR1α-CD36 binding characterization. Interestingly, the CIDR1α domain from CD36-adherent parasites is not significantly different in terms of amino acid sequences from the non CD36-adherent CIDR1α. All cysteine residues are conserved and no gross changes are found in the minimal CD36-binding region (Smith *et al.*, 2000b). Thus, it seems that small modifications in the CIDR1α sequence may modulate its ability to bind CD36. Most of the studies were based on substitutions of individual amino acids of CD36-binding CIDRα or non CD36-binding CIDRα in order to assess their binding specificity. Five mutants where amino acids from CSA-binding strain FCR3-CSA were inserted into CD36-binding strain MC (S203T, R207N, K218T, K235R and K246S) had no effects on CD36 binding activities. This indicated that these residues are not critical for the interactions of the MC CIDR1α with CD36 (Gamain *et al.*, 2001). Similarly, Robinson *et al.* reported that several signature residues of the CIDR1α domain in strain FCR3-CSA when mutated into the corresponding amino acids in strain MC, all of these single

mutations (MC Q648K, MC EQ727LK) did not affect CD36-binding activities. However, a combination of the three mutants (MC Q648K + EQ727LK + H644L) reduced the number of CD36-coated beads to 63% of wild type, indicating a contribution of these 4 residues to CD36-binding (Robinson *et al.*, 2003). In order to map the region within the r179 of MC/FCR3-CSA responsible for CD36-binding more precisely, Gamain *et al.* divided r179 region into two regions: M2a and M2b (residue 1-66 and 67-179 of MC CIDR1α, respectively) and exchanged these two parts between strain MC and strain FCR3-CSA. They observed no binding of CD36 to any construct that contained one or more fragments of the FCR3-CSA region. Thus, it is probable that several residues located within both M2a and M2b region of the CD36-binding domain are responsible for the inability of the FCR3-CSA CIDR1α to bind CD36. Alternatively, there could be some incompatibility between the M2a and M2b regions of the two proteins in forming the CD36-binding pocket (Gamain *et al.*, 2001). They also found that a 3-amino acid change from GHR to DIE in r179 region of ItG2-CS2, a strain phenotype that binds CSA (Reeder *et al.*, 1999), preserved binding activity to CD36 (**Figure 1. 13**) (Gamain *et al.*, 2001). The same mutation in the CIDR1α in the strain MC with the conversion of 51EIK sequence to GHR reduced the total binding to 64% of the wild type. It leads to the conclusion that not only these residues play a significant role in the CIDR1α-CD36 interactions but also other surrounding regions contribute to binding, thus suggesting that several discontinuous elements of the

CIDR structure participate in forming a topographical binding site (Gamain *et al.*, 2001). The mutagenesis data mentioned above are summarized in **Figure 1. 13**. We noticed that most of the experiments designed for CD36 binding assay used cell-based binding assays. The CIDR1α domains were expressed on the surface of mammalian cells (such as Cos7 cell line) and CD36 binding was tested using CD36-coated beads. Influence on binding effects was determined by counting the number of beads present on positive cells. These kinds of experiments unavoidably have some disadvantages that might affect the binding results, such as cell growth conditions, transfection efficiency etc. In addition, the bulky CD36-coated beads may have partially interfered with the interactions between CD36 and CIDR1α domains. The ELISA-based assay present in this study is relatively simple to perform, and the static anchoring CD36/Fc may provide a platform for facilitating CIDR1α domain folding in the solution. In addition, it is more sensitive than mammalian-based binding system because the protein required for signal detection is relatively low (less than 0.1 μM). Therefore, this assay has some advantages than the mammalian-based binding assay. Also, due to the diversities of CD36-binding and non CD36-binding CIDRα sequences, at present there is no study that can unambiguously identify the residues critical for the CIDR1α-CD36 interaction.

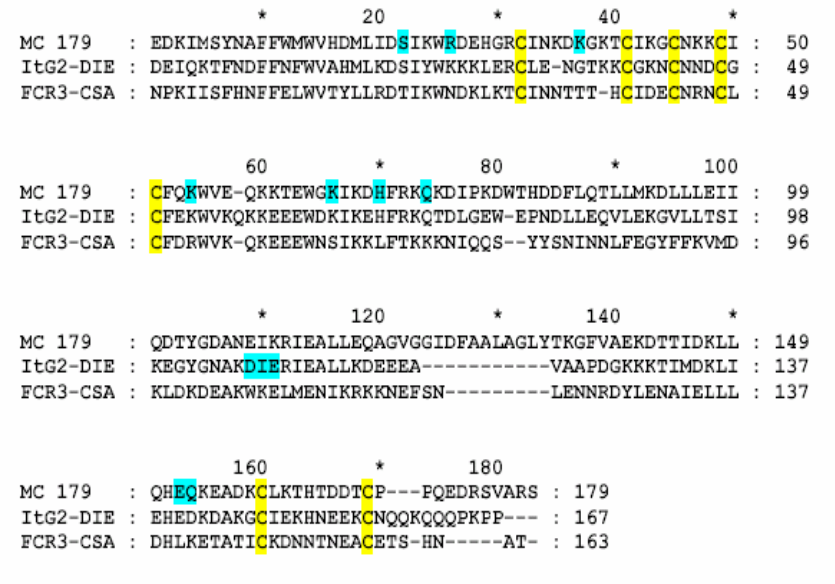

Figure 1. 13. Summary of mutagenesis data in MC r179 minimal binding domain. The conserved cysteines are indicated in yellow. The residues that have been mutated are shown in blue.

1.7 Vaccine development

With the emergence of more and more drug-resistant strains of malarial parasites, safe and effective vaccines for the control of malaria all over the world are urgently needed, especially in Africa and south-east Asia. Several experimental data support the importance of antibody mediated immunity in *P. falciparum* infection (Fried *et al.*, 1998; Duffy and Fried, 2003). Not only passive transfer of antibodies is capable of conferring protection between residents in a local area, but sera collected in Africa is also capable of reducing parasitemia of patients in Thailand (Bouharoun-Tayoun *et al.*, 1990; Sabchareon *et al.*, 1991). Humoral immunity in

P. falciparum is extremely complicated as protection seems to result from a combination of antibodies targeting several developmental stages, thereby reducing the parasitemia, blocking adhesive events and cytotoxic events. While antibodies against conserved but poorly recognized antigens certainly cannot be ruled out as an important part of immunity, the accumulation of antibodies against a repertoire of variant surface antigens (VSA) is strongly suggested by many studies (Bull *et al.*, 1998a; Bull *et al.*, 1999; Bull *et al.*, 2000; Giha *et al.*, 2000; Ofori *et al.*, 2002).

Hence, potential vaccine candidates must utilize antigens from different stages of the parasite life cycle. The objective of a vaccine targeting the pre-erythrocytic forms of the parasite, sporozoites and infected heptocytes is to induce sterile immunity. Several proteins have been investigated, including circumsporozoite protein (CSP) (Alonso *et al.*, 2004) and sporozoite protein thrombospondin-related adhesion protein (TRAP) (Gantt, *et al.*, 2000). For sexual stage vaccines, antibodies would be ingested together with the gametocytes during the mosquito's blood meal, so that target antigens can be specifically expressed during the sexual replication in the gut of the vector, to block further transmission of the disease. Antibodies to the recombinant vaccine candidate antigen Pfs28 and Pfs25 have also been reported to block transmission (Duffy & Kaslow, 1997; Gozar *et al.*, 2001). As for blood stage vaccine candidates, their target is either parasite expressed epitopes exposed on the extracellular merozoite or epitopes exposed at the surface of

PRBCs. Targeting the PRBCs is often referred to as anti-disease vaccines, since they would optimally inhibit sequestration and hence reduce the severe clinical manifestations.

PfEMP-1 is a major parasite virulence factor that undergoes antigenic variation to promote parasite survival in the host. Despite antigenic variation, it is encouraging that epidemiological data indicate that immunity against severe malaria is partly due to the acquisition of anti-PfEMP-1 antibodies, blocking the growth of many variants (Bull *et al*., 1998b; Bull *et al*., 2002). The advantage of a PfEMP-1 vaccine is that the molecule is exposed on the surface for more than 30 hours, which makes it an attractive target for antibodies. However, the highly variant nature of this molecule renders successful vaccine developments a challenging task.

Most of *P. falciparum*-infected erythrocytes bind to CD36 through CIDR1α domain, making it one of the main elements in cytoadherence (Hasler *et al*., 1990; Ockenhouse *et al*., 1991). It has been shown that immunization with recombinant CIDR1α (rCIDR1α) in *Aotus* monkeys delayed the time to onset of parasitemia when PRBCs in the inoculum (FVO1) were predominantly of the same PfEMP-1 type as the vaccine. Also, it was observed that the rCIDR1α-immunized monkeys did not develop anemia compared to the control monkeys. But rCIDR1α-immunized monkeys were not protected against high parasitemia levels, and all monkeys required the same treatment as the control monkeys (Makobongo *et al*., 2006). In another study, immunization of mice with plasmid DNA

expressing the CIDR1α domains of PfEMP-1 of three different parasite strains leads to the production of cross-reactive antibodies. This cross-reactivity was greatly enhanced by boosting with recombinant proteins from of three constructs (Baruch *et al*., 2003; Gratepanche *et al*., 2003). All this evidence indicates that CIDR1α domains are attractive targets for the development of a vaccine against cytoadherence in malaria.

1.8 Aims of the research

CIDR1α domains are potential candidates for vaccine development against malaria provoked by *P. faciparum*. However, this domain is far from being well characterized and its 3D structure is still unknown. Moreover, the exact determinants of CD36 binding are still unclear. Our long term aim is to conduct structural studies of CIDR domains to explain its adhesion properties at the molecular level.

In this research, we aim at:

1. Expressing several CIDR1α domains from *P. falciparum* clone 3D7 in a functional form.

2. Characterizing CIDR domains using biophysical methods (CD, 1DNMR).

3. Mapping the important region(s) responsible for CD36 binding using site-specific mutagenesis studies.

4. Determining the inhibitory effects conferred by murine polyclonal antibodies against this region(s).

CHAPTER 2: Experimental strategy and methods

2.1 Sequence alignment of CIDR1α domains from *P. falciparum* clone 3D7

The MC-r179 sequence was used to align similar sequences in *Plasmodium falciparum* clone 3D7 which was deposited in the Genebank database. Fourteen amino-acid sequences corresponding to CIDR1α domains of *Plasmodium falciparum* clone 3D7 were aligned with MC-r179 using program CLUSTALW, with some manual modifications to align conserved cysteines. Program NNPREDICT (http://www.cmpharm.ucsf.edu/~nomi/nnpredict.html); ProdictProtein (http://cubic.bioc.columbia.edu/predictprotein/) and Jpred (http://www.compbio.dundee.ac.uk/~www-jpred/) were used to predict the secondary structures of all CIDR1α domains.

2.2 Cloning of CIDR1α and MBP-DBPv proteins

2.2.1 Cloning of CIDR1α domain constructs for expression in *E.coli* and insect cells

2.2.1.1 Cloning of CIDR1α domain constructs for expression in *E.coli*

All PCR reactions were performed using genomic DNA of *Plasmodium falciparum* clone 3D7 as template. Primers used were: 5'-AATTAATCATATGTGTGTACTACAAAATGA-3' and 5'-AATCTCGAGAGGGGTATTTTCGCAT-3' for CIDR-f:1-177 (accession number: NP_700879, amino-acids residues 574-751); 5'-

ATTTACATATGAAGGAAGAAAAAAGTATGC-3' and 5'-AATCTCGAGAGGGGTATTTTCGCAT-3' for CIDR-f:11-177 (accession number: NP_700879, amino-acids residues 584-751); Primers 5'-CTAGCTAGCGGCGCGGAAAAAATA-3' and 5'-TATCTCGAGCTGGGAAGAGGAACATGC-3' for CIDR 1640w (accession number: NP_703663, residues 570-731). To compare the binding activity of CIDR-f with MC r179 (Brauch *et al.*, 1997), we also constructed a plasmid encoding GST-CIDRf-His_6 protein, which has the exact boundary as r179 based on the alignment and can be expressed as a N-terminal GST fusion and C-terminal 6-histidine tag protein. Primer 5'ATGGATCCGTGAAGAAAAAAGTATGCACTATCATCC3' and 5'ATTACTCGAGTCAGTGGTGGTGGTGGTGGTGTGTTTGGGAGC GGACTCCAGGGGTATT3' were used to perform PCR reaction.

PCR reactions were performed using the *Taq* polymerase (Fermentas) by heating the reaction mixture at 95 ºC for 3 minutes, followed by 30 cycles at 95 ºC for 45 seconds. Subsequently, an annealing and an elongating step were carried out at 50 ºC and at 68 ºC for 45 seconds and 1 minute, respectively. After 30 cycles, a final elongation step at 68ºC was performed for 10 minutes.

PCR reaction formula is listed below:

Name	Volume (µl)
ddH2O	41.4
10X Buffer with $MgCl_2$	5
dNTP mixture (200 µM)	0.4
Forward Primer (10 pmol/µl)	1
Reverse Primer (10 pmol/µl)	1
3D7 Genomic DNA (50 µg/µl)	1
Taq DNA polymerase (5 U/µl)	0.2

The pET-24a vector (Novagen) encoding a C-terminal hexa-histidine tag, was digested by the restriction enzymes NdeI and XhoI. The pGEX-5X-1 vector (Amersham) encoding a N-terminal GST protein, was digested by the restriction enzymes BamHI and XhoI. Purified PCR products were ligated with digested pET-24a plasmid or pGEX-5X-1 plasmid and transformed into DH5α competent cells.

2.2.1.2 Cloning of CIDR1α domain expression constructs for expression in insect cells

CIDR-f:11-177 (C-terminal 6-Histidine tagged protein) was cloned into the baculovirus transfer vector pVL1392 using primer 5'ATTAGATCTATGAAGGAAGAAAAAAGTATGC3' and 5'TATTCTAGATTAATGGTGATGATGGTGATGAGGGGTATTTTC GCATTTGTCTGG3'. Cotransfection with the vector pVL1392 and linearized baculovirus (*Autographica californica* multiple nuclear

polyhedrosis virus, AcMNPV) DNA was carried out as described by the manufacturer using the BaculoGold kit (BD Biosciences) and the infected *Spodoptera frugiperda* (Sf9) cells were maintained in a serum-free medium SF900 II (Gibco, USA) insect medium supplemented 1% penicillin-streptomycin (Invitrogen).

2.2.2 Cloning of the MBP-DBPv fusion protein

The full length Duffy-binding protein region II gene (accession number: AAZ81536, amino-acids residues 214-521) was sub-cloned from the plasmid pEGFP-HSVgD1-PvDBPII (kindly provided by Prof. John Adams, University Notre Dame, USA) into the pMAL-c2x-C-his6 vector [(pMAL-c2x (New England Biolabs) modified by adding a six-histidine tag at the C-terminus] between BamHI and HindIII sites using forward primer 5'-TAGAATTCATGAAAAACTGTAATTA-3' and reverse primer 5'-ATTAAGCTTTTATGTCACAACTTCCTGAG-3'. The construct was named MBP-DBPv. After screening and sequencing, the positive clone was transformed into *E. coli* strain BL21 (DE3) for protein expression.

2.3 Site-directed mutagenesis and domain swapping of CIDR1α

All mutations were performed using the Quick-change Site-Directed Mutagenesis Kit (Stratagene) according to the manufacturer's instructions. Briefly, the wild type DNA templates were purified (Qiagen) and replicated by PCR with the Turbo *Pfu*

polymerase (Stratagene) using the following parameters: 95ºC for 30 seconds followed by 16 cycles at 95ºC for 30seconds, 50ºC for 45 seconds and 72ºC for 7 minutes. A final elongation step was performed at 72ºC for 10 minutes. The PCR products were digested with Dpn I (Stratagene) at 37ºC for 2h and transformed into SuperBlue XL-1 competent cells (Stratagene). Domain swapping between proteins PFE1640w and CIDR-f:11-177 was performed by means of double-PCR overlapping method. All mutants were confirmed by sequencing. The list and nomenclature of mutations and primers used are listed in **Table 2. 1.**

CIDR f mutant	Sequence(5'-3')
CIDR-f: 11-133	**F:** ATTTACATATGAAGGAAGAAAAAAGTATGC **R:** ATTCTCGAGTTCATTTTCCTTTTCC
CIDR-f: 11-116	**F:** ATTTACATATGAAGGAAGAAAAAAGTATGC **R:** ATTCTCGAGTCCATAAGTATCTTTAATATTTG
CIDR-f: 117-177	**F:** ATTACATATGAATGTAAAGGAATTAGAAG **R:** AATCTCGAGAGGGGTATTTTCGCAT
CIDR-f: 133-177	**F:** ATTACATATGAATGTAAAGGAATTAGAAG **R:** ATTCTCGAGTCCATAAGTATCTTTAATATTTG
1640-f chimera	**F1:**CTAGCTAGCGGCGCGGAAAAAATA **R1:**CTAATTCCTTTACATTTTTAGAAGACTCAATT **F2:**AATTGAGTCTTCTAAAAATGTAAAGGAATTAG **R2:** AATCTCGAGAGGGGTATTTTCGCAT
f-1640 chimera	**F1:** ATTACATATGAATGTAAAGGAATTAGAAG **R1:** GCACTTTCTGAATCTTTAATTCCTTCATTTC **F2:** GAAAGACTTAGAAATTAAGGAAGTAAAC **R2:** TATCTCGAGCTGGGAAGAGGAACATGC
DeleGFSIFG	**F:**TAAAAAACAAGGAAATGATTATAATTATGCTC TTAAAGC **R:**GCATAATTATAATCATTTCCTTGTTTTTTAAAA TGCTG
Dele EQEA	**F:**GGAAAATGAAAATAATTCTGGTGGCAATAACA GTC **R:**GTTATTGCCACCAGAATTATTTTCATTTTCCTT TTCC

Table 2. 1. Primers used in the site-directed mutagenesis and domain swapping studies.

2.4 Protein expression and purification

2.4.1 Expression and purification of CIDR1α domains

2.4.1.1 Expression and purification of Histidine-tagged CIDR1α domains

CIDR-f:1-177, CIDR-f:11-177 and all mutant constructs were transformed into *E. coli* Rosetta-gami (DE3) cells (Novagen) and subjected to the same procedures described below. Cells were grown at 37°C shaking until OD_{600}=0.6. Protein expression was induced by the addition of a final concentration of 0.2 mM isopropyl-β-D-thiogalactopyranoside (IPTG), followed by overnight incubation at 20ºC before harvesting the cells. Cells were disrupted by sonication in the lysis buffer (20 mM sodium phosphate, 0.5 M NaCl, 5 mM β-mercaptoethanol, 40 mM imidazole, pH7.4). Protein was subjected to a 3-step purification protocol before proceeding with functional assays and crystallization trials (**Figure 2. 1**). After centrifugation at 30,000 g for 30 minutes, the soluble fractions were passed through HisTrap HP column (Amersham) and eluted using a linear imidazole concentration gradient of 40 mM to 500 mM at 4ºC. The eluted fractions were pooled and analyzed by SDS-PAGE gel. Following buffer exchange to 20 mM Tris-HCl, 50 mM NaCl, 2 mM DTT, pH8.5, the samples were loaded onto a HiPrep QFF column (Amersham) pre-equilibrated with the same buffer. Proteins were subsequently eluted using a linear NaCl concentration gradient of 0 to 1 M and the fractions were checked by SDS-PAGE. Pooled and concentrated proteins were then loaded onto a Superdex 200 GL

column (Amertham) pre-equilibrated with 20 mM Tris-HCl, 200 mM NaCl, 2 mM DTT, pH 8.5. The apparent molecular size of CIDR-f:11-177 was determined using the Low Molecular Weight calibration kit (Amersham). The molecular mass of purified proteins was confirmed by electron spray mass spectroscopy.

2.4.1.2 Expression and purification of GST-CIDR f

The GST-CIDRf fusion protein was induced in *E. coli* BL21 (DE3) by the addition of a final concentration of 0.4 mM isopropyl-β-D-thiogalactopyranoside (IPTG), followed by overnight incubation at 25ºC before harvesting the cells. The protein was purified by affinity chromatography using glutathione sepharose beads, according to the manufacturer's protocol.

2.4.1.3 Expression and purification of CIDR-f:11-177 in insect cells

For insect cell expression, the High Five insect cells were infected by high-titre recombinant virus, which was amplified three times in sf9 cells, and shook for 48 hours at 27°C. The cells were harvested and solublized by sonication. Subsequently, the supernatant was purified by Ni-NTA, ion-exchange, and gel-filtration chromatography.

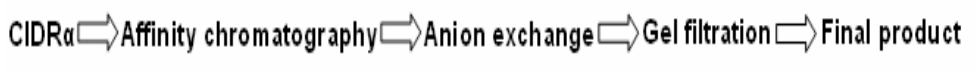

Figure 2. 1. Flowchart of CIDR1α purification protocol.

2.4.2 Expression and purification of MBP-DBPv fusion protein

The bacteria were grown in the LB media supplemented with 0.2% glucose at 37ºC until the optical density of wavelenghth 600 (OD_{600}) reached 0.6. Protein expression was induced by adding a final concentration of 0.5 mM IPTG. After 3 hours of incubation at 30ºC, cells were harvested by centrifugation at 7000g for 10 minutes. Subsequent procedures were performed at 4ºC with all buffers and rotors prechilled to 4ºC. Cells were resuspended in lysis buffer (20 mM Tris-Cl, 200 mM NaCl, 1 mM EDTA, pH7.4) and lysed by 30-minutes sonication (pulse of 6 seconds interspersed by 9 seconds). The lysate was clarified by centrifugation at 30,000g for 30 minutes.

The supernatant was loaded onto a Econo-column (Bio-Rad) packed with 5ml of amylose resin (NEB) previously equilibrated with 40ml of washing buffer (20 mM Tris-Cl, 50 mM NaCl and 1 mM EDTA, pH7.4) and incubated overnight at 4ºC on a rocking platform. The column was washed 3 times with 25 ml of buffer and the fusion protein eluted by 10 ml of elution buffer (20 mM Tris-Cl, 50 mM NaCl, 1 mM EDTA and 10 mM maltose, pH7.4) at 4ºC. Analysis of the fractions was done with SDS-PAGE using Coomassie blue staining. A major protein of about 79.5 kDa was eluted which corresponds to the total molecular weight expected for the recombinant MBP-DBPv fusion protein. Eluted samples containing approximately 80-90% purity band in SDS-PAGE gel were pooled and concentrated by ultrafiltration at 3000g (Centricon 10K MWCO,

Vivascience). The final concentration was measured by Bradford method using IgG (Bio-rad) as a standard.

2.4.3 Expression and purification of GST fusion proteins for raising antibodies in mice

In order to raise antibodies against the C-terminal end of CIDR-f:11-177, we made two constructs that were fused at its N-terminus to the GST protein and expressed them in *E. coli*. One is CIDR-f:117-177, the other is CIDR-f:133-177 which has a deletion in the region NVKELE from above CIDR1α portion (**Figure 3. 14**). Both fusion proteins were well expressed in *E. coli* and purified by affinity using glutathione sepharose beads, according to the manufacturer's protocol.

2.4.4 Construction of CD36 chimeric protein

A recombinant soluble human CD36 encompassing residues from Gly-30 to Asn-439 (fused with a human IgG1 Fc fragment at its C-terminus, hereafter named CD36/Fc) was purchased from R&D systems (USA) and used for all binding experiments (**Figure 2. 2**). The recombinant human CD36/Fc is a disulfide-linked homodimeric protein. The schematic representation of CD36/Fc structure is shown in **Figure 2. 3**.

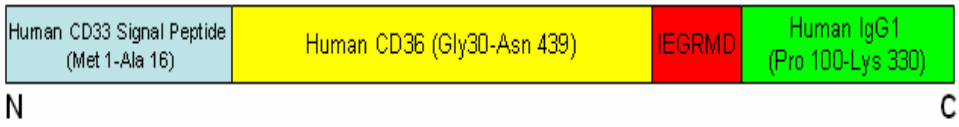

Figure 2. 2. Schematic representation of CD36/Fc protein.

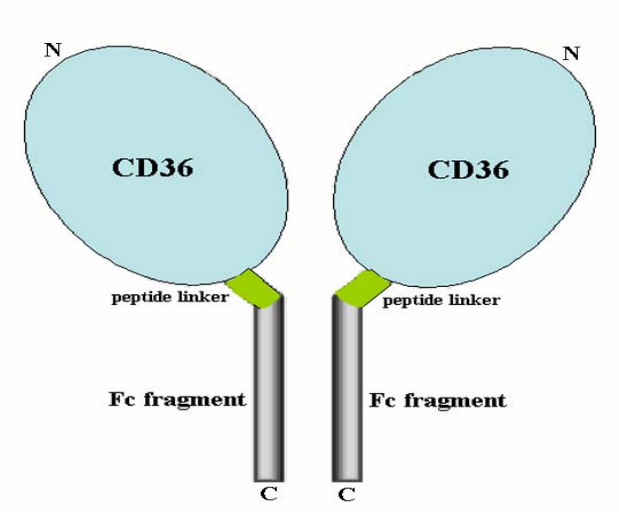

Figure 2. 3. Schematic representation of CD36/Fc structure. Two CD36 molecules are fused with Fc fragement of human IgG1 through short peptide linker IEGRMD and form a homodimeric protein.

2.5 CD and 1D ^{1}H NMR spectroscopy analyses of the CIDR1α domain

Circular Dichroism (CD) experiments were carried out using a ChiraScan CD Spectrophotometer (Applied Photophysics) with a 1 mm quartz cell at room temperature. Spectra were collected using wavelengths ranging from 190 nm to 260 nm with steps of 0.1 nm. All proteins were dissolved in PBS buffer at pH 7.4 to a final

concentration of 0.4-0.5 mg/ml. CD spectra were corrected by subtracting the spectrum obtained from the buffer solution.

For one dimensional ^{1}H NMR spectroscopy, a 500 µl of solution containing the CIDR-f:11-177 protein at a concentration of 200 µM was prepared in an aqueous buffer containing sodium phosphate buffer, 50 mM NaCl, 1 mM DTT at pH 6.0 and 10% D_2O (v/v). The NMR spectra were collected at 285 K on an Avance600 spectrometer (Bruker, Billerica, MA). The spectra were processed and analyzed with the program ZGGPW5 (Bruker).

2.6 ELISA-based CD36 and CIDR1α binding assay

2.6.1 ELISA-based CD36 and CIDR1α direct binding assay

A ELISA-based binding assay was used for evaluating the binding activity of CIDR1α to the human CD36/Fc protein which was coated at a concentration of 0.2 µg/ml on a MaxiSorp Immuno 96-wells plate (NUNC) overnight at 4ºC. After 2 hours blockage in PBS containing 1% (w/v) BSA and 0.3% (v/v) Tween-20, a range of concentrations of purified CIDR1α proteins or mutants thereof were incubated for 1 hour at 37ºC. The amount of CIDR-f:11-177 bound to the immobilized CD36/Fc protein adsorbed on the well was then detected using a mouse Penta-His antibody (Qiagen), followed by an alkaline phosphatase (AP) conjugated goat IgG specific for mouse Fab (Sigma). After 1 hour of incubation at 37ºC and washing, the Immuno Pure (P-nitrophenyl Phosphate Disodium Salt PNPP tablets,

Pierce) dissolved in diethanolamine buffer was added to the well and the resulting absorbance at 405 nm was read using a microplate spectrophotometer (Bio-Rad).

The schematic procedure of CD36/Fc and CIDR1α direct binding assay is shown in **Figure 2. 4**.

2.6.2 Peptide inhibition assay

All peptides were synthesized by the Fmoc method using an automatic peptide synthesizer (Intavis AG, Bioanalytical instruments) and purified by High-performance liquid Chromatography (HPLC) (Shimadzu) using a C8 column (Agilent). The peptide sequences were confirmed by mass spectrometry. After pre-incubation of CIDR-f:11-177, 1640-f chimera, f-1640 chimera or CIDR 1640w proteisn at a constant concentration of 2 μg/ml with peptide concentrations ranging from 10 nM to 1 mM for 1 hour at room temperature, the mixtures were added to a 96-well plate which had been previously coated with CD36/Fc (0.2 μg/ml) overnight at 4°C and incubated for 2 hours at 37 ºC. The amount of CIDR-f:11-177 bound to the immobilized CD36/Fc protein detected using a mouse Penta-His antibody, followed by an AP conjugated anti mouse antibody. After 1 hour of incubation, the PNPP substrate was added and the resulting absorbance at 405 nm was read using a microplate spectrophotometer (Bio-Rad).

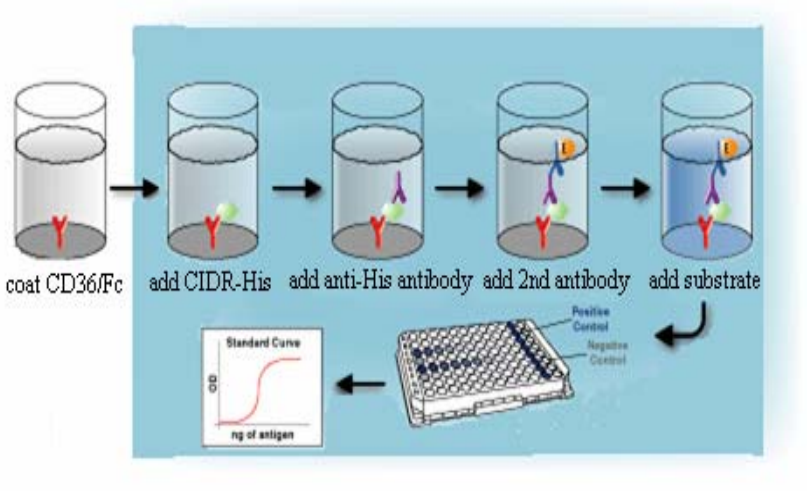

Figure 2. 4. ELISA-based CD36/Fc and CIDR1α direct binding assay. CD36/Fc was coated on the 96-well plate overnight at 4°C. Serial diluted CIDR-f:11-177 proteins (or mutants) were added to the plate and incubate for 1 hour. After mouse anti-his antibody (primary antibody) and anti-mouse AP conjugated antibody (secondary antibody) was added to the plate, binding was detected by adding AP substrate and read at an OD of 405 nm.

2.7 Generation of polyclonal antisera against the C-terminus of CIDR-f

2.7.1 Generation of antibodies

Two purified GST fusion proteins (50 µg per mouse), one GST fused with CIDR-f:117-177, the other is GST fused with CIDR-f:133-177, were injected into male BALB/C mice 7-8 weeks old with Complete Freund's adjuvant (Pierce) for the first injection and in Incomplete Freund's adjuvant (Pierce) for the subsequent injections

(Harkins *et al.*, 2000). Blood was drawn from the animals two weeks after each boost and tested for antibody titre by ELISA (Doolan *et al.*, 2001) and Western Blotting (Doolan *et al.*, 2001) on 96-wells polystyrene plates.

2.7.2 ELISA and Western blotting analyses of polyclonal antibodies

5 µg of each CIDR-f:11-177, chimera and CIDR 1640w:12-172 (**Figure 3. 14**) were loaded on a 12% SDS-PAGE gel and separated by electrophoresis. Proteins were transferred to a PVDF membrane (Bio-rad) and blocked with TBST (20 mM Tris-HCl, 150 mM NaCl, 0.01% Tween 20, pH7.4) supplemented with 5% (w/v) of non-fat dry milk for 1 hour at room temperature. The membranes were incubated with mouse anti GST-CIDRf:117-177 and GST-CIDRf:133-177 polyclonal sera at 1:1000 dilution overnight at 4°C. After washing 3 times with TBST, horseradish peroxidase (HRP)-conjugated goat anti-mouse secondary antibody (Pierce) was used at dilution of 1:2000 and incubated with the membrane for 1 hour at room temperature. After washing 3 times with TBST, chemiluminescence (ECL) substrate (Amersham) was added and images were detected using Kodak processor.

2.8 Immunofluorescence microscopy

Fixed-cell immunofluorescence assay (IFA) was conducted with 20% parasitemia (clone 3D7) blood smear onto a glass slide. Blood

cells were fixed with acetone for 5 minutes and air dried. Anti-serum against GST-CIDRf:117-177 was used as primary antibody at a dilution of 1:200 and pre-immunized sera and anti-GST sera were used as negative control at the same dilution. The slides were incubated in the dark with sera in the humid box at room temperature for 60 minutes, followed by 3 times wash with PBS. Goat anti-mouse FITC-conjugated IgG (Jackson ImmunoRearch Laboratories) was then incubated with the slides at the dilution of 1:100 for 30 minutes at room temperature. After washing 3 times, the slides were stained with 4', 6-Diamidino-2-phenylindole dihydrochloride (DAPI) (Sigma) and mounted using a fluorescence mounting medium Citifluor (DAKO). The imagines were visualized by using an inverted fluorescence microscopy (Olympus).

To further demonstrate that the polyclonal antisera can recognize surface expressed PfEMP-1, Liquid-phase immunofluorescence microscopy (L-IFA) was performed. After 3 washes of mature-blood stage infected erythrocytes with culture medium without Albumax, the PEs were incubated with polyclonal antisera against CIDR-f: 117-177 at dilution 1:20 to 1:50 at 4°C for 30 minutes. The PEs were then washed 3 times with PBS, and incubated at 4°C for an additional 30 minutes with a FITC-conjugate goat anti-mouse antibody (Jackson immunoresearch laboratory). Preimmunized sera and anti-GST antibody were used as negative control. Vectorshield mounting medium with Dapi (Vector

laboratories) was applied to the slides. Immunofluorescence staining was analyzed with Olympus fluorescence microscope.

2.9 Polyclonal antisera inhibit the interaction between CIDR-f and CD36

A procedure similar to the peptide inhibition assay described in section 2.6.2 was used to evaluate the inhibition effect by the antisera on the interactions between CD36/Fc and CIDR-f:11-177. Human CD36/Fc protein was coated at a concentration of 0.2 µg/ml on a MaxiSorp Immuno 96-wells plate (NUNC) overnight at 4ºC. After pre-incubation for 2 hours at room temperature of constant concentration of CIDR-f:11-177 (4µg/ml) with serial dilutions of two antisera ranging from 1:8 to 1: 1024, the mixtures were added to a 96-wells plate and incubated for 2 hours at 37 ºC. The amount of CIDR-f:11-177 binding to the plate was detected using a Penta-His antibody conjugated with HRP, followed by addition of HRP substrate O-Phenylenediamine Dihydrochloride (OPD) (Sigma) and reading at an OD of 492 nm. A pre-immune serum, an anti-GST serum and an irrelevant polyclonal serum directed against unrelated rhoptry protein of *P. falciparum* were used as negative controls.

2.10 Mammalian cell culture and Parasites culture

Human lung endothelial cells (HLECs) expressing CD36 at the cell surface (donated as HLEC-CD36) and Chinese hamster ovary K1

cells (CHO-K1), transferred CHO cells expressing CSA at the cell surface (donated as CHO-CSA) were cultured using RPMI 1640 medium with 10% FBS (kindly provided by University of Heidelberg). Three *Plasmodium falciparum* strains, 3D7, HB3 and FCR3 were grown in human erythrocytes from malaria-negative donors with daily changed RPMI media under standard conditions as described previously (Pouvelle *et al*., 1998) replacing 10% human serum with 2.5% Albumax. Highly synchronized parasites in mature blood stage-infected erythrocytes of the CD36 or CSA adhesive phenotype were obtained by regular panning on HLECs or CHO-K1 cells as described elsewhere (Pouvelle *et al*., 1997).

2.11 Western Blotting of parasites extracts

Parasites were cultivated to late trophozoite-schizont stages and extracted as described previously (Florens *et al*., 2004). The extracted mature-stage parasites were lysed directly into sample buffer and frozen-thawed 3 times. The supernatant were used for SDS-PAGE electrophoresis using 4% to 12% NuPAGE gradient gel (Invitrogen). After the proteins were transferred onto nitrocellulose membranes, polyclonal antisera against CIDR-f: 117-177 were used to detect the expression of PfEMP-1 at the dilution of 1:200, followed by secondary antibodies and enhanced chemiluminescence (Pierce) as described in section 2.7.2.

2.12 PE inhibition assay using recombinant proteins and polyclonal antisera

HLECs-CD36 and CHO-K1-CSA cells were cultured in 48-well plate for at least 3 days to approximately 80% confluence before performing the assay. The PEs to be assayed were fractionated on a Percoll gradient to yield about 95% late stage PEs. These PEs were diluted in the binding buffer (RPMI 1640/HEPES, 10% FBS, pH 6.8) at the concentration of $5x10^6$/ml were incubated with different dilutions of polyclonal antisera against CIDR-f: 117-177 for 30 to 45 min at room temperature before adding to HLEC-CD36/CHO-K1-CSA cells. HLECs-CD36/CHO-K1-CSA cells incubated with different recombinant proteins from concentration 1.5μM to 12μM for 30 min at RT before adding parasites. After 60-min incubation with gentle rocking, the plate was washed 3-4 times and fixed using 2% glutaraldehyde. The average number of PEs bound to 100 HLEC-CD36/CHO-K1-CSA cell for three (40x) microscopic fields were calculated and the percentage inhibition of parasite binding compared to the untreated control without adding any antibodies or proteins were determined. Each assay was triplicated.

2.13 Crystallization trials of CIDR1α

CIDR-f:11-177 and CIDR 1640w proteins were screened for crystallization conditions using Hampton Crystal screen Kit 1, 2 and PEG/ION screen (Hampton Research) at concentrations of 20 mg/ml, 10 mg/ml, 5 mg/ml and 3mg/ml, respectively. 1 μl of protein

solution was mixed with 1 µl of the reservoir solution using the hanging-drop vapour diffusion method and incubated at 18°C.

CHAPTER 3: Results and Discussion

3.1 Sequence alignment of CIDR1α domains

This study aimed to characterize several CIDR1α domains derived from the clone 3D7 of PfEMP-1, whose complete genome sequences have been reported (Gardner *et al.*, 2002). Thus, 14 different CIDR1α domains were chosen and expressed individually in *E. coli*. All these fourteen CIDR1α domains showed 20-30% sequence identities to MC-r179 (**Figure 3. 1**). A sequence alignment of the MC r179 with the five proteins that could be successfully expressed in *E. coli* (CIDR a, c, f, i, l) and one CIDR1α domain named PFE1640w from clone 3D7 which was demonstrated not to bind CD36 (Robinson *et al.*, 2003) is shown in **Figure 3. 2**. Regardless of their abilities to bind CD36, CIDR1α domains contain eight strictly conserved cysteine residues that have been sequentially numbered from 0 to 7 to match the nomenclature originally proposed by Baruch *et al.* (1997). The overall amino-acid sequence identities between five CD36 binders CIDR-f:1-177, CIDR-a, CIDR-c, CIDR-i and CIDR-l and the non CD36 binding CIDR 1640w:12-172 were 31.1 % , 24.1%, 25.3%, 24.7 % and 23.6 %, respectively. This was not much different from the overall sequence identity amongst the CD36 binders across the *P. falciparum* strains where identities ranged from 28.5% to 42%. Regardless of the low overall sequence identities between the CD36-binding and non-binding domains, the secondary structure prediction suggests a grossly conserved tertiary

structure between the various CIDR1α domains expressed in this study. Three secondary structure programs had been used and showed consistent secondary structure prediction. CIDR molecules contain four to five helices, with variations in their respective lengths. The exact location and lengths of the putative connecting loops are shown in **Figure 3. 2**. Interestingly, their N-terminal sequences, spanning residues 1 to 90 are more conserved than their C-terminal sequences (residues 91-177), including two long segments corresponding to the predicted helices 1 and 2 (**Figure 3. 2**). Consistent in all predictions is the indication that the secondary structure of CIDRα domain is mainly composed of α helices, which is consistent with spectra obtained from CD measurements (see below).

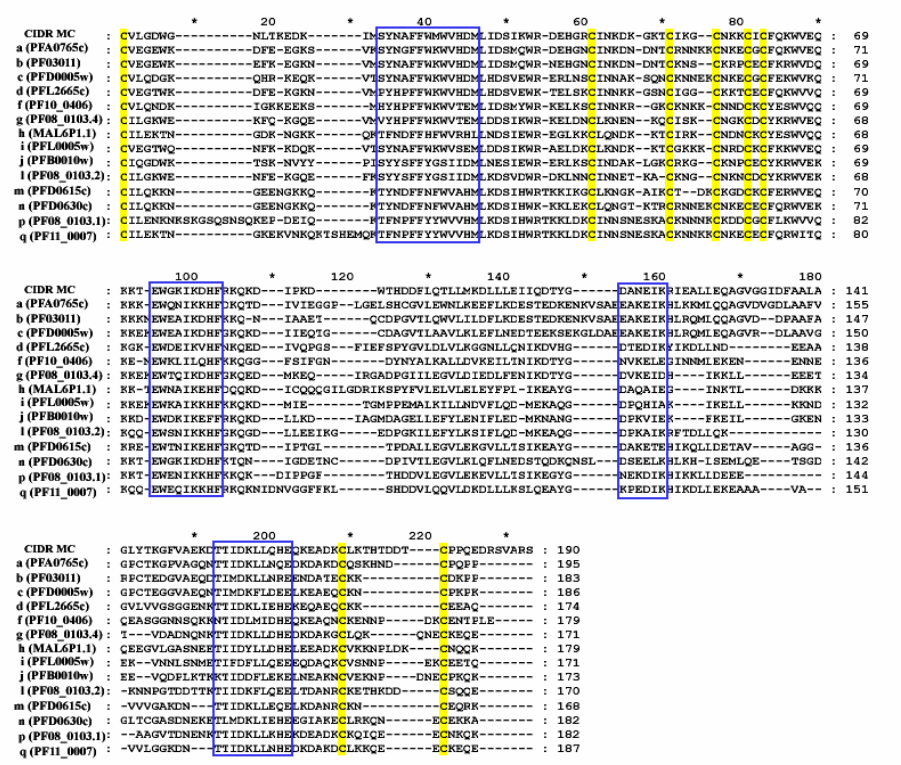

Figure 3. 1. Sequence alignment of 14 CIDR1α domains in *P. falciparum* clone 3D7. Accession number for each protein is: a: NP_703350.1, residues 598-793; b: NP_701891, residues 595-758; c: NP_702661.1, residues 622-807; d: NP_701891, residues 596-768; f: NP_700879, residues 574-751; g: NP_704544, residues 664-734; h: NP_703834, residues 543-711; i: NP_701366, residues 578-748; j: NP_472931, residues 574-746; l: NP_704464, residues 572-741; m: NP_702779, residues 655-822; n: NP_702780, residues 611-792; p: NP_704468, residues 632-813; q: NP_700880, residues 622-808. MC-r179 includes four conserved motifs: $CX_8CX_3CX_3CXC$, LEX(V/L)LXKXXLL, $GX_4IX(H/R)XX(L/M)LXXE$ and TTIDKXLXHE which are marked as blue rectangles. All cysteine residues are colored yellow.

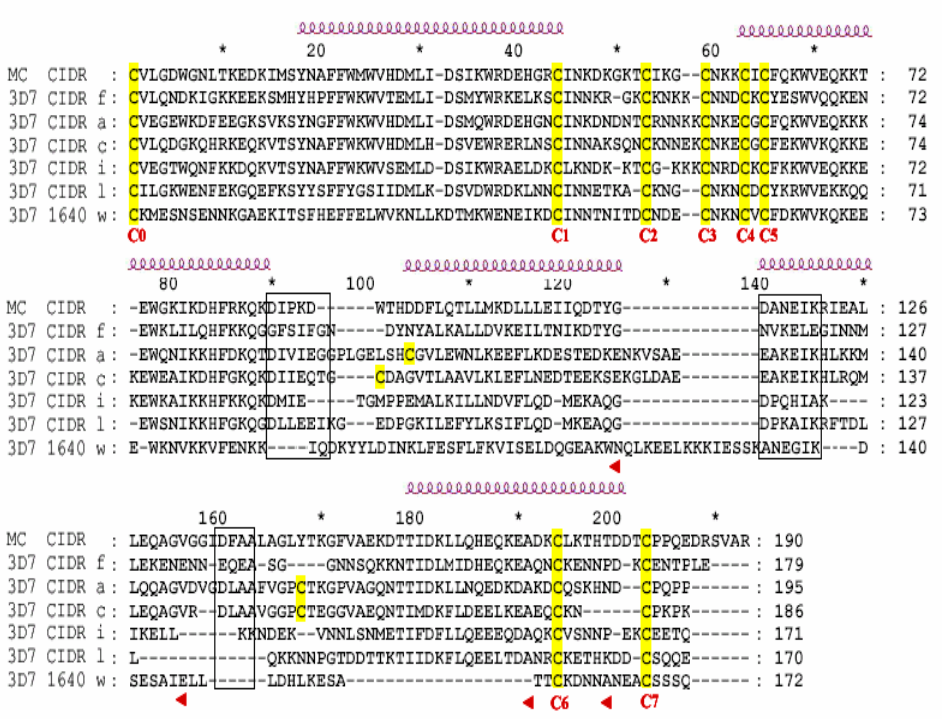

Figure 3. 2. Amino acid sequence alignment of CIDR1α domains from the clone 3D7 of *P. falciparum* and the MC strain. One CIDR1α domain from the MC clone and six CIDR1α domains from clone 3D7 which were used for further studies are included in the alignment: CIDR-f:1-177, PFE1640w (see Methods), CIDR a, CIDR c, CIDR i and CIDR l (See **Figure 3. 1**). The eight conserved cysteine residues are numbered from 0 to 7, in line with the convention introduced by Baruch *et al.* (1997). The five predicted α helices of CIDR-f:11-177 are represented by red helices.

3.2 Protein expression and characterization

3.2.1 Expression of CIDR1α domain and mutants

14 different CIDR1α domains were chosen and expressed individually in *E. coli*. However, 3 out of 14 CIDR domains (CIDR g,

CIDR J and CIDR n) did not yield any PCR products (**Figure 3. 3**) and the other 6 either failed to express in *E. coli* or were poorly soluble (CIDR b, CIDR d, CIDR h, CIDR m, CIDR p and CIDR q), thus their study was discontinued (**Figure 3. 4**). We chose one of the well expressed CIDR1α domains: CIDR-f in our later studies. The CIDR-f:11-177 wild type protein and all the mutants were purified using the same procedure. Three steps of protein purification (affinity purification, ion-exchange purification and size exclusion purification) by Fast Performance Liquid Chromatography (FPLC) were carried out **(Figure 3. 5**). All CIDR-f proteins had more than 90% purity as judged by SDS-PAGE analysis (**Figure 3. 7**).

GST-CIDRf fusion protein was purified by affinity chromatography and checked in 12% SDS-PAGE gel (**Figure 3. 7**).

CIDR-f:11-177 protein, named CIDR-f:11-177(Bac) was expressed in High Five insect cells and purified using similar three-step purification protocol. However, the final product only showed about 70% purity (**Figure 3. 8**).

A:

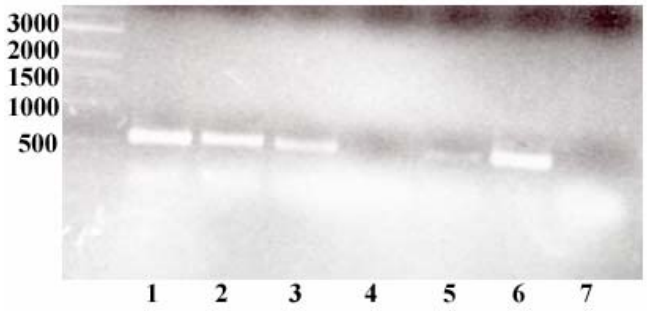

B:

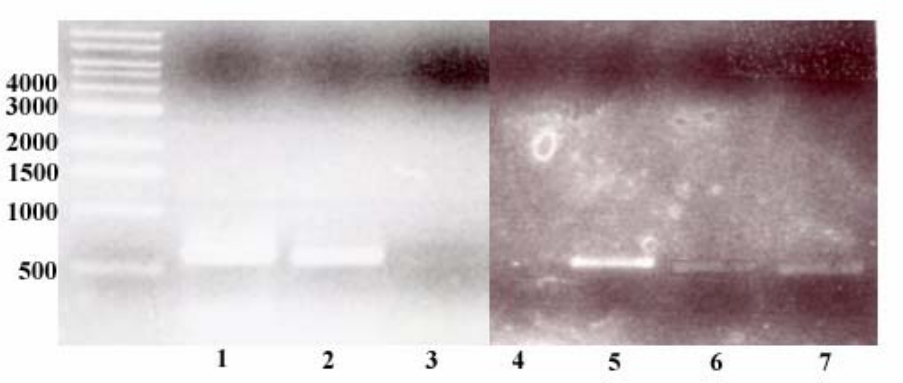

Figure 3. 3. PCR products of CIDR1α domains from *P. falciparum* 3D7 clone. PCR were performed using genomic DNA of *P. falciparum* clone 3D7 as templates. However, we only successfully obtained PCR products (around 500 base pairs) of the following proteins: 1: CIDR d, 2: CIDR f, 3: CIDR i, 5: CIDR l, 6: CIDR a in figure A and 1: CIDR b, 2. CIDR c, 3: CIDR h, 5: CIDR m, 6: CIDR p and 7. CIDR q in figure B; No PCR products were obtained for 4: CIDR j, 7: CIDR n in figure A and 4: CIDR g in figure B.

A:

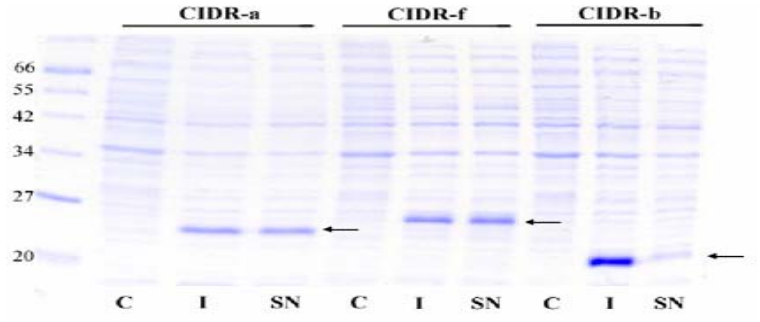

B:

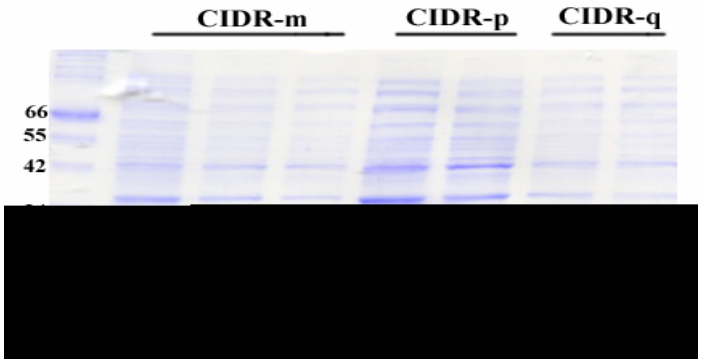

C:

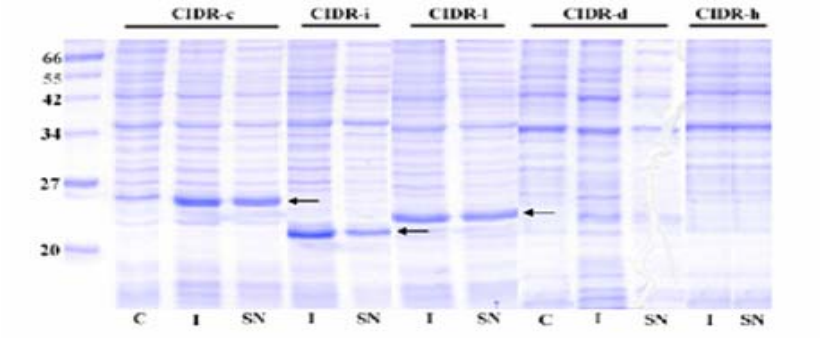

Figure 3. 4. Expression of eleven CIDR1α domains of *P. falciparum* clone 3D7 *in E. coli*. Different CIDR1α domains were induced using final concentration of 0.2 mM IPTG at 20°C overnight. Each sample was analyzed using SDS-PAGE gel. CIDR a, CIDR f (figure A),

CIDR c, CIDR i and CIDR l (figure C) were well induced and soluble in the solution (C: samples without addition of IPTG; I: induced sample; SN: supernatant), thus can be used for further experiments. However, CIDR b (figure A), CIDR m, CIDR p, CIDR q (figure B), CIDR d and CIDR h (figure C) either failed to express or were poorly soluble. The expressed CIDR domains were indicated by arrow.

A:

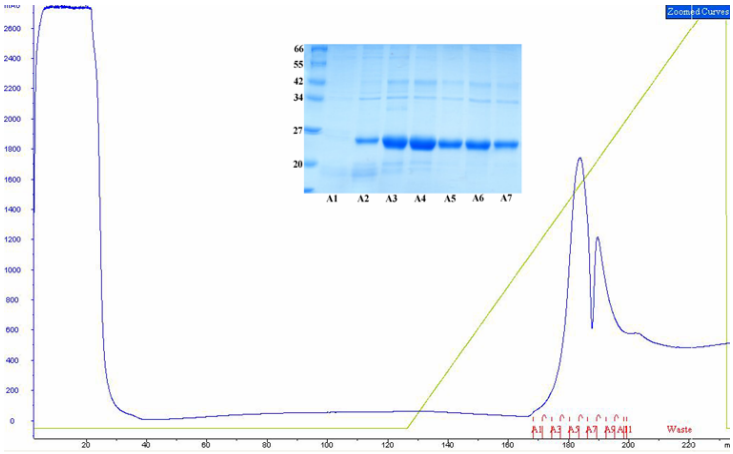

B:

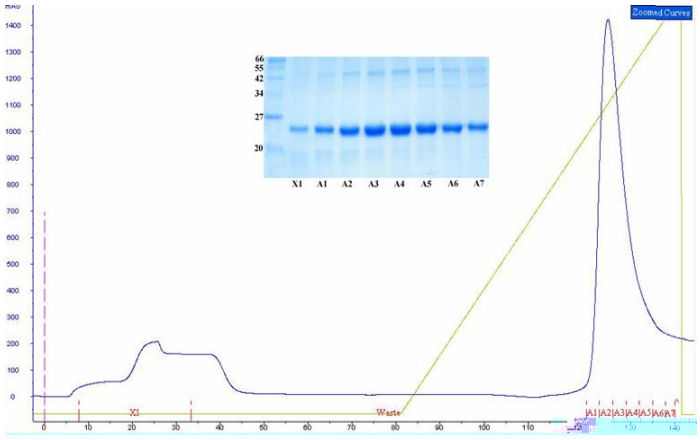

C:

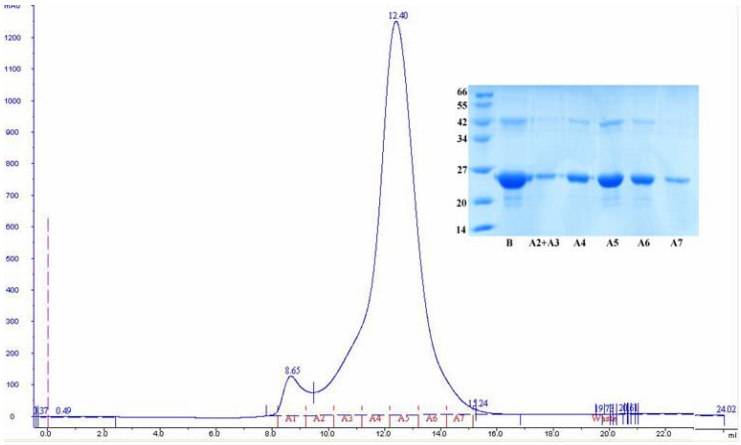

Figure 3. 5. Purification of CIDR-f:11-177 using FPLC. Soluble fractions of CIDR-f:11-177 were purified using HisTrap HP (figure A), HiPrep QFF (figure B) and Superdex 200 (figure C). Firstly, CIDR-f:11-177 was eluted at a concentration of about 250mM Imidazole using HisTrap HP column and fractions from the first peak (fractions from A1-A7 in figure A) were pooled and exchanged for a buffer containing 20 mM Tris-HCl, 50 mM NaCl, 2mM DTT, pH8.5. The sample was then loaded onto a HiPrep QFF column and eluted at a concentration of 700 mM NaCl (fractions from A1 to A7 in figure B). After exchanging for a buffer containing 20 mM Tris-HCl, 200 mM NaCl, 2 mM DTT, pH 8.5, the concentrated sample (around 400 µl) was then loaded onto a Superdex 200 GL column (fraction A2-A7 in figure C).

3.2.2 MBP-DBPv fusion protein expression and purification

Only about 40% of the total induced MBP-DBPv fusion protein was soluble even after lowering the temperature of induction to 16°C

using 0.02 mM IPTG. After affinity chromatography (amylose resin), about 90% purity of the recombinant MBP-DBPv protein were obtained for further experiments (**Figure 3. 6**).

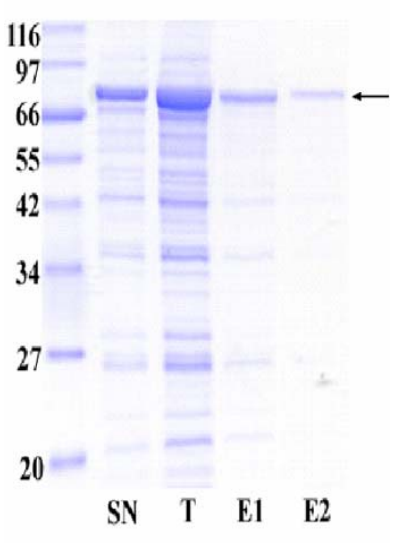

Figure 3. 6. Purification of MBP-DBPv fusion protein. After induction, the soluble fraction of MBP-DBPv fusion proteins indicated by black arrow was purified using an amylose resin. T: total cell after induction; SN: supernatant of MBP-DBPv fusion proteins before loading onto amylose column; E1: elution sample one, E2: elution sample two.

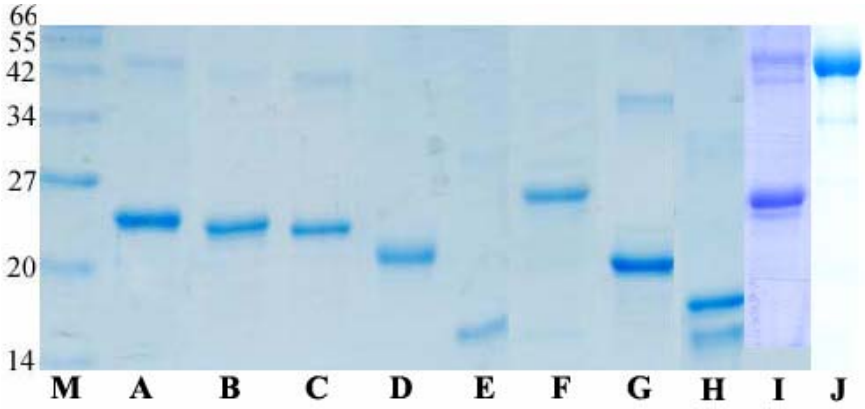

Figure 3. 7. Expression and purification of the CIDR1α mutants in *E. coli*. All proteins purified by affinity chromatography, HiPrep QFF and Superdex 200 column were separated on a 12% SDS-PAGE gel. M: molecular mass standard. A: CIDR-f:11-177; B: Dele GFSIFG; C: Dele EQEA; D: CIDR 1640w: 12-172; E: CIDR-f: 11-116; F: 1640-f chimera; G: f-1640 chimera; H: CIDR-f: 11-132; I: CIDR-f:1-177; J: GST-CIDRf.

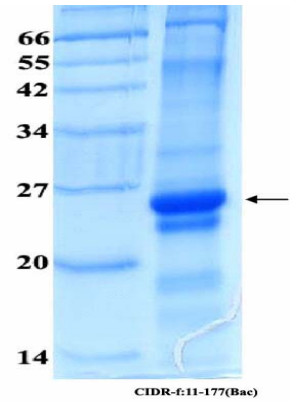

Figure 3. 8. Express and purification CIDR-f:11-177 in insect cells. Protein was expressed in High Five cells shaking for 48 hour at 28°C. Protein was purified by affinity chromatography, ion exchange and

gel filtration chromatography. Final purification product was shown in 12% SDS-PAGE gel and indicated by arrow.

3.2.3 Biophysical characterization of CIDR1α

3.2.3.1 Circular Dichroism spectrometry

Circular Dichroism (CD) is a common used biophysical tool to evaluate protein secondary structure and folding in solution. CD relies on the differential absorption of left and right circularly polarized radiation by chromophores which either possess intrinsic chirality or are placed in chiral environments. In far UV region (240-180nm), which corresponds to peptide bond absorption, the CD spectrum can be analyzed to give the content of regular secondary structural features such as α-helix and β-sheet. The CD spectrum in the near UV region (320-260nm) refects the environments of the aromatic amino acid side chains and thus gives information about the tertiary of the protein. The main advantages of CD is, compared with X-ray crystallography and NMR, it can be carried out rapidly; thus good quality spectra in the far and near UV can each be obtained within 30 min. The main limitation of CD is that it only provides relatively low resolution structural information. Although far UV CD can give reasonably reliable estimates of the secondary structure content of a protein, it must be noted that these are overall figures and do not indicate which regions of the protein are of which structural type. A further limitation of CD is that it gives little detailed information on the quaternary structure of proteins.

The CD spectra of CIDR-f:11-177 and CIDR 1640w:12-172 proteins showed a similar pattern with a maximum at 190 nm and two shallow minima at 208 nm and 222 nm (**Figure 3. 9**), regardless of their binding capacity to the CD36 analogue. These spectra are typical of proteins with a high content of α helices. This result also confirms that the CIDR1α domains which can bind to CD36 molecule (eg CIDR-f, CIDR-c and CIDR-i) share a common secondary structure with the CIDR1α domains which cannot bind to CD36 (eg CIDR1640w).

A:

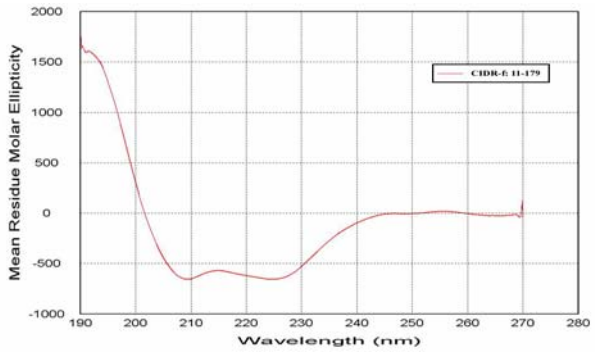

B:

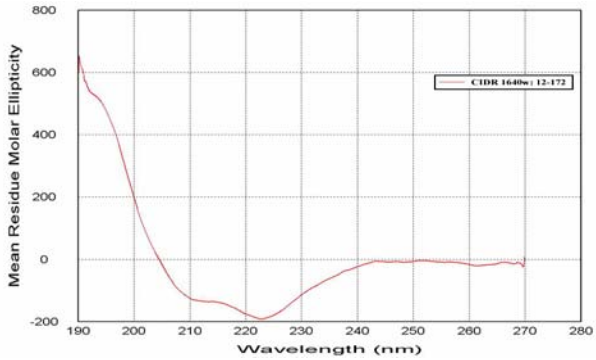

Figure 3. 9**.** CD spectra of CD36 binder vs non binder. The far UV CD spectra of CIDR-f:11-177 (A) and CIDR 1640w (B) both showed

a maximum at 190nm and two minima curves at 208nm and 222nm, indicating the presence of predominantly α-helix secondary structure.

3.2.3.2 1D ^{1}H NMR spectrometry

For further biophysical characterization of the recombinant CIDR1α domains, 1D ^{1}H NMR spectroscopy was used to check their folding state (Page *et al.*, 2005).

1D ^{1}H NMR is another biophysical method to evalutate protein folding in solution. When place in a magnetic field, NMR active nuclei (like ^{1}H, ^{13}C or ^{15}N) resonate at a specific frequency, dependent on strength of the magnetic field. Different protons in a molecule each resonate at slightly different frequencies depending on the local chemical environment. Because this frequency is dependent on the strength of the magnetic field, it is converted into a field-independent value known as the chemical shift. The chemical shift is reported as a relative measure from some reference resonance frequency. The difference between the frequency of the signal and the frequency of the reference is divided by frequency of the magnetic field to give the chemical shift. The units of chemical shift are parts per million (ppm). A typical methyl group, α-protons and amide protons have a shift around -0.5-1.5ppm, 3.5-6ppm and 6-10ppm, respectively. 1D ^{1}H NMR can be used to verify the protein folded state. It only needs 50-100μM purified protein and the spectra can be recorded within a few minutes. However, the reliability of 1D ^{1}H NMR to verify the folded state is limited by protein size and

possibly by multimerization state. Monomeric proteins of sizes up to 50kDa are good candidates for 1D ^{1}HNMR screening, but oligomerization can cause the data on such proteins to be more difficult to interpret.

1D ^{1}H NMR spectra of CIDR-f:11-177 protein showed a clear dispersion of resonance lines in the region of amide protons (between 6 and 10 ppm), and downfield-shifted methyl protons (-0.5-1.5 ppm) resonances, indicating at least partial protein was proper folding (**Figure 3. 10**). However, the spectra also confirmed a tendency of CIDR domains to oligomerize and/or to aggregate, as shown by a comparison with typical ^{1}H 1D NMR spectra obtained from a large group of proteins subjected to crystallization trials (Page *et al.*, 2005). Indeed, our crystallization assays with the current CIDR-f protein constructs have so far failed to yield crystals.

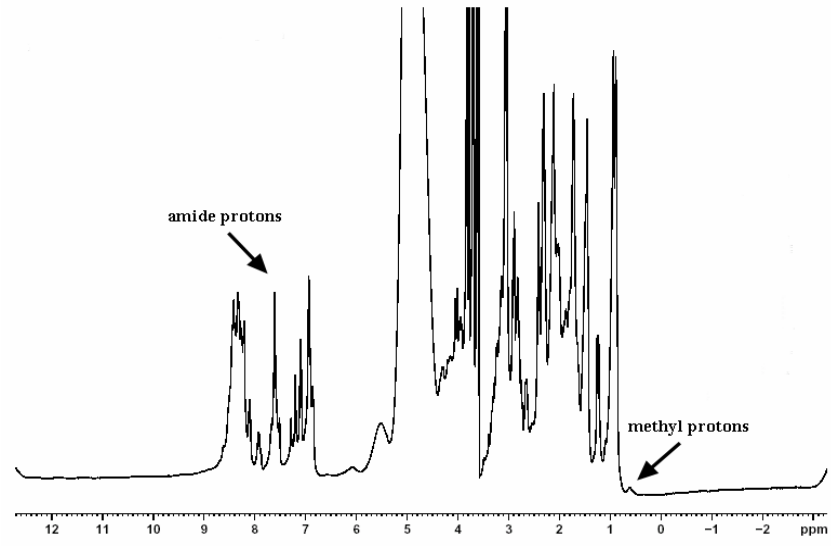

Figure 3. 10. 1D ^{1}H NMR spectra of CIDR-f:11-177. The NMR spectra of CIDR-f proteins showed a clear dispersion of resonance

lines in the region of amide protons (between 6 and 10 ppm), and downfield-shifted methyl protons (-0.5-1.5 ppm) resonances.

3.3 The recombinant CIDR-f proteins expressed in *E. coli* are functional

ELISA is a convenient and reliable method to evaluate protein-protein interactions in a semi-quantitative manner (Hans *et al.*, 2005). Using ELISA, CIDR-f:11-177 proteins showed strong binding activities with CD36/Fc in a concentration-dependent manner, while MBP-DBPv did not (**Figure 3. 11**). Using the same direct binding assay, strong binding of proteins CIDR-c and CIDR-i to coated CD36 molecules were also found (approximately 85% and 90% binding activities respectively compared to CIDR-f:11-177). The CIDR-f:1-177 binds to CD36 in a concentration dependent manner, while the negative control MBP-DBPv and CD36 non-binder CIDR 1640w:12-172 did not. Due to extensive degradation, CIDR-a and CIDR-l could not be used in this binding experiment. As there was no apparent difference in the binding to CD36 of any of the different CIDR domains, all subsequent studies focused on CIDR-f.

To compare the binding activity of CIDR-f:11-177 with MC r-179, we perform ELISA-based binding assay using CIDR-f:11-177, GST-CIDRf and CIDR-f (Bac). Previous study by Baruch *et al.*(1997) performed binding assay using N-terminal GST protein fused with MC r179, thus GST-CIDRf was used in present CD36-binding assay. Baculovirus expression system has been used for expressing some

proteins which have problems of proper folding or lack of post-translational processing. Insect cells are known to express proteins with better folding than those of expressed in *E. coli*, especially for some heterologous genes produce the inclusion body in *E. coli*. CIDR-f:11-177 and GST-CIDRf showed comparable CD36-binding activity, whereas CIDR-f:11-177(Bac) showed about 50% of binding activity compared to CIDR-f:11-177, probably due to some contaminant protein present in the solution which potentially decreased the functional CIDR-f in the solution (**Figure 3. 12**). Therefore, this experiment showed that the CIDR-f:11-177 histidine-tagged protein expressed in *E. coli* has compatible CD36-binding activity as GST fusion protein and insect cell-expressed protein, thus could be used for further mutagenesis studies.

In order to check that the binding of CIDR1α domains were specific for the same region that had been previously mapped on the human CD36 receptor (Baruch *et al.*, 1999), we performed the inhibition assays using two synthetic peptides derived from the CD36 sequence which had previously demonstrated to specifically disrupt the binding between CD36 and the CIDR1α from the MC strain (Baruch *et al.*, 1997). Both peptides CD36:145-171 (NH_2-ASHIYQNQFVQMILNSLINKSKSSMFQ-COOH) and CD36:146-164 (NH_2-SHIYQNQFVQMILNSLINK-COOH) disrupt the binding between CIDR-f:11-177 and CD36 in a concentration dependent manner, whilst an unrelated peptide having sequence (NH_2-KAFTTTLRGAQRLAALGDTA-COOH), used as a negative control, did not display any significant

inhibition activity (**Figure 3. 13**). This result further confirmed that the CIDR-f domains expressed in *E. coli* could specifically bind to CD36 molecules, and were thus functional. It also rules out any significant interference with binding interactions that might have been introduced by the presence of the bulky Fc moiety fused to the CD36 molecule in our binding assay. Peptide CD36 145-171 showed about 85% of inhibition at the concentration of 100 μM, while CD36 146-164 only showed about 60% of inhibition at the same concentration. The different effect of inhibition was probably due to the poor solubility of peptide CD36 146-164, which made the actual final concentration in the solution lower than calculated. A concentration of ~0.1μM of CD36:145-171 produces 40% inhibition of binding.

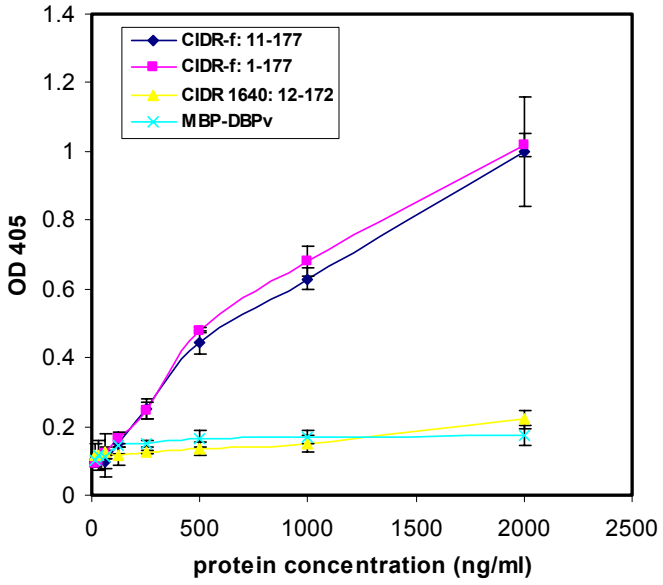

Figure 3. 11. Binding of different lengths of CIDR-f protein to CD36. Different lengths of CIDR-f were used to test binding with CD36/Fc.

CIDR-f:1-179 (with eight cysteines), CIDR-f:11-179 (with seven cysteines) showed comparable binding activity, whereas MBP-DBPv and CD36 non-binder CIDR 1640w:12-172 did not show binding activities. Results are expressed as mean and SD of three independent experiments.

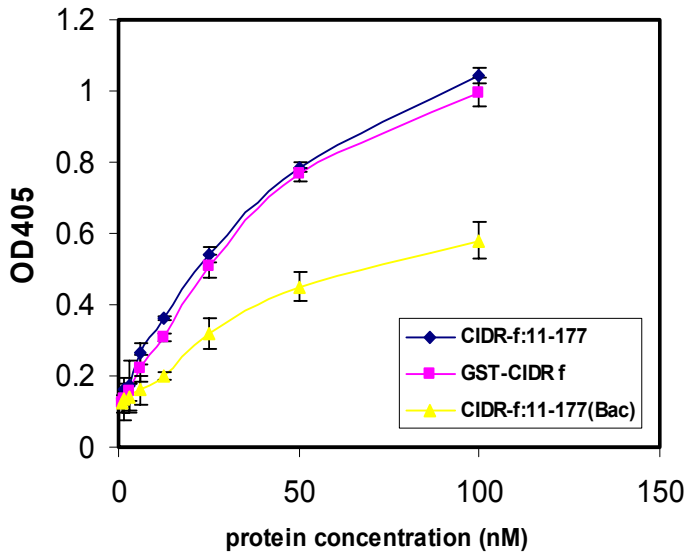

Figure 3. 12. Binding of different constructs of CIDR-f proteins to CD36/Fc. Purified CIDR-f:11-177, GST-CIDRf and CIDR-f:11-177(Bac) were used to test binding with CD36/Fc. CIDR-f:11-177 and GST-CIDRf showed comparable binding activity, whereas CIDR-f:11-177(Bac) showed about 50% of binding activity compared to CIDR-f:11-177. Results are expressed as the mean and SD of three independent experiments.

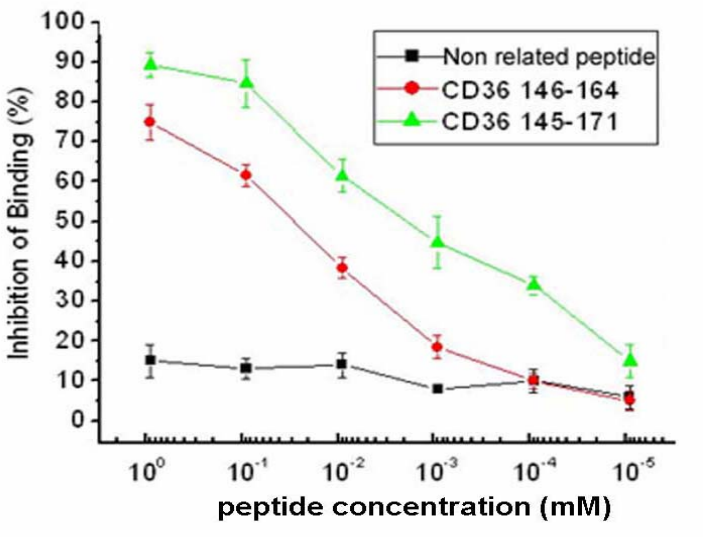

Figure 3. 13. Peptide inhibition of CIDR-CD36 interactions. Three peptides: CD36 145-171 (circle), CD36 146-164 (triangle) and a non related peptide (rectangle) were tested for their inhibitory effects of CIDR-f:11-177 and CD36/Fc binding. Percentage of inhibition = $\frac{OD405\ (w/o\ inhibitor)-OD405\ (w\ inhibitor)}{OD405\ (\ w/o\ inhibitor)}$ Results are expressed as the mean and SD of three independent experiments.

3.4 The CIDR1α C-terminal region is the main determinant for CD36 binding

3.4.1 Mapping CD36-binding region within CIDR-f domain

To date, there were no experimental data that has unambiguously mapped the region of the CIDR1α domain that binds CD36. It is suggested that the CD36 binding relies on the discontinuous amino acid sequence throughout the domain (Gamain *et al.*, 2002; Robinson *et al.*, 2003). Thus we made different

mutation constructs based on the putative secondary structure instead of on primary amino acid sequence. Schematic representations of all the constructs made were shown in **Figure 3. 14**. Very early on during this study, it was established that deletion of the first 11 amino acids from CIDR-f had no effect on overall binding and therefore this deletion mutant CIDR-f:11-177 was used in all subsequent studies (**Figure 3. 11**). This result also confirmed previous study (Burach *et al.*, 1997) that cysteine residue C_0 is not essential for binding.

It has been demonstrated that the nine amino acids at the N-terminus of MC r179 play an important role for the proper folding of CIDR molecules in *E. coli* (Baruch *et al.*, 1997). Based on the sequence alignment of CIDR-f with MC r179 (**Figure 3. 2**), the N-terminal domain of CIDR-f:11-177 was retained and truncation experiments at the C-terminus were performed. Truncation of the putative C-terminal α-helix α5 (construct CIDR-f:11-133) led to a decrease of about 60-70% in binding activities. Further truncation encompassing the region surrounding putative helix α4 (construct CIDR-f:11-116) completely abolished the binding activities (**Figure 3. 15**). It suggested that the region comprising residues 117 to 177 of the CIDR-f:11-177 plays a major role in mediating binding to CD36.

To establish whether this region alone can bind specifically to CD36, we expressed the C-terminal fragment of CIDR-f spanning residues 117-177 and assayed for CD36 binding (**Figure 3. 14**). No

binding above background could be detected and consistent with this the CD spectra indicated that this domain is largely unfolded, showing a negative peak near 200nm (Adler *et al.*, 1973) (**Figure 3. 18**). This would imply that while this region is important for specificity, other parts of CIDR are important for proper folding into a functional CD36 binding domain.

In order to demonstrate that this region contains the structural determinants necessary and sufficient for strong binding to the CD36 molecule, we constructed two chimeric CIDR molecules: the first, 1640-f chimera, fused N-terminal region of the the non-CD36 binding CIDR 1640w (residues 1 to 122) (Gamain *et al.*, 2001a; Robinson *et al.*, 2003) with C-terminal region of the CIDR-f molecule (residues 116 to 177); the second, f-1640 chimera, fused N-terminal region of CIDR-f (residues 11 to 117) with C-terminal region of non-binder CIDR 1640w (residues 133 to 172) (**Figure 3. 14)**. These chimeric CIDR molecules expressed in *E. coli* and could be purified using the same protocol as the wild type CIDR-f (**Figure 3. 7**). The CD analysis showed that these two chimeric CIDR molecules as well as CIDR-f:11-116 had a similar content of secondary structure elements as to the wild type CIDR-f protein (**Figure 3. 17)**, and therefore, the lack of CD36-binding activity of CIDR-f:11-116 was not due to collapse of the whole structure. However, f-1640 chimera is prone to aggregation and precipitates readily in various buffer conditions. Remarkably, the 1640-f chimera converted the non-CD36 binder to about 98% of wild type levels of

CD36 binding activity, while the f-1640 chimera showed only minimal binding activity (**Figure 3. 16**). To further investigate whether the binding observed in the 1640-f chimera is CD36 specific, we tested the ability of the CD36 peptide 145-171 to compete for the interaction. The peptide is able to compete for CD36 binding with either CIDR-f:11-177 or the 1640-f chimera with no effect being seen for either the CIDR 1640w and 1640-f chimera (**Figure 3. 19**) confirming the specificity of the 1640-f chimera for CD36.

Our results demonstrate that although the C-terminal region is the determinant for the CD36 binding activities, the N-terminal region is crucial for maintaining the overall structural integrity of the CIDR molecule, possibly acting as a scaffold to present the CD36 binding determinant present in the C-terminal region. This is reminiscent of the Fab fragment of immunoglobulin molecules where a limited number of loops variable in length and in sequence determine the binding specificity of the molecule (Novotny *et al.*, 1983; Chothia *et al.*, 1985). These loops are presented on an essentially conserved structural framework. However, in the case of Fab, the framework is based on β-sandwiches whereas in CIDR molecules, it appears to consist of α-helices.

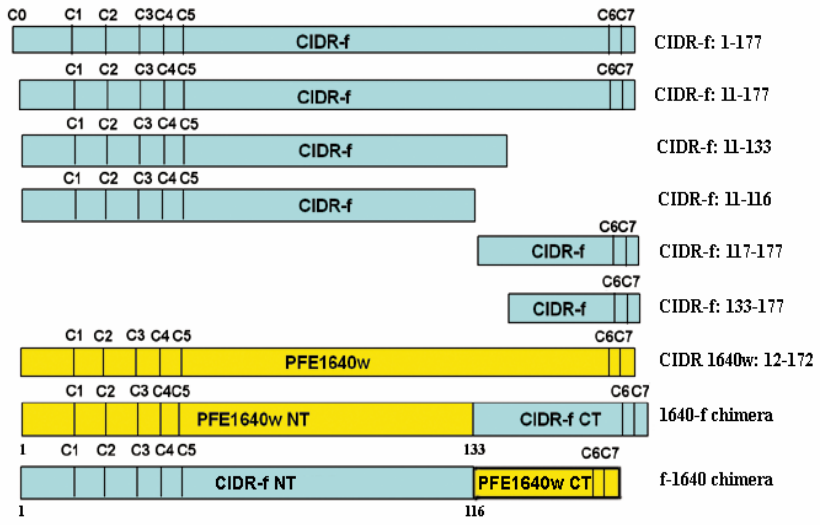

Figure 3. 14. Schematic view of the various constructs used for the binding experiment. The positions of conserved cysteines are indicated.

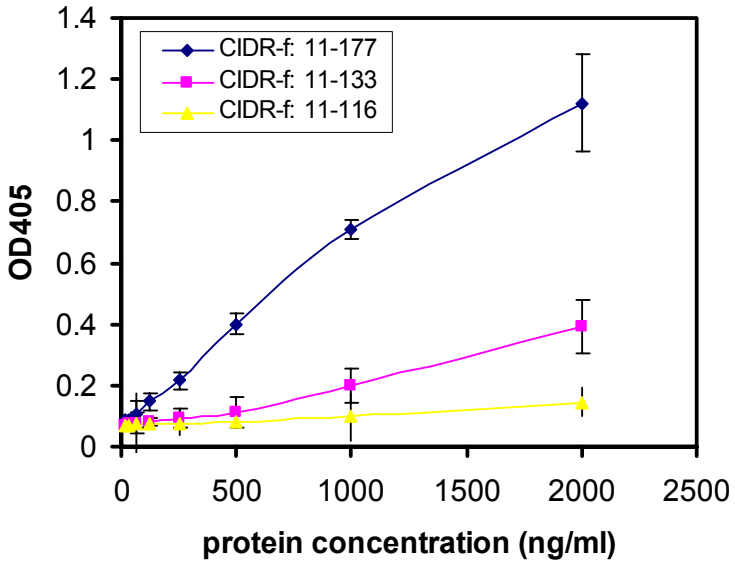

Figure 3. 15. Binding of different C-terminally truncated fragments of CIDR-f proteins to CD36. Different lengths of CIDR-f were used to test binding with CD36/Fc. Truncations were made based on the

predicted CIDR1α secondary structure. CIDR-f:11-133 lost about 70% of binding activities to CD36/Fc and CIDR-f:11-116 totally lost the binding activities to CD36/Fc. Results are expressed as the mean and SD of three independent experiments.

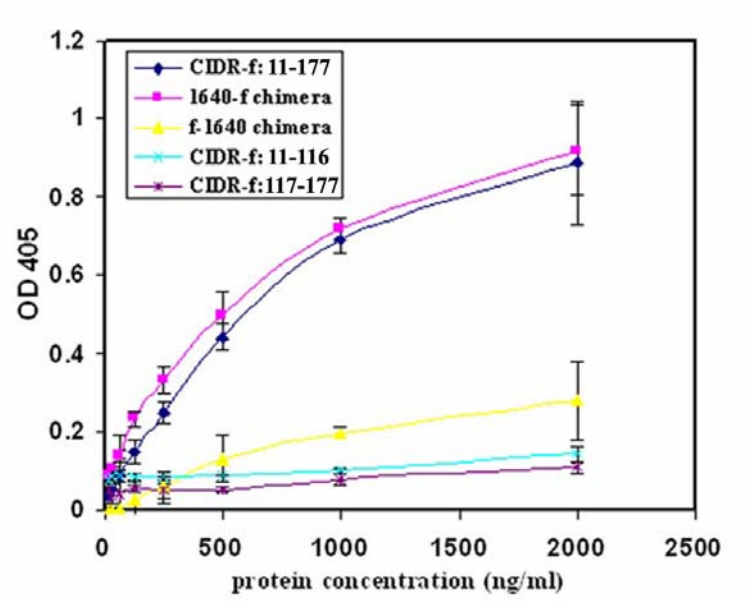

Figure 3. 16. Direct binding assay of CD36/FC and chimera. Several constructs were used to test binding ability to CD36/Fc. CIDR-f:11-116 and CIDR-f:117-177 totally lost binding ability. However, 1640-f chimera and f-1640 chimera showed about 98% and ~20% of wild type of CD36 binding activities respectively. Results are expressed as mean and SD of three independent experiments.

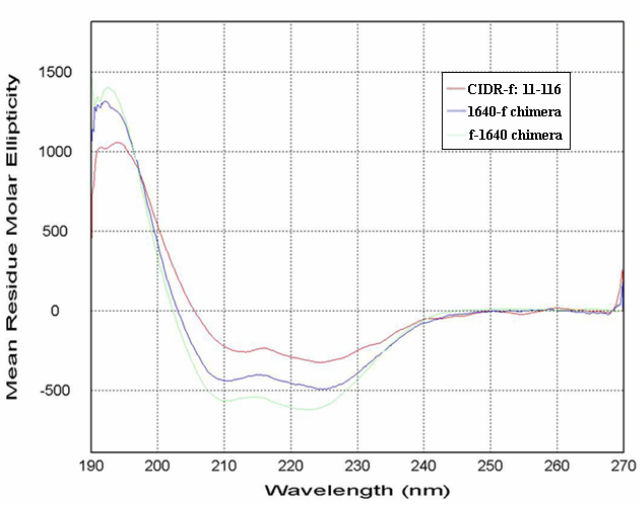

Figure 3. 17. CD spectra of the chimera. CD spectra were collected with steps of 0.1 nm from wavelength 190nm to 260nm. Mutants CIDR-f:11-116 and chimera all showed similar spectra which had maximum at 190nm and two minima curves at 208nm and 222nm.

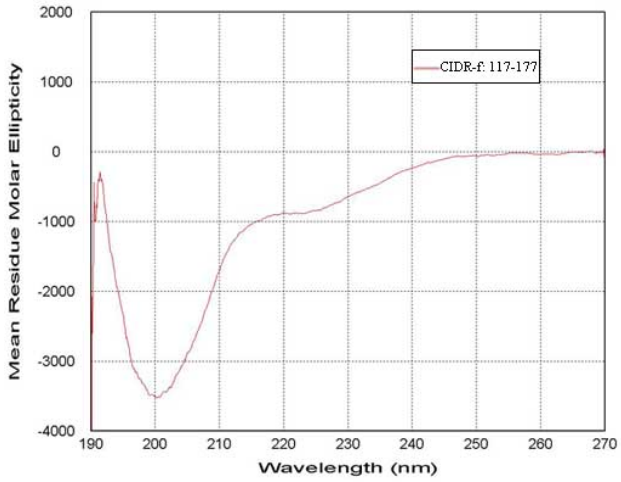

Figure 3. 18. CD spectra of CIDR-f: 117-177. The CD spectrum was recorded using 0.5mg/ml protein in PBS. CD spectrum is characterized by a negative peak near 200 nm, indicating random coil structure.

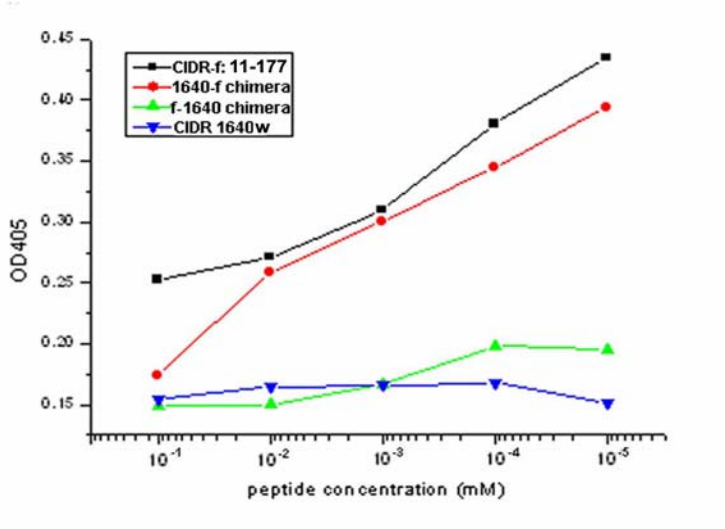

Figure 3. 19. Peptide inhibition of CIDR-CD36 interactions. Peptide: CD36 145-171 was tested for their inhibitory effects of binding between CIDR-f:11-177, 1640-f chimera, f-1640 chimera and CIDR 1640w and CD36/Fc. The peptide can inhibit the interaction between CIDR-f: 11-177 or 160-f chimera and CD36/Fc in concentration-dependent manner, while only showed minor inhibitory effects on CIDR 1640w or f-1640 chimera.

3.4.2 Binding activity of loop regions

According to the sequence alignment presented in **Figure 3. 2**, two putative loops connecting helices α2 and α3 with sequence 86GFSIFG and α4 to α5 with sequence 136EQEA vary significantly in length and amino-acids between various CIDR domains, including between CD36 binders and non-binders. Two expression constructs deleting the two putative loops (Dele GFSIFG and Dele EQEA) were constructed. These two constructs expressed well in *E. coli* and their binding activities were reduced by approximately 25-35%,

suggesting some involvement in CIDR1α-CD36 binding interaction (**Figure 3. 20**). Although there is no protein structure available now, we propose a model to explain this reduction of CD36-binding activity. Upon binding between CD36 and CIDR1α, the loop regions might form a cover to protect binding interface against exposed solvent. This cover may not direct involved in binding, thus the absence of it would not dramatically reduce the binding activity.

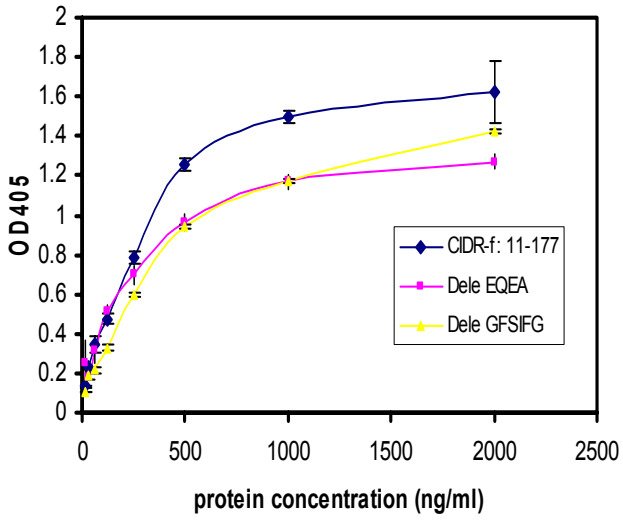

Figure 3. 20. CD36/Fc binding assay using 2 deletion mutants. Both of Dele EQEA and Dele GFSIFG showed reduced binding ability to CD36/Fc by approximately 25-35%.

3.4.3 PE inhibition assay using recombinant CIDR-f proteins

To establish whether the ELISA-based *in vitro* binding assays did indeed reflect differences in binding ability of the different CIDR constructs to CD36 under *in vivo* like conditions, we utilized

HLEC and CHO-K1 cell lines that are known to express either CD36 or CSA on their surface. *P. falciparum* infected erythrocytes where selected for a number of cycles on either cell line to enrich for parasite populations that predominately expressed CD36 or CSA binding PfEMP-1 (Pouvelle *et al*., 1997; Lekana Douki *et al*., 2002). The ability of the different recombinant CIDR constructs to inhibit the binding of these selected parasites was then determined. Preincubation of the HLEC-CD36 cell with CIDR-f:11-177 inhibited binding of the CD36 selected 3D7 parasites in a concentration dependent manner, while preincubation of the CHO-CSA cell line with the same protein followed by binding of CSA selected parasites showed no inhibition (**Figure 3. 21)**. 50% inhibitory effects appeared at around 5 μM, which was 3 times higher than previous studies (Cooke *et al*., 1998; Yipp *et al*., 2003), indicating around 60% proteins were misfolded or aggregated during the assay. Using the same assay, we tested blockage of PEs adherence on *P. falciparum* strains 3D7, HB3 and FCR3 using truncated and chimeric proteins at a concentration of 6 μM. While CIDR-f:11-177 and 1640-f chimera showed ~60% inhibition of PE adherence in all three strains, the inhibitory effect of CIDR-f:11-116 and CIDR 1640w:12-172 showed only less than 10% inhibitory effects. All these 4 proteins showed minor inhibitory effects (0-20%) on CSA-adherent PEs of three strains (**Figure 3. 22**).

Our current data demonstrates that the C-terminal region of CIDRα is the determinant for the CD36 binding activity without

which the binding ability to CD36 would be lost as demonstrated by the studies on the 1640-f chimera and CIDR-f:11-116 truncation mutant. The replacement of the 60 amino acid C-terminal end from a non-binding CD36 CIDRα domain with one from a CD36 binding domain as demonstrated in the 1640-f chimera is sufficient to convert the non-binder to a binder. The reverse experiment leads to a nearly complete loss of binding.

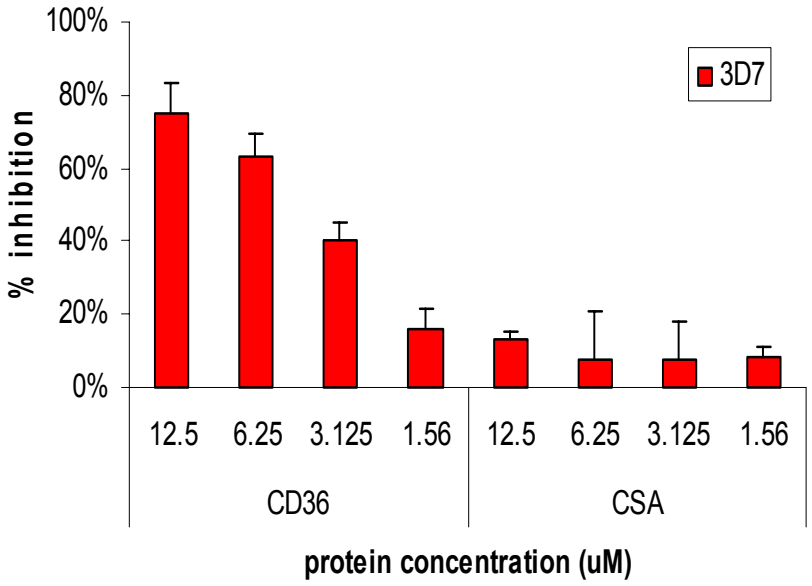

Figure 3. 21. Blockade of CD36-adherent PEs of strain 3D7 using recombinant proteins CIDR-f:11-177. 1.56 µM to 12 µM recombinant proteins were preincubated with HLEC-CD36/CHO-K1-CSA cells in the binding buffer. After 30 mins of incubation, both CD36-adherent and CSA-adherent PEs of strain 3D7 were added to each well and test for binding. The average number of PEs bound to 100 HLECs-CD36/CHO-K1-CSA cell for three (40x) microscopic fields were calculated. The percentage inhibition of parasite binding compared

to the untreated control without adding any proteins were determined. SD was determined from 3 independent experiments.

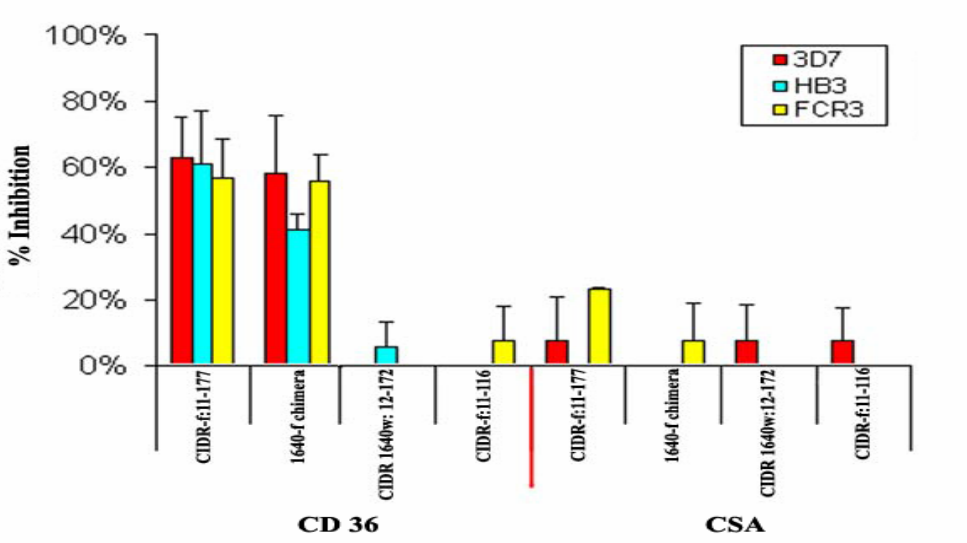

Figure 3. 22. Blockage of CD36-adherent PEs of three strains 3D7, HB3 and FCR3 using recombinant proteins CIDR-f:11-177, 1640-f chimera, CIDR-f:11-116 and CIDR 1640w:12-172. 6 μM of each recombinant protein preincubated with HLEC-CD36/CHO-K1-CSA cells in the binding buffer. The average number of PEs bound to 100 HLECs/CHO-K1 cell for three (40x) microscopic fields were calculated. The percentage inhibition of parasite binding compared to the untreated control without adding any proteins were determined. SD was determined from 3 independent experiments.

3.5 Polyclonal antibodies characterization

To confirm that the region 117-177 of CIDR-f is crucial for CD36-CIDR1α binding, murine polyclonal antibodies against the

region CIDR-f:117-177 and CIDR-f:133-177 were produced and used to test inhibitory effect on CD36-CIDR1α binding interactions. The two constructs were well expressed in *E. coli* and successfully purified by using Glutathione Sepharose beads (**Figure 3. 23**). Blood was drawn from the animals two weeks after each boost and tested for antibody titer by ELISA on 96-well polystyrene plates (**Figure 3. 24**). For protein GST-CIDRf:117-177, sera from mouse 2, 3 and 4 which had better immune responses were combined for further assays. For protein GST-CIDRf:133-177, sera from mouse 2 and 4 were combined. To confirm that the antibodies had been raised against the region 117-177 and 133-177 of CIDR-f domain, Western blotting assay was performed. Bands corresponding to the sizes of CIDR-f:11-177 and the chimeric protein were detected using anti-GST CIDRf:117-177 and anti-GST CIDRf:133-177 polyclonal sera, respectively, while no signals were detected for CIDR 1640w (**Figure 3. 25**). It showed that the polyclonal antibodies were specific for the C-terminal region of CIDR-f:11-177, and can be used for the inhibition assay described below.

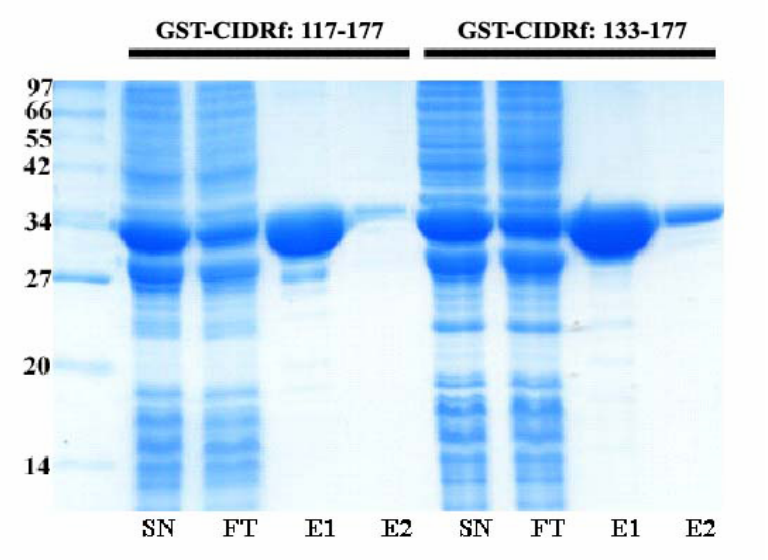

Figure 3. 23. Expression and purification of GST-CIDRf:117-177 and GST-CIDRf:133-177. Both constructs were well expressed in *E. coli*. After sonication and separation, the soluble fractions were passed through Glutathione Sepharose beads and washed several times. The beads-bound fractions were then eluted. GST-CIDRf:117-177 and GST-CIDRf:133-177 soluble fractions (SN), flow through fractions (FT) and eluted fraction one (E1) and eluted fraction two (E2) were indicated.

A:

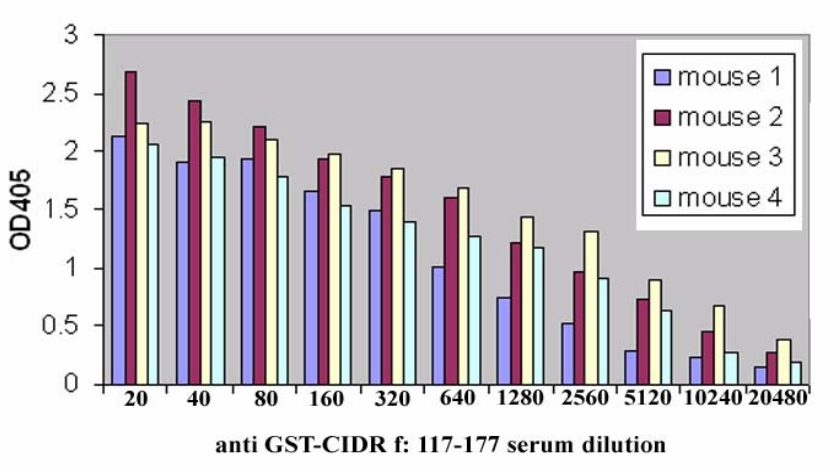

B:

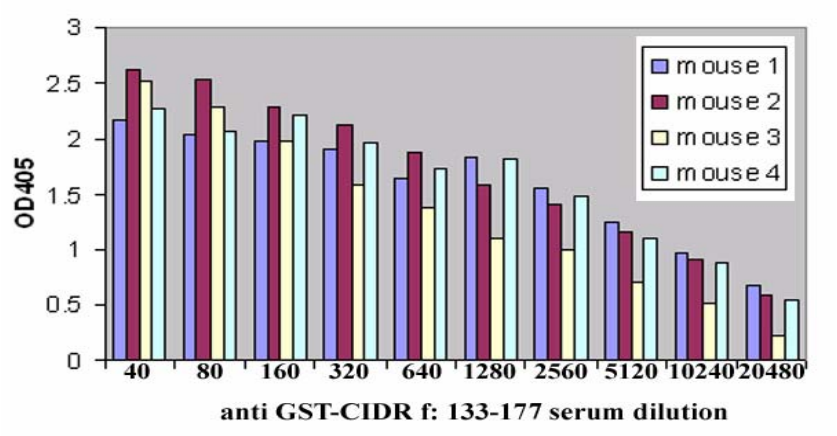

Figure 3. 24. Polyclonal antibodies titer using ELISA. We tested the titers of two antibodies by ELISA on 96-well microtiter plates 7-8 weeks after the first injection. Blood was drawn from eight mice (each protein injected into 4 mice) and sera were used to test antibody titer. For anti GST-CIDRf:117-177, mouse number 2, 3 and 4 had good immune responses (figure A); for anti GST-CIDRf:133-177, mouse number 2 and 4 had good immune responses (figure B). These sera were pooled separately and used for inhibition assay.

Figure 3. 25. Western blotting of polyclonal antibodies. CIDR-f:11-177, CIDR 1640w, 1640-f chimera, GST-CIDRf:117-177 and GST-CIDRf:133-177 were used for Western blotting to test the reactivity and specificity of polyclonal antibodies. After separation by SDS-PAGE gel, the two membranes were incubated with the sera against GST-CIDRf:117-177 and sera against GST-CIDRf:133-177, respectively. Then anti-mouse HRP conjugated secondary antibody was used as the secondary antibody, followed by ECL substrates detection. The two anti sera can recognize CIDR-f:11-177, 1640-f chimera, GST-CIDRf:117-177 and GST-CIDRf:133-177, but cannot recognize CIDR 1640w.

3.6 Polyclonal antibodies specific recognize PfEMP-1

To test whether the polyclonal antisera can specific recognize PfEMP-1 on native PEs, we performed Western blotting on both CD36-adherent and CSA-adherent PEs, including strain 3D7, HB3

and FCR3, using polyclonal antisera against 117-177. The polyclonal antibodies recognized full length PfEMP-1 from different parasite strains with a specific protein of > 250kDa in size (**Figure 3. 26**). Some small size variations between the protein detected in the 3D7 strain selected on CD36 compared to that selected on CSA were shown, consistent with the expected change PfEMP-1 expression in different binding phenotypes (Smith *et al.*, 2000a; Robinson *et al.*, 2003). To test whether the C-termial region of CIDR-f:11-177 would elicit antibodies reactive to PfEMP-1 expressed by PEs, antibodies against GST-CIDRf:117-177 were used to perform IFA. To exclude the possibilities of non-specific IgM and non-immune IgG binding to PEs, as well as the possibility of antibody against GST binding to PEs, preimmune serum and mice anti-GST antibody were used as the negative controls. IFA tested positive for GST-CIDRf:117-177 mouse antiserum, while no labeling was observed using the corresponding preimmune serum and GST antibodies (**Figure 3. 27**). This result demonstrated that the polyclonal antibody raised against the recombinant C-terminal region of CIDR-f molecules could recognize the PfEMP-1 proteins expressed by *P. falciparum* parasites. To further confirm that the murine polyclonal antisera can recognize native PfEMP-1 expressed on the surface of PEs, L-IFA was performed. The antisera against CIDR-f:117-177 reacted only with the CD36-adherent PEs of 3D7 strain (**Figure 3. 28**), but not with the corresponding preimmmune or anti-GST sera (data not shown).

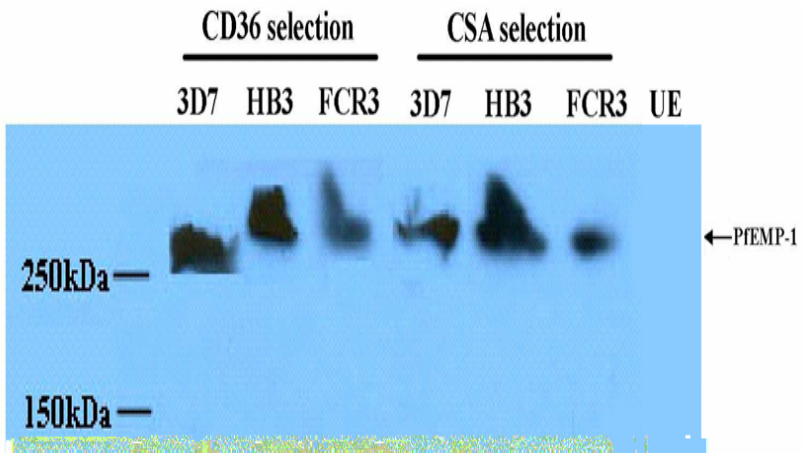

Figure 3. 26. Western blotting on PEs. Mature-stage parasites were extracted and lysed. Proteins were separated by SDS-PAGE electrophoresis and transferred onto nitrocellulose membranes. Murine polyclonal antisera against CIDR-f:117-177 were used to detect the expression of PfEMP-1 at the dilution 1:200, followed by secondary antibodies and enhanced chemiluminescence. PfEMP-1 of around 250KDa can be detected on both CD36-adherent and CSA-adherent PEs of strain 3D7, HB3 and FCR3, while no signal can be detected in uninfected erythrocytes (UE).

1) Murine polyclonal antisera against CIDR-f: 117-177

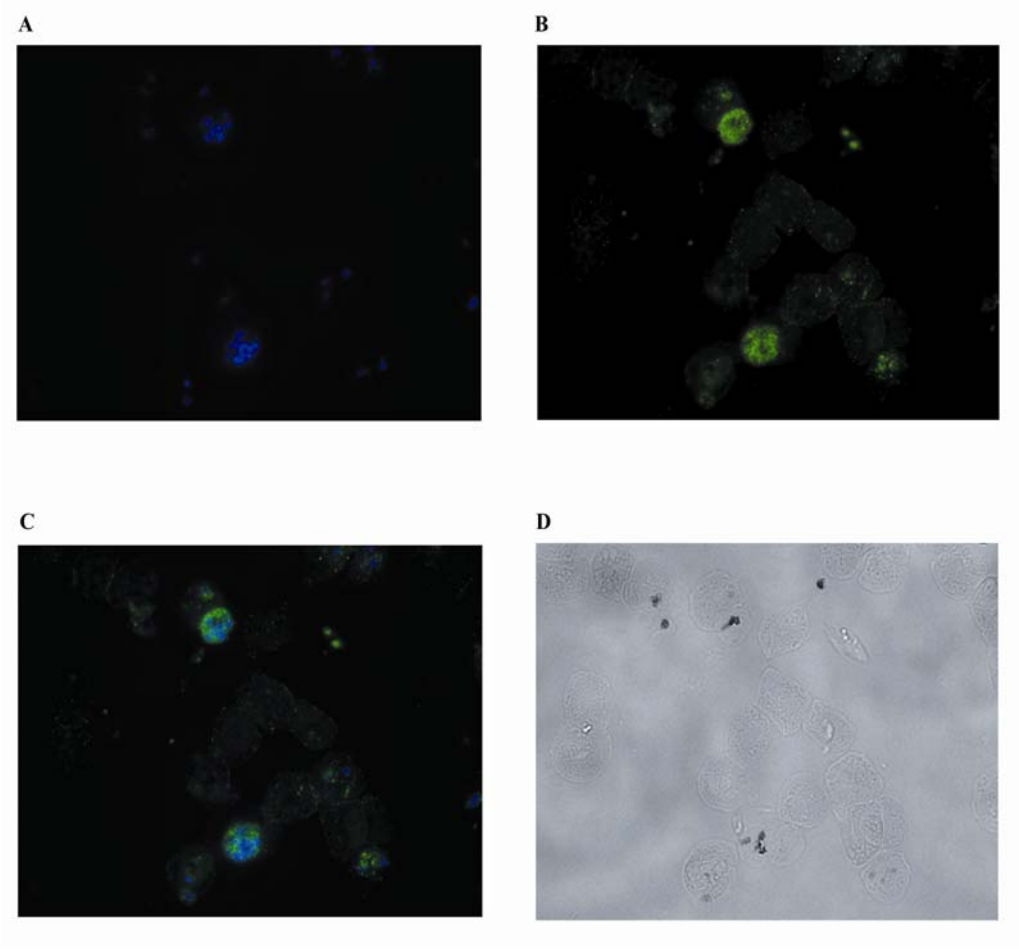

2) anti-GST antibody

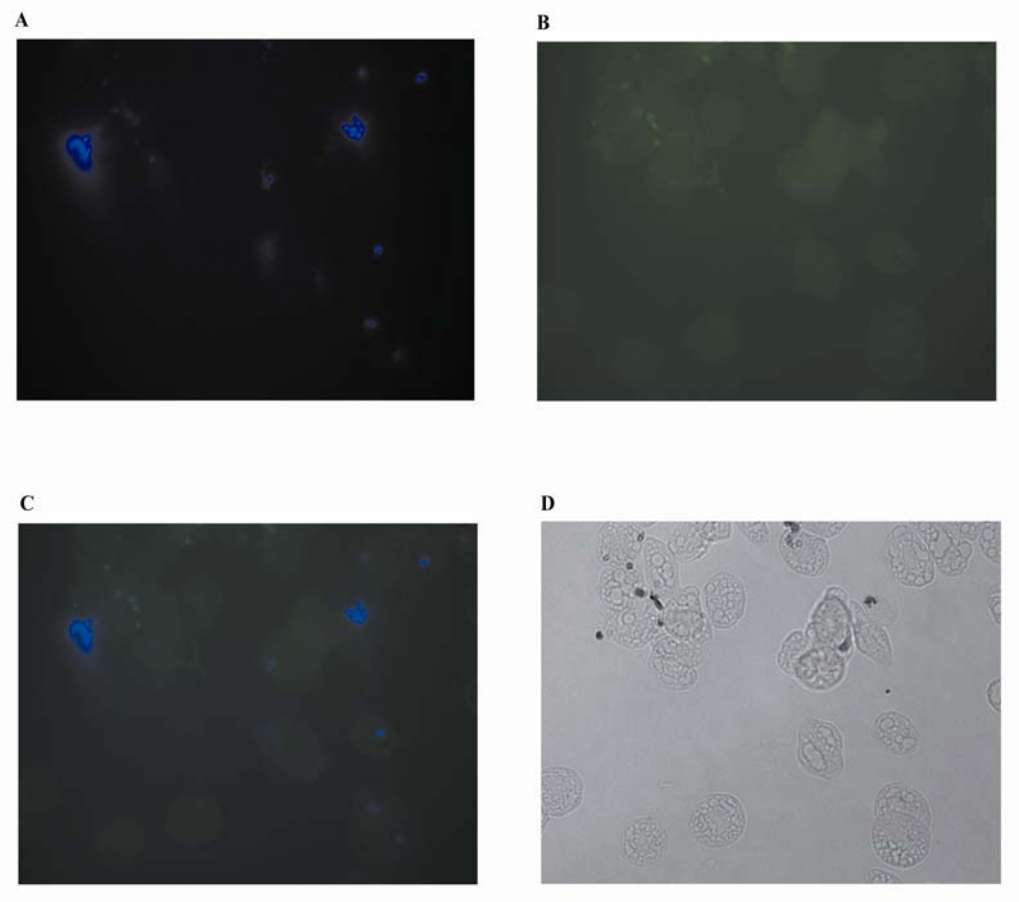

3) Preimmune serum

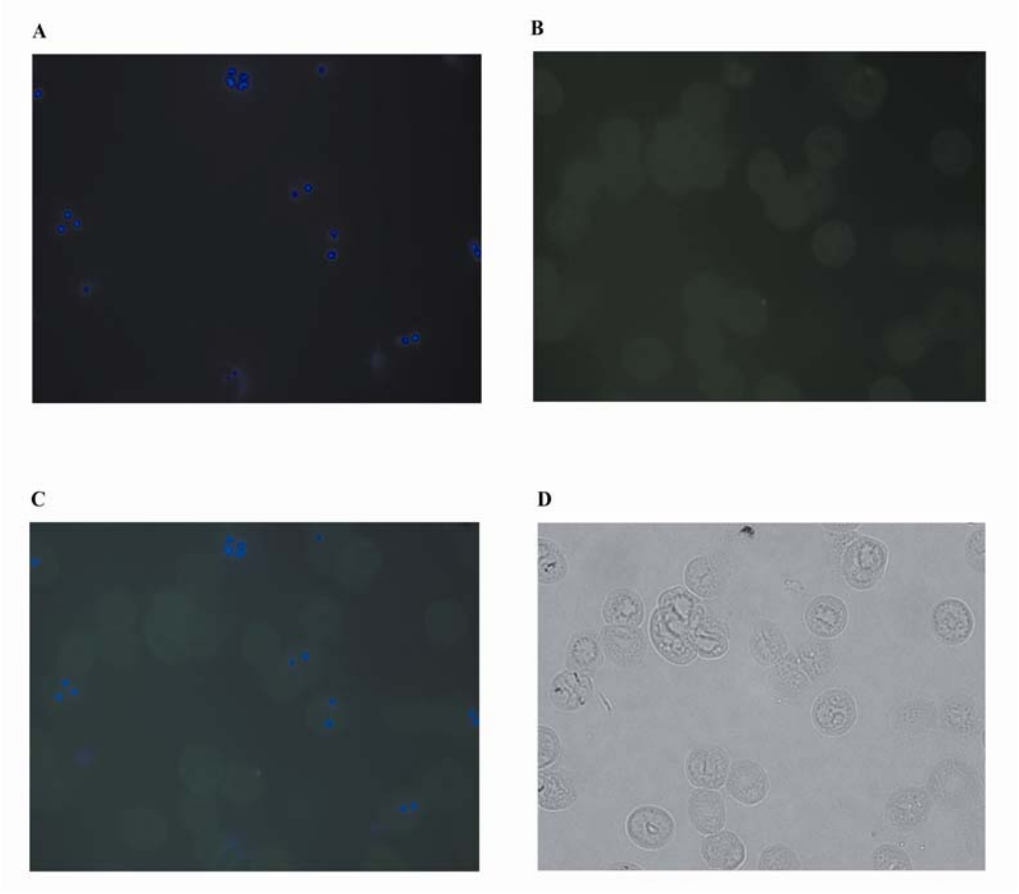

Figure 3. 27. Immuno-labeling of PEs with an antiserum raised against the C-terminal domain of CIDR-f:11-177. The antibody against C-terminus of CIDR-f:11-177 can recognize PEs in a specific manner (Figure 1), while no labeling on PEs was detected for anti-GST antibody (Figure 2) and preimmune serum (Figure 3). A: the nuclei of parasitized erythrocytes stained with DAPI; B: surface labeling detection by FITC; C: the merged images of figure A and B; D: optical phase.

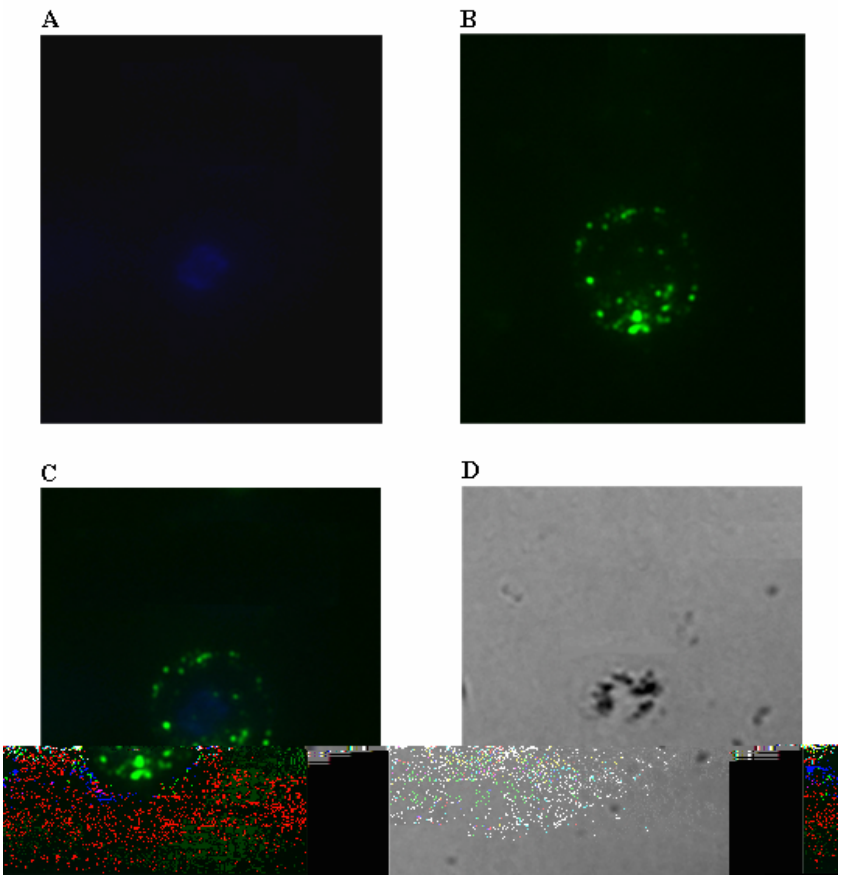

Figure 3. 28. Surface labeling of CD36-adherent PEs of strain 3D7 with murine polyclonal antisera raised against CIDR-f: 117-177. A: parasite's nuclei staining using DAPI; B: surface labeling of FITC; C: merge image; D: phase image.

3.7 Murine polyclonal antisera against C-terminus of CIDR-f inhibit CD36-CIDR1α binding

Compared to region 117-177, region 133-177 was shorter by 26 amino acids downstream from N-terminal region which was devoid of amino acids NVKELE. This region had been shown to be involved in CD36 binding in *P. falciparum* MC strain (Gamain *et al.*, 2001).

Inhibition assays were carried out with a series of dilutions for two antisera. For the region 117-177, there was about 90% inhibition at the dilution of 1:8. However, an exponential decrease in the degree of inhibitory effect reaching about 5% was observed when the dilution factor was 1:1024. In contrast, the region 133-177 was only partially inhibited (about 70%) at a dilution of 1:8 and its degree of inhibition decreased faster than region 117-177 (**Figure 3. 29**). For control reactions, pre-immune serum, anti-GST antibodies and other irrelevant antibodies did not show any inhibitory effects. To establish whether the inhibitory antisera were also able to inhibit binding of PEs to CD36 and whether the antisera had cross-reactive effects on different strains of *P. falciprum*, we investigated their effect on blockade of binding of CD36-adherent/CSA-adherent PEs on HLEC-CD36/CHO-CSA cells. The antisera against CIDR-f:117-177 inhibited more than 60% binding between mammalian cell expressed CD36 and CD36-adherent PEs at the dilution of 1:20 in strain 3D7, HB3 and FCR3, while had less than 10% inhibitory effects on CSA-binding PEs, indicating both specificity as well as cross-reactivity (**Figure 3. 30**). It supports the model that the different domains of PfEMP-1 alters the adhesion phenotype of PEs and structural difference between CD36-binding and CSA-binding PfEMP-1 determining their binding specificity (Gamain *et al.*, 2002). It suggested that these two antibodies could inhibit the CIDR1α and CD36/Fc binding, presumably directly interacting with the CD36/Fc binding site(s). Although these two antibodies raised against CIDR-f

antigen with different amino acid lengths, both showed inhibitory effects, the antisera against longer region (residues 117-177) showed better inhibitory effects than the shorter region (residues 133 to 177). Thus, the CD36-CIDR1α interaction is most probably involved in the longer region (residue 117-177). However, to unveil the mechanism of the interactions, the structure of CIDR1α domain and the complex of CIDR1α protein with CD36 receptor are still required.

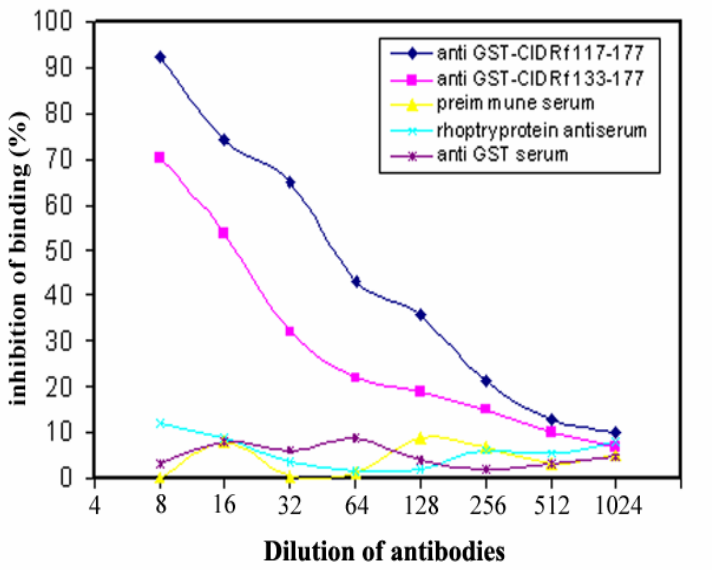

Figure 3. 29. Two sera raised against GST fused with CIDR-f:117-177 and GST fused with CIDR-f:133-177, respectively were tested for the inhibition effects of CIDR-f:11-177 and CD36/Fc binding. Both anti GST-CIDRf:117-177 and anti GST-CIDRf:133-177 showed dose-dependent inhibition effects on CD36/Fc-CIDR1α binding. Preimmunized serum, anti-GST serum and an unrelated anti-serum (rhoptry protein polyclonal antisera) did not show inhibition effects. The percentage of inhibition of binding was indicated by the ratio of

OD405 reading of control sample (without any serum) minus each sample with different dilution of serum relative to OD405 reading of control sample.

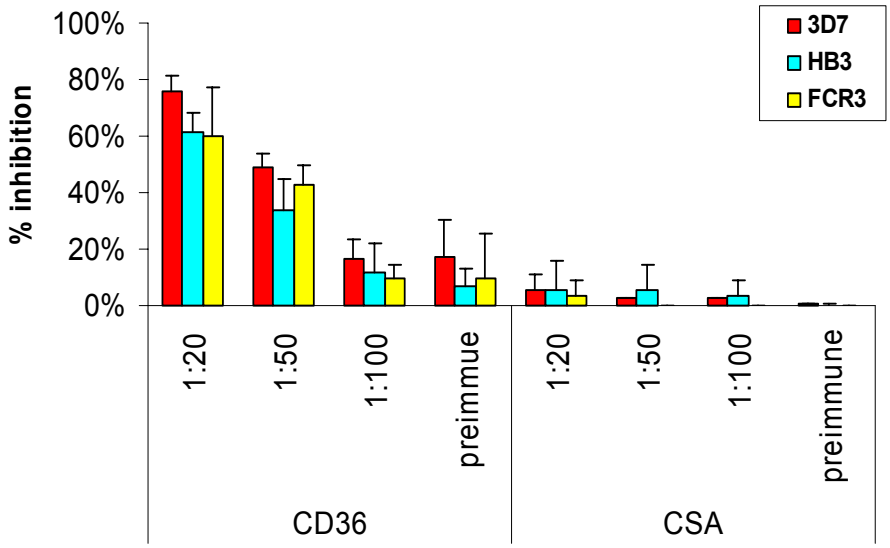

Figure 3. 30. Blockage of CD36-adherent PEs of three strains 3D7, HB3 and FCR3 using murine polyclonal antisera against CIDR-f:117-177. PEs were preincubated with binding buffer alone or binding buffer containing antisera diluted from 1:20 to 1:100, or preimmune sera. After 30-min incubation, the PEs were added to HLEC-CD36/CHO-K1-CSA cells and tested for binding. The average number of PEs bound to 100 HLEC-CD36/CHO-K1-CSA cells for three (40x) microscopic fields were calculated. The percentage inhibition of parasite binding compared to the untreated control without adding any proteins were determined. SD was determined from 3 independent experiments.

3.8 Crystallization screens of CIDR1α domains

Crystallization screens were performed for both CIDR-f:11-177 and CIDR 1640w. Four Hampton crystallization kits (total of 242 conditions) were used but no crystals were seen throughout a period of 6 months. Most of the crystallization conditions (about 80% of total screen conditions) showed heavy precipitation within 3 days even when the protein concentration was at 3 mg/ml (**Table 3. 1)**. This observation indicates that either the relative supersaturation of the protein sample and reagent is too high, the sample has denatured, or the sample is heterogeneous. Since we had diluted the sample up to 3 mg/ml and the ELISA-based binding assay showed the binding activities of CIDR-f:11-177, the chances of supersaturation and denaturation of the sample is relative low. The failure of crystal growth was probably due to the heterogeneity of the samples.

Screen kit	Observation of the drop	CIDR-f: 11-177	CIDR 1640w
crystal screen 1	clear drop skin precipitate	5 10 35	11 11 28
crystal screen 2	clear drop skin precipitate	8 10 32	12 13 25
PEG/Ion screen	clear drop skin precipitate	9 11 32	12 12 26
Index screen	clear drop skin precipitate	19 15 62	27 17 52

Table 3. 1. Summary of crystallization screens of CIDR domains. Four Hampton crystallization screen kits were used and total of 242

conditions were screened. The number of screened conditions observed using microscope is as shown in this table.

3.9 Expression of CIDR-f protein

CIDR1α domains has been expressed as the recombinant proteins in different expression systems, such as *E. coli* (Baruch *et al.*, 1997; Baruch *et al.*, 1999; Gamain *et al.*, 2001a), mammalian cells (Gamain *et al.*, 2001b) and *Pichia pastoris* (Yipp *et al.*, 2003). All proteins expressed in these three systems were functional and were used to map domain binding activities in different binding assays. In this study, I expressed the different CIDR1α domains, including both CD36-binders and non CD36-binders, from the strain 3D7 in *E. coli*. To compare the CD36-binding activity, one of the CD36-binders, CIDR-f, was expressed as C-terminal histidine-tagged protein, N-terminal GST fusion protein in *E. coli* and C-terminal histidine-tagged protein in insect cells at the beginning of the studies. The large-affinity tagged protein-GST (26 kDa) shows effects to increase protein solubility and formation of active protein, especially when it is fused at the N-terminal end of the construct (Toye *et al.*, 1990; Kaelin *et al.*, 1991). However, when the C-terminal histidine-tagged protein was compared with N-terminal GST fusion protein, they showed compatible CD36-binding activity in ELISA-based binding assay (**Figure 3. 12)**, thus the simplest C-

terminal histidine-tagged CIDR-f protein was used in subsequent studies.

As with other eukaryotic expression systems, baculovirus expression of heterologous genes permits folding, post-translational modification and oligomerization in manners that are often identical to those that occur in mammalian cells. Also, unlike the reducing environment of the *E. coli* cytoplasm, the insect cytoplasmic environment allows proper folding and S-S bond formation (O'Reilly *et al.*, 1992). So far, there has been no studies reported using baculovirus expression system to express CIDR1α domain. I successfully expressed the heterologous CIDR-f protein in insected cells with high yield (~5mg recombinant proteins/L culture medium). CIDR-f:11-177 (Bac) is not glycosylated in the insect cells although it contains one potential N-glycosylation site(N_{147}) (data not shown). It showed only about 50% binding activity compared with *E. coli* expressed CIDR-f protein, probably due to relative low purity after purification (**Figure 3. 12**). Therefore, it appears that the CIDR-f protein expressed in insect cells is no better in quality if not worse than that expressed in *E. coli*. In addition, protein expression in insect cells is much more time- and labor-consuming than expression in *E. coli*. Therefore, *E. coli* expression of C-terminal histindine-tagged CIDR-f protein was employed and recombinant protein purified from *E. coli* expression was used throughout the study.

3.10 Disulfide bonds formation in CIDR1α domain

The minimal CD36-binding domain from the MC strain (MC r179) contains seven conserved cysteine residues (Baruch *et al.*, 1997). These seven cysteine residues are suggested to be of functional importance for this domain. Reduction and alkylation of whole MC r-179 lost its ability to bind CD36. Out of the 7 cysteine-to-serine mutants in MC r-179, three mutants (C606S (C1), C615S (C2) and C625S (C5)) were poorly expressed in *E. coli* thus can not be used for further binding assay. One mutant (C619S (C3)) failed to bind CD36 molecule, two mutants (C733S (C6) and C742S (C7)) had a decreased binding activity, while one mutant (C623S, (C4)) had a comparable binding activity as the wild type protein (Baruch *et al.*, 1997). Therefore, disulfide bond(s) is present within this domain, however, at least one conserved cysteine residue (C4) is unpaired, or is not required to maintain an active conformation of the CIDR1α domain.

Both DBL domains and CIDR domains are cysteine-rich molecules. Based on the two DBLs structures solved so far, all cysteines within these two molecules are crucial since they are involved in formation of disulfide bonds and maintaining the integrity of three-dimensional structure (Tolia *et al.*, 2005; Singh *et al.*, 2006). However, it seems that the structure of CIDR1α domain is different from those of DBLs, at least in the content of disulfide bonds. DBLs have 12 conserved cysteines, whereas CIDR1α only has 7 cysteines. Thus some of cysteines have to be unpaired within the

CIDR1α domain. However, the possibility that the odd-number of cysteines might be involve in the formation of intermolecular disulfide bonds and in the determination of the oligmerization state of this protein cannot be ruled out.

In the beginning of this study, we have mutated the five cysteines at the N-terminus individually into serine and truncated the last two cysteines from the C-terminus to pinpoint the important cysteines for CD36-binding activity. These N-terminus cysteine-to-serine mutants and C-terminus truncations had shown compatible binding activities to the wild type CIDR-f:11-177 (data not shown). However, in later PE blockage adhesion assay, these results cannot be futher substantiated as they all lost inhibitory effects on PE adhesion (data not shown). The explanations for this discrepancy are complicated. The CIDR-f protein might not be expressed as 100% percentage correctly folded in *E.coli*. The ELISA-based binding assay is much more sensitive than PE blockage adhesion assay, as it only requires less than 0.1 μM proteins to obtain the final detectible signals, while PE blockage adhesion assay needs at least 1-2 μM protein to observe the inhibitory effects. Thus the binding activity of correctly folded protein detected by ELISA-based binding assay might not be detectible in PE blockage adhesion assay. Moreover, in the ELISA-based binding assay, if the protein is mostly misfold or aggregated in the solution, it might increase the chances of the protein sticking to the plate non-specifically, thus obtaining false-positive signals. Therefore, this type of assay might not be suitable

for detection of binding activity for cysteine-to-serine mutants. To conclude, I was unable convincingly map disulfide bonds formation within CIDR-f protein, due to the limitation of assays applied and the quality of expressed proteins.

3.11 Molecular dichotomy of PfEMP-1

Molecular dichotomy is present in PfEMP-1 molecule, providing the evidence that parasites isolated from non-pregnant people can bind CD36, while parasites isolated from human placenta can bind CSA but not to CD36 (Fried *et al.*, 1996; Beeson *et al.*, 2000; Scherf *et al.*, 2001; Flick *et al.*, 2001). PfEMP-1 proteins from CD36-binding parasites have type 1 head structure, containing CIDR1α domain which binds CD36; while PfEMP-1 proteins from CSA-binding parasites have a combination of a CSA-binding DBLγ domain and a non-CD36-binding CIDR1α (Buffet *et al.*, 1999; Gamain *et al.*, 2001a). Thus, the different domains within PfEMP-1, especially CIDRα and DBLγ domains are mutually exclusive to express one phenotype to bind CD36 or CSA (Gamain *et al.*, 2001a).

In our study, the polyclonal antisera against C-terminal region of CIDR-f recognized PfEMP-1 proteins selected from both CD36-adherent and CSA-adherent PEs from three different strains (3D7, HB3 and FCR3) by Western blotting (**Figure 3. 26**), indicating there is some conserve epitope(s) present on both CD36-adherent and non-CD36-adherent genotype. However, these polyclonal antisera only

showed inhibitory effects on CD36-adherent PEs but not on CSA-adherent PEs (**Figure 3. 30**). This is consistent with the previous study which showed CSA-binding PEs fail to bind CD36 owing to a dysfunctional CIDRα domain (Gamain *et al.*, 2001a; Gamain *et al.*, 2002).

3.12 Antibody strain specificity and cross strain specificity

As antibodies to PfEMP-1 correlate with development of clinical immunity, it makes PfEMP-1 a potential vaccine candidate (Bull *et al.*, 1998a; Giha *et al.*, 2000). Amongst the various domains in PfEMP-1, CIDR domain is relatively conserved and mediates an important CD36-binding function in most clones of PfEMP-1, making it an attractive target for vaccine development against PfEMP-1. Previous work and the study presented here clearly demonstrates that recombinant PfEMP-1 CIDR can prevent binding of a variety of strains of *P. falciparum* infected erythrocytes to CD36 and even reverse cytoadherance *in vivo* (Cooke *et al.*, 1998). This is in contrast to the properties that antibodies raised against the same recombinant protein inhibit CD36-binding by the parasite is predominantly observed in a strain specific fashion (Baruch *et al.*, 1997). While previous work focused on immunizations using the correctly folded and functional full length CIDR1α domain, we investigated whether smaller unfolded regions of CIDR1α could circumvent this strain specificity of antibody response. Our studies show murine polyclonal antisera raised against short peptides

located at C-terminal region of CIDR-f inhibit CIDRf-CD36 binding and cross-reactive across different *P. falciparum* strains.

Vaccine development focusing on C-terminal region of CIDRα we mapped may thus provide a successful tool in targeting specifically CD36-CIDR interaction as it is much shorter and less conformationally sensitive than previous defined CD36 binding domain. However, due to the highly variant nature of CIDR1α domains across the genome of *P. falciparum*, further studies are still required to address whether antibodies raised against this region is applicable in blockage PE adhesion in other CD36-binding strains.

3.13 Conclusion and perspectives

In conclusion, I have expressed several CIDR1α molecules from strain 3D7 in *E. coli* in the functional forms, as demonstrated by their abilities to bind to a soluble analogue of the human CD36 receptor and by the ability of the antibodies raised against the C-terminal region of this recombinant protein to specifically recognize PE expressed surface protein: PfEMP-1. The secondary structure of CIDR1α is predominantly α-helical, according to an analysis using circular dichroism. I have mapped the CD36 binding domain of the CIDR1α module to its C-terminal region using site-directed mutagenesis, truncation and domain swapping experiments. This C-terminal region is presumably involved in the direct/indirect interactions with CD36, providing the evidence that polyclonal antisera raised against this region could inhibit CIDR1α-CD36

interactions. The N-terminus of CIDR1α might work as a scaffold to maintain the integrity of the whole structure. All these findings may help us to develop CIDR-based vaccines against the variant antigen on *P. falciparum* infected erythrocytes.

Although I have tried to crystallize CIDR-f proteins with extensive efforts, no crystals were grown so far. Further studies will focus on understanding the structural basis for the interaction between CD36 and CIDR1α by deciphering the structure of CD36-binding CIDR1α domains and non CD36-binding domains or the complex of CIDR1α with CD36.

Since the CD36 molecule appears to be a critical receptor for anchoring of parasitized erythrocytes to the microvascular endothelium, disruption of these protein-protein interactions with small molecule compounds or by specific antibodies that would bind to either of the partners hold great promise for the development of new therapeutics or vaccines against malaria. Taken together, this study will enhance our understanding of the interaction between CIDRα domain and CD36 molecule and will hopefully contribute to the development of specific anti-malaria compounds.

REFERENCES

1. **Adams, J. H., P. L. Blair, O. Kaneko, and D. S. Peterson.** 2001. An expanding ebl family of Plasmodium falciparum. Trends Parasitol **17:**297-9.
2. **Adams, J. H., D. E. Hudson, M. Torii, G. E. Ward, T. E. Wellems, M. Aikawa, and L. H. Miller.** 1990. The Duffy receptor family of Plasmodium knowlesi is located within the micronemes of invasive malaria merozoites. Cell **63:**141-53.
3. **Adams, J. H., B. K. Sim, S. A. Dolan, X. Fang, D. C. Kaslow, and L. H. Miller.** 1992. A family of erythrocyte binding proteins of malaria parasites. Proc Natl Acad Sci U S A **89:**7085-9.
4. **Aikawa, M.** 1971. Parasitological review. Plasmodium: the fine structure of malarial parasites. Exp Parasitol **30:**284-320.
5. **Aikawa, M., M. Iseki, J. W. Barnwell, D. Taylor, M. M. Oo, and R. J. Howard.** 1990. The pathology of human cerebral malaria. Am J Trop Med Hyg **43:**30-7.
6. **Aikawa, M., L. H. Miller, J. Johnson, and J. Rabbege.** 1978. Erythrocyte entry by malarial parasites. A moving junction between erythrocyte and parasite. J Cell Biol **77:**72-82.
7. **Aikawa, M., M. Torii, A. Sjolander, K. Berzins, P. Perlmann, and L. H. Miller.** 1990. Pf155/RESA antigen is localized in dense granules of Plasmodium falciparum merozoites. Exp Parasitol **71:**326-9.
8. **Alonso, P. L., J. Sacarlal, J. J. Aponte, A. Leach, E. Macete, J. Milman, I. Mandomando, B. Spiessens, C. Guinovart, M. Espasa, Q. Bassat, P. Aide, O. Ofori-Anyinam, M. M. Navia, S. Corachan, M. Ceuppens, M. C. Dubois, M. A. Demoitie, F. Dubovsky, C. Menendez, N. Tornieporth, W. R. Ballou, R. Thompson, and J. Cohen.** 2004. Efficacy of the RTS,S/AS02A vaccine against Plasmodium falciparum infection and disease in young African children: randomised

controlled trial. Lancet **364:**1411-20.

9. **Ampudia, E., M. A. Patarroyo, M. E. Patarroyo, and L. A. Murillo.** 1996. Genetic polymorphism of the Duffy receptor binding domain of Plasmodium vivax in Colombian wild isolates. Mol Biochem Parasitol **78:**269-72.
10. **Angus, B. J., K. Chotivanich, R. Udomsangpetch, and N. J. White.** 1997. *In vivo* removal of malaria parasites from red blood cells without their destruction in acute falciparum malaria. Blood **90:**2037-40.
11. **Asch, A. S., I. Liu, F. M. Briccetti, J. W. Barnwell, F. Kwakye-Berko, A. Dokun, J. Goldberger, and M. Pernambuco.** 1993. Analysis of CD36 binding domains: ligand specificity controlled by dephosphorylation of an ectodomain. Science **262:**1436-40.
12. **Bai, T., M. Becker, A. Gupta, P. Strike, V. J. Murphy, R. F. Anders, and A. H. Batchelor.** 2005. Structure of AMA1 from Plasmodium falciparum reveals a clustering of polymorphisms that surround a conserved hydrophobic pocket. Proc Natl Acad Sci U S A **102:**12736-41.
13. **Baldi, D. L., K. T. Andrews, R. F. Waller, D. S. Roos, R. F. Howard, B. S. Crabb, and A. F. Cowman.** 2000. RAP1 controls rhoptry targeting of RAP2 in the malaria parasite Plasmodium falciparum. Embo J **19:**2435-43.
14. **Bannister, L. H., G. A. Butcher, E. D. Dennis, and G. H. Mitchell.** 1975. Structure and invasive behaviour of Plasmodium knowlesi merozoites *in vitro*. Parasitology **71:**483-91.
15. **Bannister, L. H., and A. R. Dluzewski.** 1990. The ultrastructure of red cell invasion in malaria infections: a review. Blood Cells **16:**257-92; discussion 293-7.
16. **Bannister, L. H., J. M. Hopkins, R. E. Fowler, S. Krishna, and G. H. Mitchell.** 2000. Ultrastructure of rhoptry development in Plasmodium falciparum erythrocytic schizonts. Parasitology **121 (Pt 3):**273-87.

17. **Bannister, L. H., and G. H. Mitchell.** 1989. The fine structure of secretion by Plasmodium knowlesi merozoites during red cell invasion. J Protozool **36:**362-7.

18. **Barnwell, J. W., A. S. Asch, R. L. Nachman, M. Yamaya, M. Aikawa, and P. Ingravallo.** 1989. A human 88-kD membrane glycoprotein (CD36) functions *in vitro* as a receptor for a cytoadherence ligand on Plasmodium falciparum-infected erythrocytes. J Clin Invest **84:**765-72.

19. **Barragan, A., V. Fernandez, Q. Chen, A. von Euler, M. Wahlgren, and D. Spillmann.** 2000. The duffy-binding-like domain 1 of Plasmodium falciparum erythrocyte membrane protein 1 (PfEMP1) is a heparan sulfate ligand that requires 12 mers for binding. Blood **95:**3594-9.

20. **Baruch, D. I., B. Gamain, and L. H. Miller.** 2003. DNA immunization with the cysteine-rich interdomain region 1 of the Plasmodium falciparum variant antigen elicits limited cross-reactive antibody responses. Infect Immun **71:**4536-43.

21. **Baruch, D. I., X. C. Ma, B. Pasloske, R. J. Howard, and L. H. Miller.** 1999. CD36 peptides that block cytoadherence define the CD36 binding region for Plasmodium falciparum-infected erythrocytes. Blood **94:**2121-7.

22. **Baruch, D. I., X. C. Ma, H. B. Singh, X. Bi, B. L. Pasloske, and R. J. Howard.** 1997. Identification of a region of PfEMP1 that mediates adherence of Plasmodium falciparum infected erythrocytes to CD36: conserved function with variant sequence. Blood **90:**3766-75.

23. **Baruch, D. I., B. L. Pasloske, H. B. Singh, X. Bi, X. C. Ma, M. Feldman, T. F. Taraschi, and R. J. Howard.** 1995. Cloning the P. falciparum gene encoding PfEMP1, a malarial variant antigen and adherence receptor on the surface of parasitized human erythrocytes. Cell **82:**77-87.

24. **Baum, J., A. W. Thomas, and D. J. Conway.** 2003. Evidence for diversifying selection on erythrocyte-binding antigens of Plasmodium falciparum and P. vivax. Genetics **163:**1327-36.

25. **Beeson, J. G., S. J. Rogerson, B. M. Cooke, J. C. Reeder, W. Chai, A. M. Lawson, M. E. Molyneux, and G. V. Brown.** 2000. Adhesion of Plasmodium falciparum-infected erythrocytes to hyaluronic acid in placental malaria. Nat Med **6:**86-90.

26. **Berendt, A. R., D. L. Simmons, J. Tansey, C. I. Newbold, and K. Marsh.** 1989. Intercellular adhesion molecule-1 is an endothelial cell adhesion receptor for Plasmodium falciparum. Nature **341:**57-9.

27. **Bian, Z., and G. Wang.** 2000. Antigenic variation and cytoadherence of PfEMP1 of Plasmodium falciparum-infected erythrocyte from malaria patients. Chin Med J (Engl) **113:**981-4.

28. **Bir, N., S. S. Yazdani, M. Avril, C. Layez, J. Gysin, and C. E. Chitnis.** 2006. Immunogenicity of Duffy binding-like domains that bind chondroitin sulfate A and protection against pregnancy-associated malaria. Infect Immun **74:**5955-63.

29. **Black, C. G., L. Wang, T. Wu, and R. L. Coppel.** 2003. Apical location of a novel EGF-like domain-containing protein of Plasmodium falciparum. Mol Biochem Parasitol **127:**59-68.

30. **Black, C. G., T. Wu, L. Wang, A. R. Hibbs, and R. L. Coppel.** 2001. Merozoite surface protein 8 of Plasmodium falciparum contains two epidermal growth factor-like domains. Mol Biochem Parasitol **114:**217-26.

31. **Blackman, M. J., H. Fujioka, W. H. Stafford, M. Sajid, B. Clough, S. L. Fleck, M. Aikawa, M. Grainger, and F. Hackett.** 1998. A subtilisin-like protein in secretory organelles of Plasmodium falciparum merozoites. J Biol Chem **273:**23398-409.

32. **Blackman, M. J., H. Whittle, and A. A. Holder.** 1991. Processing of the Plasmodium falciparum major merozoite surface protein-1: identification of a 33-kilodalton secondary processing product which is shed prior to erythrocyte invasion. Mol Biochem Parasitol **49:**35-44.

33. **Blair, P. L., S. H. Kappe, J. E. Maciel, B. Balu, and J. H. Adams.** 2002. Plasmodium falciparum MAEBL is a unique member of the ebl family. Mol Biochem Parasitol **122:**35-44.

34. **Bouharoun-Tayoun, H., P. Attanath, A. Sabchareon, T. Chongsuphajaisiddhi, and P. Druilhe.** 1990. Antibodies that protect humans against Plasmodium falciparum blood stages do not on their own inhibit parasite growth and invasion *in vitro*, but act in cooperation with monocytes. J Exp Med **172:**1633-41.

35. **Brabin, B. J.** 1983. An analysis of malaria in pregnancy in Africa. Bull World Health Organ **61:**1005-16.

36. **Brown, H., G. Turner, S. Rogerson, M. Tembo, J. Mwenechanya, M. Molyneux, and T. Taylor.** 1999. Cytokine expression in the brain in human cerebral malaria. J Infect Dis **180:**1742-6.

37. **Buffet, P. A., B. Gamain, C. Scheidig, D. Baruch, J. D. Smith, R. Hernandez-Rivas, B. Pouvelle, S. Oishi, N. Fujii, T. Fusai, D. Parzy, L. H. Miller, J. Gysin, and A. Scherf.** 1999. Plasmodium falciparum domain mediating adhesion to chondroitin sulfate A: a receptor for human placental infection. Proc Natl Acad Sci U S A **96:**12743-8.

38. **Bull, P. C., M. Kortok, O. Kai, F. Ndungu, A. Ross, B. S. Lowe, C. I. Newbold, and K. Marsh.** 2000. Plasmodium falciparum-infected erythrocytes: agglutination by diverse Kenyan plasma is associated with severe disease and young host age. J Infect Dis **182:**252-9.

39. **Bull, P. C., B. S. Lowe, M. Kortok, and K. Marsh.** 1999a. Antibody recognition of Plasmodium falciparum erythrocyte surface antigens in Kenya: evidence for rare and prevalent variants. Infect Immun **67:**733-9.

40. **Bull, P. C., B. S. Lowe, M. Kortok, C. S. Molyneux, C. I. Newbold, and K. Marsh.** 1998b. Parasite antigens on the infected red cell surface are targets for naturally acquired immunity to malaria. Nat Med **4:**358-60.

41. **Bull, P. C., and K. Marsh.** 2002. The role of antibodies to Plasmodium falciparum-infected-erythrocyte surface antigens in naturally acquired immunity to malaria. Trends Microbiol **10:**55-8.

42. **Burgmann, H.** 1996. Serum levels of erythropoietin production in acute plasmodium falciparum malria. Am. J. Trop. Med. Hyg. **54:**280-283.

43. **Camus, D., and T. J. Hadley.** 1985. A Plasmodium falciparum antigen that binds to host erythrocytes and merozoites. Science **230:**553-6.

44. **Carlton, J. M., S. V. Angiuoli, B. B. Suh, T. W. Kooij, M. Pertea, J. C. Silva, M. D. Ermolaeva, J. E. Allen, J. D. Selengut, H. L. Koo, J. D. Peterson, M. Pop, D. S. Kosack, M. F. Shumway, S. L. Bidwell, S. J. Shallom, S. E. van Aken, S. B. Riedmuller, T. V. Feldblyum, J. K. Cho, J. Quackenbush, M. Sedegah, A. Shoaibi, L. M. Cummings, L. Florens, J. R. Yates, J. D. Raine, R. E. Sinden, M. A. Harris, D. A. Cunningham, P. R. Preiser, L. W. Bergman, A. B. Vaidya, L. H. van Lin, C. J. Janse, A. P. Waters, H. O. Smith, O. R. White, S. L. Salzberg, J. C. Venter, C. M. Fraser, S. L. Hoffman, M. J. Gardner, and D. J. Carucci.** 2002. Genome sequence and comparative analysis of the model rodent malaria parasite Plasmodium yoelii yoelii. Nature **419:**512-9.

45. **Carruthers, V. B., O. K. Giddings, and L. D. Sibley.** 1999. Secretion of micronemal proteins is associated with toxoplasma invasion of host cells. Cell Microbiol **1:**225-35.

46. **Carruthers, V. B., and L. D. Sibley.** 1997. Sequential protein secretion from three distinct organelles of Toxoplasma gondii accompanies invasion of human fibroblasts. Eur J Cell Biol **73:**114-23.

47. **Chattopadhyay, R., T. Taneja, K. Chakrabarti, C. R. Pillai, and C. E. Chitnis.** 2004. Molecular analysis of the cytoadherence phenotype of a Plasmodium falciparum field

isolate that binds intercellular adhesion molecule-1. Mol Biochem Parasitol **133:**255-65.

48. **Chen, Q., A. Barragan, V. Fernandez, A. Sundstrom, M. Schlichtherle, A. Sahlen, J. Carlson, S. Datta, and M. Wahlgren.** 1998. Identification of Plasmodium falciparum erythrocyte membrane protein 1 (PfEMP-1) as the rosetting ligand of the malaria parasite P. falciparum. J Exp Med **187:**15-23.
49. **Chen, Q., A. Heddini, A. Barragan, V. Fernandez, S. F. Pearce, and M. Wahlgren.** 2000. The semiconserved head structure of Plasmodium falciparum erythrocyte membrane protein 1 mediates binding to multiple independent host receptors. J Exp Med **192:**1-10.
50. **Cheng, Q., N. Cloonan, K. Fischer, J. Thompson, G. Waine, M. Lanzer, and A. Saul.** 1998. stevor and rif are Plasmodium falciparum multicopy gene families which potentially encode variant antigens. Mol Biochem Parasitol **97:**161-76.
51. **Chitnis, C. E., A. Chaudhuri, R. Horuk, A. O. Pogo, and L. H. Miller.** 1996. The domain on the Duffy blood group antigen for binding Plasmodium vivax and P. knowlesi malarial parasites to erythrocytes. J Exp Med **184:**1531-6.
52. **Chitnis, C. E., and L. H. Miller.** 1994. Identification of the erythrocyte binding domains of Plasmodium vivax and Plasmodium knowlesi proteins involved in erythrocyte invasion. J Exp Med **180:**497-506.
53. **Choe, H., M. J. Moore, C. M. Owens, P. L. Wright, N. Vasilieva, W. Li, A. P. Singh, R. Shakri, C. E. Chitnis, and M. Farzan.** 2005. Sulphated tyrosines mediate association of chemokines and Plasmodium vivax Duffy binding protein with the Duffy antigen/receptor for chemokines (DARC). Mol Microbiol **55:**1413-22.
54. **Chothia, C., J. Novotny, R. Bruccoleri, and M. Karplus.** 1985. Domain association in immunoglobulin molecules. The packing of variable domains. J Mol Biol **186:**651-63.

55. **Clark, I. A., M. M. Awburn, R. O. Whitten, C. G. Harper, N. G. Liomba, M. E. Molyneux, and T. E. Taylor.** 2003. Tissue distribution of migration inhibitory factor and inducible nitric oxide synthase in falciparum malaria and sepsis in African children. Malar J **2:**6.

56. **Clark, I. A., and G. Chaudhri.** 1988. Tumor necrosis factor in malaria-induced abortion. Am J Trop Med Hyg **39:**246-9.

57. **Cole-Tobian, J., and C. L. King.** 2003. Diversity and natural selection in Plasmodium vivax Duffy binding protein gene. Mol Biochem Parasitol **127:**121-32.

58. **Cooke, B. M., A. R. Berendt, A. G. Craig, J. MacGregor, C. I. Newbold, and G. B. Nash.** 1994. Rolling and stationary cytoadhesion of red blood cells parasitized by Plasmodium falciparum: separate roles for ICAM-1, CD36 and thrombospondin. Br J Haematol **87:**162-70.

59. **Cooke, B. M., C. L. Nicoll, D. I. Baruch, and R. L. Coppel.** 1998. A recombinant peptide based on PfEMP-1 blocks and reverses adhesion of malaria-infected red blood cells to CD36 under flow. Mol Microbiol **30:**83-90.

60. **Cortes, A., M. Mellombo, C. S. Mgone, H. P. Beck, J. C. Reeder, and B. M. Cooke.** 2005. Adhesion of Plasmodium falciparum-infected red blood cells to CD36 under flow is enhanced by the cerebral malaria-protective trait South-East Asian ovalocytosis. Mol Biochem Parasitol **142:**252-7.

61. **Costa, F. T., T. Fusai, D. Parzy, Y. Sterkers, M. Torrentino, J. B. Douki, B. Traore, S. Petres, A. Scherf, and J. Gysin.** 2003. Immunization with recombinant duffy binding-like-gamma3 induces pan-reactive and adhesion-blocking antibodies against placental chondroitin sulfate A-binding Plasmodium falciparum parasites. J Infect Dis **188:**153-64.

62. **Cowman, A. F., and B. S. Crabb.** 2006. Invasion of red blood cells by malaria parasites. Cell **124:**755-66.

63. **Cranston, H. A., C. W. Boylan, G. L. Carroll, S. P. Sutera, J. R. Williamson, I. Y. Gluzman, and D. J. Krogstad.** 1984.

Plasmodium falciparum maturation abolishes physiologic red cell deformability. Science **223:**400-3.

64. **Crawley, J., S. Smith, F. Kirkham, P. Muthinji, C. Waruiru, and K. Marsh.** 1996. Seizures and status epilepticus in childhood cerebral malaria. Qjm **89:**591-7.

65. **Crewther, P. E., J. G. Culvenor, A. Silva, J. A. Cooper, and R. F. Anders.** 1990. Plasmodium falciparum: two antigens of similar size are located in different compartments of the rhoptry. Exp Parasitol **70:**193-206.

66. **Culvenor, J. G., K. P. Day, and R. F. Anders.** 1991. Plasmodium falciparum ring-infected erythrocyte surface antigen is released from merozoite dense granules after erythrocyte invasion. Infect Immun **59:**1183-7.

67. **Daly, T. M., and C. A. Long.** 1993. A recombinant 15-kilodalton carboxyl-terminal fragment of Plasmodium yoelii yoelii 17XL merozoite surface protein 1 induces a protective immune response in mice. Infect Immun **61:**2462-7.

68. **David A Warrel, H. M. G.** 2001. Essential Malariology, Fourth ed. Arnold.

69. **David, P. H., T. J. Hadley, M. Aikawa, and L. H. Miller.** 1984. Processing of a major parasite surface glycoprotein during the ultimate stages of differentiation in Plasmodium knowlesi. Mol Biochem Parasitol **11:**267-82.

70. **Daviet, L., R. Buckland, M. D. Puente Navazo, and J. L. McGregor.** 1995. Identification of an immunodominant functional domain on human CD36 antigen using human-mouse chimaeric proteins and homologue-replacement mutagenesis. Biochem J **305 (Pt 1):**221-4.

71. **Davis, T. M., S. Krishna, S. Looareesuwan, W. Supanaranond, S. Pukrittayakamee, K. Attatamsoonthorn, and N. J. White.** 1990. Erythrocyte sequestration and anemia in severe falciparum malaria. Analysis of acute changes in venous hematocrit using a simple mathematical model. J Clin Invest **86:**793-800.

72. **Day, N. P., T. T. Hien, T. Schollaardt, P. P. Loc, L. V. Chuong, T. T. Chau, N. T. Mai, N. H. Phu, D. X. Sinh, N. J. White, and M. Ho.** 1999. The prognostic and pathophysiologic role of pro- and antiinflammatory cytokines in severe malaria. J Infect Dis **180:**1288-97.

73. **Dondorp, A. M., B. J. Angus, K. Chotivanich, K. Silamut, R. Ruangveerayuth, M. R. Hardeman, P. A. Kager, J. Vreeken, and N. J. White.** 1999. Red blood cell deformability as a predictor of anemia in severe falciparum malaria. Am J Trop Med Hyg **60:**733-7.

74. **Dondorp, A. M., P. A. Kager, J. Vreeken, and N. J. White.** 2000. Abnormal blood flow and red blood cell deformability in severe malaria. Parasitol Today **16:**228-32.

75. **Doolan, D.** 2001. Malaria Methods and Protocols.

76. **Dorman, E. K., C. E. Shulman, J. Kingdom, J. N. Bulmer, J. Mwendwa, N. Peshu, and K. Marsh.** 2002. Impaired uteroplacental blood flow in pregnancies complicated by falciparum malaria. Ultrasound Obstet Gynecol **19:**165-70.

77. **Dorn, A., S. R. Vippagunta, H. Matile, C. Jaquet, J. L. Vennerstrom, and R. G. Ridley.** 1998. An assessment of drug-haematin binding as a mechanism for inhibition of haematin polymerisation by quinoline antimalarials. Biochem Pharmacol **55:**727-36.

78. **Dowse, T. J., J. C. Pascall, K. D. Brown, and D. Soldati.** 2005. Apicomplexan rhomboids have a potential role in microneme protein cleavage during host cell invasion. Int J Parasitol **35:**747-56.

79. **Dubremetz, J. F., A. Achbarou, D. Bermudes, and K. A. Joiner.** 1993. Kinetics and pattern of organelle exocytosis during Toxoplasma gondii/host-cell interaction. Parasitol Res **79:**402-8.

80. **Duffy, P. E., and M. Fried.** 2003. Plasmodium falciparum adhesion in the placenta. Curr Opin Microbiol **6:**371-6.

81. **Duffy, P. E., and D. C. Kaslow.** 1997. A novel malaria

protein, Pfs28, and Pfs25 are genetically linked and synergistic as falciparum malaria transmission-blocking vaccines. Infect Immun **65:**1109-13.

82. **Duraisingh, M. T., A. G. Maier, T. Triglia, and A. F. Cowman.** 2003a. Erythrocyte-binding antigen 175 mediates invasion in Plasmodium falciparum utilizing sialic acid-dependent and -independent pathways. Proc Natl Acad Sci U S A **100:**4796-801.

83. **Duraisingh, M. T., T. Triglia, S. A. Ralph, J. C. Rayner, J. W. Barnwell, G. I. McFadden, and A. F. Cowman.** 2003b. Phenotypic variation of Plasmodium falciparum merozoite proteins directs receptor targeting for invasion of human erythrocytes. Embo J **22:**1047-57.

84. **Eggleson, K. K., K. L. Duffin, and D. E. Goldberg.** 1999. Identification and characterization of falcilysin, a metallopeptidase involved in hemoglobin catabolism within the malaria parasite Plasmodium falciparum. J Biol Chem **274:**32411-7.

85. **el Hassan, A. M., A. M. Saeed, J. Fandrey, and W. Jelkmann.** 1997. Decreased erythropoietin response in Plasmodium falciparum malaria-associated anaemia. Eur J Haematol **59:**299-304.

86. **English, M., C. Waruiru, E. Amukoye, S. Murphy, J. Crawley, I. Mwangi, N. Peshu, and K. Marsh.** 1996a. Deep breathing in children with severe malaria: indicator of metabolic acidosis and poor outcome. Am J Trop Med Hyg **55:**521-4.

87. **English, M., C. Waruiru, and K. Marsh.** 1996b. Transfusion for respiratory distress in life-threatening childhood malaria. Am J Trop Med Hyg **55:**525-30.

88. **English, M. C., C. Waruiru, C. Lightowler, S. A. Murphy, G. Kirigha, and K. Marsh.** 1996c. Hyponatraemia and dehydration in severe malaria. Arch Dis Child **74:**201-5.

89. **Etzion, Z., M. C. Murray, and M. E. Perkins.** 1991.

Isolation and characterization of rhoptries of Plasmodium falciparum. Mol Biochem Parasitol **47:**51-61.

90. **Febbraio, M., N. A. Abumrad, D. P. Hajjar, K. Sharma, W. Cheng, S. F. Pearce, and R. L. Silverstein.** 1999. A null mutation in murine CD36 reveals an important role in fatty acid and lipoprotein metabolism. J Biol Chem **274:**19055-62.
91. **Fitch, C. D., G. Z. Cai, and J. D. Shoemaker.** 2000. A role for linoleic acid in erythrocytes infected with Plasmodium berghei. Biochim Biophys Acta **1535:**45-9.
92. **Flick, K., C. Scholander, Q. Chen, V. Fernandez, B. Pouvelle, J. Gysin, and M. Wahlgren.** 2001. Role of nonimmune IgG bound to PfEMP1 in placental malaria. Science **293:**2098-100.
93. **Foley, M., L. Tilley, W. H. Sawyer, and R. F. Anders.** 1991. The ring-infected erythrocyte surface antigen of Plasmodium falciparum associates with spectrin in the erythrocyte membrane. Mol Biochem Parasitol **46:**137-47.
94. **Freeman, R. R., and A. A. Holder.** 1983. Surface antigens of malaria merozoites. A high molecular weight precursor is processed to an 83,000 mol wt form expressed on the surface of Plasmodium falciparum merozoites. J Exp Med **158:**1647-53.
95. **Fried, M., and P. E. Duffy.** 1996. Adherence of Plasmodium falciparum to chondroitin sulfate A in the human placenta. Science **272:**1502-4.
96. **Fried, M., F. Nosten, A. Brockman, B. J. Brabin, and P. E. Duffy.** 1998. Maternal antibodies block malaria. Nature **395:**851-2.
97. **Gamain, B., S. Gratepanche, L. H. Miller, and D. I. Baruch.** 2002. Molecular basis for the dichotomy in Plasmodium falciparum adhesion to CD36 and chondroitin sulfate A. Proc Natl Acad Sci U S A **99:**10020-4.
98. **Gamain, B., L. H. Miller, and D. I. Baruch.** 2001b. The surface variant antigens of Plasmodium falciparum contain

cross-reactive epitopes. Proc Natl Acad Sci U S A **98:**2664-9.

99. **Gamain, B., J. D. Smith, M. Avril, D. I. Baruch, A. Scherf, J. Gysin, and L. H. Miller.** 2004. Identification of a 67-amino-acid region of the Plasmodium falciparum variant surface antigen that binds chondroitin sulphate A and elicits antibodies reactive with the surface of placental isolates. Mol Microbiol **53:**445-55.

100. **Gamain, B., J. D. Smith, L. H. Miller, and D. I. Baruch.** 2001a. Modifications in the CD36 binding domain of the Plasmodium falciparum variant antigen are responsible for the inability of chondroitin sulfate A adherent parasites to bind CD36. Blood **97:**3268-74.

101. **Gantt, S., C. Persson, K. Rose, A. J. Birkett, R. Abagyan, and V. Nussenzweig.** 2000. Antibodies against thrombospondin-related anonymous protein do not inhibit Plasmodium sporozoite infectivity *in vivo*. Infect Immun **68:**3667-73.

102. **Gardner, M. J., N. Hall, E. Fung, O. White, M. Berriman, R. W. Hyman, J. M. Carlton, A. Pain, K. E. Nelson, S. Bowman, I. T. Paulsen, K. James, J. A. Eisen, K. Rutherford, S. L. Salzberg, A. Craig, S. Kyes, M. S. Chan, V. Nene, S. J. Shallom, B. Suh, J. Peterson, S. Angiuoli, M. Pertea, J. Allen, J. Selengut, D. Haft, M. W. Mather, A. B. Vaidya, D. M. Martin, A. H. Fairlamb, M. J. Fraunholz, D. S. Roos, S. A. Ralph, G. I. McFadden, L. M. Cummings, G. M. Subramanian, C. Mungall, J. C. Venter, D. J. Carucci, S. L. Hoffman, C. Newbold, R. W. Davis, C. M. Fraser, and B. Barrell.** 2002. Genome sequence of the human malaria parasite Plasmodium falciparum. Nature **419:**498-511.

103. **Giha, H. A., T. Staalsoe, D. Dodoo, C. Roper, G. M. Satti, D. E. Arnot, L. Hviid, and T. G. Theander.** 2000. Antibodies to variable Plasmodium falciparum-infected erythrocyte surface antigens are associated with protection from novel malaria infections. Immunol Lett **71:**117-26.

104. **Gilberger, T. W., J. K. Thompson, M. B. Reed, R. T. Good, and A. F. Cowman.** 2003a. The cytoplasmic domain of the Plasmodium falciparum ligand EBA-175 is essential for invasion but not protein trafficking. J Cell Biol **162:**317-27.

105. **Gilberger, T. W., J. K. Thompson, T. Triglia, R. T. Good, M. T. Duraisingh, and A. F. Cowman.** 2003b. A novel erythrocyte binding antigen-175 paralogue from Plasmodium falciparum defines a new trypsin-resistant receptor on human erythrocytes. J Biol Chem **278:**14480-6.

106. **Ginsburg, H.** 1994. Transport pathways in the malaria-infected erythrocyte. Their characterization and their use as potential targets for chemotherapy. Biochem Pharmacol **48:**1847-56.

107. **Ginsburg, H., O. Famin, J. Zhang, and M. Krugliak.** 1998. Inhibition of glutathione-dependent degradation of heme by chloroquine and amodiaquine as a possible basis for their antimalarial mode of action. Biochem Pharmacol **56:**1305-13.

108. **Glushakova, S., D. Yin, T. Li, and J. Zimmerberg.** 2005. Membrane transformation during malaria parasite release from human red blood cells. Curr Biol **15:**1645-50.

109. **Gozar, M. M., O. Muratova, D. B. Keister, C. R. Kensil, V. L. Price, and D. C. Kaslow.** 2001. Plasmodium falciparum: immunogenicity of alum-adsorbed clinical-grade TBV25-28, a yeast-secreted malaria transmission-blocking vaccine candidate. Exp Parasitol **97:**61-9.

110. **Gratepanche, S., B. Gamain, J. D. Smith, B. A. Robinson, A. Saul, and L. H. Miller.** 2003. Induction of crossreactive antibodies against the Plasmodium falciparum variant protein. Proc Natl Acad Sci U S A **100:**13007-12.

111. **Grau, G. E., C. D. Mackenzie, R. A. Carr, M. Redard, G. Pizzolato, C. Allasia, C. Cataldo, T. E. Taylor, and M. E. Molyneux.** 2003. Platelet accumulation in brain microvessels in fatal pediatric cerebral malaria. J Infect Dis **187:**461-6.

112. **Grau, G. E., T. E. Taylor, M. E. Molyneux, J. J. Wirima, P.**

Vassalli, M. Hommel, and P. H. Lambert. 1989. Tumor necrosis factor and disease severity in children with falciparum malaria. N Engl J Med **320:**1586-91.

113. **Hans, D., P. Pattnaik, A. Bhattacharyya, A. R. Shakri, S. S. Yazdani, M. Sharma, H. Choe, M. Farzan, and C. E. Chitnis.** 2005. Mapping binding residues in the Plasmodium vivax domain that binds Duffy antigen during red cell invasion. Mol Microbiol **55:**1423-34.

114. **Harkins, E. W.** Current Protocols in Molecular Biology.Unit 11.4 Immuniation of Mice.

115. **Harris, P. K., S. Yeoh, A. R. Dluzewski, R. A. O'Donnell, C. Withers-Martinez, F. Hackett, L. H. Bannister, G. H. Mitchell, and M. J. Blackman.** 2005. Molecular identification of a malaria merozoite surface sheddase. PLoS Pathog **1:**241-51.

116. **Hasler, T., S. M. Handunnetti, J. C. Aguiar, M. R. van Schravendijk, B. M. Greenwood, G. Lallinger, P. Cegielski, and R. J. Howard.** 1990. *In vitro* rosetting, cytoadherence, and microagglutination properties of Plasmodium falciparum-infected erythrocytes from Gambian and Tanzanian patients. Blood **76:**1845-52.

117. **Healer, J., S. Crawford, S. Ralph, G. McFadden, and A. F. Cowman.** 2002. Independent translocation of two micronemal proteins in developing Plasmodium falciparum merozoites. Infect Immun **70:**5751-8.

118. **Ho, M., and N. J. White.** 1999. Molecular mechanisms of cytoadherence in malaria. Am J Physiol **276:**C1231-42.

119. **Ho, M., N. J. White, S. Looareesuwan, Y. Wattanagoon, S. H. Lee, M. J. Walport, D. Bunnag, and T. Harinasuta.** 1990. Splenic Fc receptor function in host defense and anemia in acute Plasmodium falciparum malaria. J Infect Dis **161:**555-61.

120. **Hodder, A. N., P. E. Crewther, M. L. Matthew, G. E. Reid, R. L. Moritz, R. J. Simpson, and R. F. Anders.** 1996. The disulfide bond structure of Plasmodium apical membrane

antigen-1. J Biol Chem **271:**29446-52.

121. **Hodder, A. N., D. R. Drew, V. C. Epa, M. Delorenzi, R. Bourgon, S. K. Miller, R. L. Moritz, D. F. Frecklington, R. J. Simpson, T. P. Speed, R. N. Pike, and B. S. Crabb.** 2003. Enzymic, phylogenetic, and structural characterization of the unusual papain-like protease domain of Plasmodium falciparum SERA5. J Biol Chem **278:**48169-77.

122. **Holder, A. A., M. J. Blackman, M. Borre, P. A. Burghaus, J. A. Chappel, J. K. Keen, I. T. Ling, S. A. Ogun, C. A. Owen, and K. A. Sinha.** 1994. Malaria parasites and erythrocyte invasion. Biochem Soc Trans **22:**291-5.

123. **Holder, A. A., and R. R. Freeman.** 1982. Biosynthesis and processing of a Plasmodium falciparum schizont antigen recognized by immune serum and a monoclonal antibody. J Exp Med **156:**1528-38.

124. **Holder, A. A., and R. R. Freeman.** 1984. The three major antigens on the surface of Plasmodium falciparum merozoites are derived from a single high molecular weight precursor. J Exp Med **160:**624-9.

125. **Holder, A. A., J. S. Sandhu, Y. Hillman, L. S. Davey, S. C. Nicholls, H. Cooper, and M. J. Lockyer.** 1987. Processing of the precursor to the major merozoite surface antigens of Plasmodium falciparum. Parasitology **94 (Pt 2):**199-208.

126. **Ibrahimi, A., Z. Sfeir, H. Magharaie, E. Z. Amri, P. Grimaldi, and N. A. Abumrad.** 1996. Expression of the CD36 homolog (FAT) in fibroblast cells: effects on fatty acid transport. Proc Natl Acad Sci U S A **93:**2646-51.

127. **Jootar, S., W. Chaisiripoomkere, P. Pholvicha, A. Leelasiri, W. Prayoonwiwat, W. Mongkonsvitragoon, and T. Srichaikul.** 1993. Suppression of erythroid progenitor cells during malarial infection in Thai adults caused by serum inhibitor. Clin Lab Haematol **15:**87-92.

128. **Kaelin, W. G., Jr., D. C. Pallas, J. A. DeCaprio, F. J. Kaye, and D. M. Livingston.** 1991. Identification of cellular

proteins that can interact specifically with the T/E1A-binding region of the retinoblastoma gene product. Cell **64:**521-32.

129. **Kai, O.** 1999. Innune haemolysis associated with severe malaria anaemia. Trans. R. Soc. Med. Hyg. **93:**119.

130. **Kaneko, O., J. Mu, T. Tsuboi, X. Su, and M. Torii.** 2002. Gene structure and expression of a Plasmodium falciparum 220-kDa protein homologous to the Plasmodium vivax reticulocyte binding proteins. Mol Biochem Parasitol **121:**275-8.

131. **Kaviratne, M., S. M. Khan, W. Jarra, and P. R. Preiser.** 2002. Small variant STEVOR antigen is uniquely located within Maurer's clefts in Plasmodium falciparum-infected red blood cells. Eukaryot Cell **1:**926-35.

132. **Keeley, A., and D. Soldati.** 2004. The glideosome: a molecular machine powering motility and host-cell invasion by Apicomplexa. Trends Cell Biol **14:**528-32.

133. **Kho, W. G., J. Y. Chung, E. J. Sim, D. W. Kim, and W. C. Chung.** 2001. Analysis of polymorphic regions of Plasmodium vivax Duffy binding protein of Korean isolates. Korean J Parasitol **39:**143-50.

134. **Kumar, S., A. Yadava, D. B. Keister, J. H. Tian, M. Ohl, K. A. Perdue-Greenfield, L. H. Miller, and D. C. Kaslow.** 1995. Immunogenicity and *in vivo* efficacy of recombinant Plasmodium falciparum merozoite surface protein-1 in Aotus monkeys. Mol Med **1:**325-32.

135. **Kurtzhals, J. A., V. Adabayeri, B. Q. Goka, B. D. Akanmori, J. O. Oliver-Commey, F. K. Nkrumah, C. Behr, and L. Hviid.** 1998. Low plasma concentrations of interleukin 10 in severe malarial anaemia compared with cerebral and uncomplicated malaria. Lancet **351:**1768-72.

136. **Kwiatkowski, D., A. V. Hill, I. Sambou, P. Twumasi, J. Castracane, K. R. Manogue, A. Cerami, D. R. Brewster, and B. M. Greenwood.** 1990. TNF concentration in fatal cerebral, non-fatal cerebral, and uncomplicated Plasmodium

falciparum malaria. Lancet **336:**1201-4.

137. **Kyes, S., P. Horrocks, and C. Newbold.** 2001. Antigenic variation at the infected red cell surface in malaria. Annu Rev Microbiol **55:**673-707.
138. **Kyes, S. A., J. A. Rowe, N. Kriek, and C. I. Newbold.** 1999. Rifins: a second family of clonally variant proteins expressed on the surface of red cells infected with Plasmodium falciparum. Proc Natl Acad Sci U S A **96:**9333-8.
139. **Lackner, P., R. Beer, R. Helbok, G. Broessner, K. Engelhardt, C. Brenneis, E. Schmutzhard, and K. Pfaller.** 2006. Scanning electron microscopy of the neuropathology of murine cerebral malaria. Malar J **5:**116.
140. **Langreth, S. G., J. B. Jensen, R. T. Reese, and W. Trager.** 1978. Fine structure of human malaria *in vitro*. J Protozool **25:**443-52.
141. **Leech, J. H., J. W. Barnwell, L. H. Miller, and R. J. Howard.** 1984. Identification of a strain-specific malarial antigen exposed on the surface of Plasmodium falciparum-infected erythrocytes. J Exp Med **159:**1567-75.
142. **Lekana Douki, J. B., B. Traore, F. T. Costa, T. Fusai, B. Pouvelle, Y. Sterkers, A. Scherf, and J. Gysin.** 2002. Sequestration of Plasmodium falciparum-infected erythrocytes to chondroitin sulfate A, a receptor for maternal malaria: monoclonal antibodies against the native parasite ligand reveal pan-reactive epitopes in placental isolates. Blood **100:**1478-83.
143. **Ling, I. T., S. A. Ogun, and A. A. Holder.** 1994. Immunization against malaria with a recombinant protein. Parasite Immunol **16:**63-7.
144. **Looareesuwan, S., M. Ho, Y. Wattanagoon, N. J. White, D. A. Warrell, D. Bunnag, T. Harinasuta, and D. J. Wyler.** 1987. Dynamic alteration in splenic function during acute falciparum malaria. N Engl J Med **317:**675-9.
145. **MacKenzie, K. R., J. H. Prestegard, and D. M. Engelman.** 1997. A transmembrane helix dimer: structure and

implications. Science **276:**131-3.

146. **MacPherson, G. G., M. J. Warrell, N. J. White, S. Looareesuwan, and D. A. Warrell.** 1985. Human cerebral malaria. A quantitative ultrastructural analysis of parasitized erythrocyte sequestration. Am J Pathol **119:**385-401.

147. **Makobongo, M. O., B. Keegan, C. A. Long, and L. H. Miller.** 2006. Immunization of Aotus monkeys with recombinant cysteine-rich interdomain region 1 alpha protects against severe disease during Plasmodium falciparum reinfection. J Infect Dis **193:**731-40.

148. **Maneerat, Y., P. Viriyavejakul, B. Punpoowong, M. Jones, P. Wilairatana, E. Pongponratn, G. D. Turner, and R. Udomsangpetch.** 2000. Inducible nitric oxide synthase expression is increased in the brain in fatal cerebral malaria. Histopathology **37:**269-77.

149. **Marshall, V. M., A. Silva, M. Foley, S. Cranmer, L. Wang, D. J. McColl, D. J. Kemp, and R. L. Coppel.** 1997. A second merozoite surface protein (MSP-4) of Plasmodium falciparum that contains an epidermal growth factor-like domain. Infect Immun **65:**4460-7.

150. **Marshall, V. M., W. Tieqiao, and R. L. Coppel.** 1998. Close linkage of three merozoite surface protein genes on chromosome 2 of Plasmodium falciparum. Mol Biochem Parasitol **94:**13-25.

151. **Marshall, V. M., L. Zhang, R. F. Anders, and R. L. Coppel.** 1996. Diversity of the vaccine candidate AMA-1 of Plasmodium falciparum. Mol Biochem Parasitol **77:**109-13.

152. **Mayer, D. C., O. Kaneko, D. E. Hudson-Taylor, M. E. Reid, and L. H. Miller.** 2001. Characterization of a Plasmodium falciparum erythrocyte-binding protein paralogous to EBA-175. Proc Natl Acad Sci U S A **98:**5222-7.

153. **Mayer, D. C., J. B. Mu, O. Kaneko, J. Duan, X. Z. Su, and L. H. Miller.** 2004. Polymorphism in the Plasmodium falciparum erythrocyte-binding ligand JESEBL/EBA-181

alters its receptor specificity. Proc Natl Acad Sci U S A **101:**2518-23.

154. **Mayor, A., N. Bir, R. Sawhney, S. Singh, P. Pattnaik, S. K. Singh, A. Sharma, and C. E. Chitnis.** 2005. Receptor-binding residues lie in central regions of Duffy-binding-like domains involved in red cell invasion and cytoadherence by malaria parasites. Blood **105:**2557-63.

155. **McColl, D. J., and R. F. Anders.** 1997. Conservation of structural motifs and antigenic diversity in the Plasmodium falciparum merozoite surface protein-3 (MSP-3). Mol Biochem Parasitol **90:**21-31.

156. **McGregor, I. A., M. E. Wilson, and W. Z. Billewicz.** 1983. Malaria infection of the placenta in The Gambia, West Africa; its incidence and relationship to stillbirth, birthweight and placental weight. Trans R Soc Trop Med Hyg **77:**232-44.

157. **McGuire, W., J. C. Knight, A. V. Hill, C. E. Allsopp, B. M. Greenwood, and D. Kwiatkowski.** 1999. Severe malarial anemia and cerebral malaria are associated with different tumor necrosis factor promoter alleles. J Infect Dis **179:**287-90.

158. **McHenry, A. M., and J. H. Adams.** 2006. The crystal structure of P. knowlesi DBPalpha DBL domain and its implications for immune evasion. Trends Biochem Sci **31:**487-91.

159. **Menendez, C., A. F. Fleming, and P. L. Alonso.** 2000a. Malaria-related anaemia. Parasitol Today **16:**469-76.

160. **Menendez, C., J. Ordi, M. R. Ismail, P. J. Ventura, J. J. Aponte, E. Kahigwa, F. Font, and P. L. Alonso.** 2000b. The impact of placental malaria on gestational age and birth weight. J Infect Dis **181:**1740-5.

161. **Miller, L. H., M. Aikawa, J. G. Johnson, and T. Shiroishi.** 1979. Interaction between cytochalasin B-treated malarial parasites and erythrocytes. Attachment and junction formation. J Exp Med **149:**172-84.

162. **Miller, L. H., D. I. Baruch, K. Marsh, and O. K. Doumbo.** 2002a. The pathogenic basis of malaria. Nature **415:**673-9.

163. **Miller, L. H., S. Usami, and S. Chien.** 1971. Alteration in the rheologic properties of Plasmodium knowlesi--infected red cells. A possible mechanism for capillary obstruction. J Clin Invest **50:**1451-5.

164. **Miller, S. K., R. T. Good, D. R. Drew, M. Delorenzi, P. R. Sanders, A. N. Hodder, T. P. Speed, A. F. Cowman, T. F. de Koning-Ward, and B. S. Crabb.** 2002b. A subset of Plasmodium falciparum SERA genes are expressed and appear to play an important role in the erythrocytic cycle. J Biol Chem **277:**47524-32.

165. **Mitchell, G. H., A. W. Thomas, G. Margos, A. R. Dluzewski, and L. H. Bannister.** 2004. Apical membrane antigen 1, a major malaria vaccine candidate, mediates the close attachment of invasive merozoites to host red blood cells. Infect Immun **72:**154-8.

166. **Morrissette, N. S., and L. D. Sibley.** 2002. Cytoskeleton of apicomplexan parasites. Microbiol Mol Biol Rev **66:**21-38; table of contents.

167. **Mota, M. M., J. C. Hafalla, and A. Rodriguez.** 2002. Migration through host cells activates Plasmodium sporozoites for infection. Nat Med **8:**1318-22.

168. **Mota, M. M., G. Pradel, J. P. Vanderberg, J. C. Hafalla, U. Frevert, R. S. Nussenzweig, V. Nussenzweig, and A. Rodriguez.** 2001. Migration of Plasmodium sporozoites through cells before infection. Science **291:**141-4.

169. **Mota, M. M., and A. Rodriguez.** 2004. Migration through host cells: the first steps of Plasmodium sporozoites in the mammalian host. Cell Microbiol **6:**1113-8.

170. **Newton, C. R., T. E. Taylor, and R. O. Whitten.** 1998. Pathophysiology of fatal falciparum malaria in African children. Am J Trop Med Hyg **58:**673-83.

171. **Nichols, B. A., and M. L. Chiappino.** 1987. Cytoskeleton of

Toxoplasma gondii. J Protozool **34:**217-26.

172. **Novotny, J., R. Bruccoleri, J. Newell, D. Murphy, E. Haber, and M. Karplus.** 1983. Molecular anatomy of the antibody binding site. J Biol Chem **258:**14433-7.

173. **Ockenhouse, C. F., M. Ho, N. N. Tandon, G. A. Van Seventer, S. Shaw, N. J. White, G. A. Jamieson, J. D. Chulay, and H. K. Webster.** 1991. Molecular basis of sequestration in severe and uncomplicated Plasmodium falciparum malaria: differential adhesion of infected erythrocytes to CD36 and ICAM-1. J Infect Dis **164:**163-9.

174. **Ockenhouse, C. F., T. Tegoshi, Y. Maeno, C. Benjamin, M. Ho, K. E. Kan, Y. Thway, K. Win, M. Aikawa, and R. R. Lobb.** 1992. Human vascular endothelial cell adhesion receptors for Plasmodium falciparum-infected erythrocytes: roles for endothelial leukocyte adhesion molecule 1 and vascular cell adhesion molecule 1. J Exp Med **176:**1183-9.

175. **Ofori, M. F., D. Dodoo, T. Staalsoe, J. A. Kurtzhals, K. Koram, T. G. Theander, B. D. Akanmori, and L. Hviid.** 2002. Malaria-induced acquisition of antibodies to Plasmodium falciparum variant surface antigens. Infect Immun **70:**2982-8.

176. **Oo, M. M., M. Aikawa, T. Than, T. M. Aye, P. T. Myint, I. Igarashi, and W. C. Schoene.** 1987. Human cerebral malaria: a pathological study. J Neuropathol Exp Neurol **46:**223-31.

177. **O'Reilly, D. R., L. K. Miller, and V. A. Luckow.** 1992. Baculovirus Expression Vectors.

178. **Othoro, C., A. A. Lal, B. Nahlen, D. Koech, A. S. Orago, and V. Udhayakumar.** 1999. A low interleukin-10 tumor necrosis factor-alpha ratio is associated with malaria anemia in children residing in a holoendemic malaria region in western Kenya. J Infect Dis **179:**279-82.

179. **Page, R., W. Peti, I. A. Wilson, R. C. Stevens, and K. Wuthrich.** 2005. NMR screening and crystal quality of bacterially expressed prokaryotic and eukaryotic proteins in a

structural genomics pipeline. Proc Natl Acad Sci U S A **102:**1901-5.

180. **Peterson, D. S., L. H. Miller, and T. E. Wellems.** 1995. Isolation of multiple sequences from the Plasmodium falciparum genome that encode conserved domains homologous to those in erythrocyte-binding proteins. Proc Natl Acad Sci U S A **92:**7100-4.

181. **Peterson, D. S., and T. E. Wellems.** 2000. EBL-1, a putative erythrocyte binding protein of Plasmodium falciparum, maps within a favored linkage group in two genetic crosses. Mol Biochem Parasitol **105:**105-13.

182. **Phillips, R. E., S. Looareesuwan, D. A. Warrell, S. H. Lee, J. Karbwang, M. J. Warrell, N. J. White, C. Swasdichai, and D. J. Weatherall.** 1986. The importance of anaemia in cerebral and uncomplicated falciparum malaria: role of complications, dyserythropoiesis and iron sequestration. Q J Med **58:**305-23.

183. **Phillips, R. E., and G. Pasvol.** 1992. Anaemia of Plasmodium falciparum malaria. Baillieres Clin Haematol **5:**315-30.

184. **Pizarro, J. C., B. Vulliez-Le Normand, M. L. Chesne-Seck, C. R. Collins, C. Withers-Martinez, F. Hackett, M. J. Blackman, B. W. Faber, E. J. Remarque, C. H. Kocken, A. W. Thomas, and G. A. Bentley.** 2005. Crystal structure of the malaria vaccine candidate apical membrane antigen 1. Science **308:**408-11.

185. **Pober, J. S., L. A. Lapierre, A. H. Stolpen, T. A. Brock, T. A. Springer, W. Fiers, M. P. Bevilacqua, D. L. Mendrick, and M. A. Gimbrone, Jr.** 1987. Activation of cultured human endothelial cells by recombinant lymphotoxin: comparison with tumor necrosis factor and interleukin 1 species. J Immunol **138:**3319-24.

186. **Pongponratn, E., M. Riganti, T. Harinasuta, and D. Bunnag.** 1985. Electron microscopy of the human brain in cerebral malaria. Southeast Asian J Trop Med Public Health **16:**219-27.

187. **Preiser, P., M. Kaviratne, S. Khan, L. Bannister, and W. Jarra.** 2000. The apical organelles of malaria merozoites: host cell selection, invasion, host immunity and immune evasion. Microbes Infect **2:**1461-77.

188. **Preiser, P. R., W. Jarra, T. Capiod, and G. Snounou.** 1999. A rhoptry-protein-associated mechanism of clonal phenotypic variation in rodent malaria. Nature **398:**618-22.

189. **Rayner, J. C., M. R. Galinski, P. Ingravallo, and J. W. Barnwell.** 2000. Two Plasmodium falciparum genes express merozoite proteins that are related to Plasmodium vivax and Plasmodium yoelii adhesive proteins involved in host cell selection and invasion. Proc Natl Acad Sci U S A **97:**9648-53.

190. **Rayner, J. C., E. Vargas-Serrato, C. S. Huber, M. R. Galinski, and J. W. Barnwell.** 2001. A Plasmodium falciparum homologue of Plasmodium vivax reticulocyte binding protein (PvRBP1) defines a trypsin-resistant erythrocyte invasion pathway. J Exp Med **194:**1571-81.

191. **Reed, M. B., S. R. Caruana, A. H. Batchelor, J. K. Thompson, B. S. Crabb, and A. F. Cowman.** 2000. Targeted disruption of an erythrocyte binding antigen in Plasmodium falciparum is associated with a switch toward a sialic acid-independent pathway of invasion. Proc Natl Acad Sci U S A **97:**7509-14.

192. **Reeder, J. C., A. F. Cowman, K. M. Davern, J. G. Beeson, J. K. Thompson, S. J. Rogerson, and G. V. Brown.** 1999. The adhesion of Plasmodium falciparum-infected erythrocytes to chondroitin sulfate A is mediated by P. falciparum erythrocyte membrane protein 1. Proc Natl Acad Sci U S A **96:**5198-202.

193. **Reeder, J. C., A. N. Hodder, J. G. Beeson, and G. V. Brown.** 2000. Identification of glycosaminoglycan binding domains in Plasmodium falciparum erythrocyte membrane protein 1 of a chondroitin sulfate A-adherent parasite. Infect Immun **68:**3923-6.

194. **Ricke, C. H., T. Staalsoe, K. Koram, B. D. Akanmori, E. M.**

Riley, T. G. Theander, and L. Hviid. 2000. Plasma antibodies from malaria-exposed pregnant women recognize variant surface antigens on Plasmodium falciparum-infected erythrocytes in a parity-dependent manner and block parasite adhesion to chondroitin sulfate A. J Immunol **165:**3309-16.

195. **Ridley, R. G., B. Takacs, H. W. Lahm, C. J. Delves, M. Goman, U. Certa, H. Matile, G. R. Woollett, and J. G. Scaife.** 1990. Characterisation and sequence of a protective rhoptry antigen from Plasmodium falciparum. Mol Biochem Parasitol **41:**125-34.

196. **Roberts, D. D., J. A. Sherwood, S. L. Spitalnik, L. J. Panton, R. J. Howard, V. M. Dixit, W. A. Frazier, L. H. Miller, and V. Ginsburg.** 1985. Thrombospondin binds falciparum malaria parasitized erythrocytes and may mediate cytoadherence. Nature **318:**64-6.

197. **Robinson, B. A., T. L. Welch, and J. D. Smith.** 2003. Widespread functional specialization of Plasmodium falciparum erythrocyte membrane protein 1 family members to bind CD36 analysed across a parasite genome. Mol Microbiol **47:**1265-78.

198. **Roger, N., J. F. Dubremetz, P. Delplace, B. Fortier, G. Tronchin, and A. Vernes.** 1988. Characterization of a 225 kilodalton rhoptry protein of Plasmodium falciparum. Mol Biochem Parasitol **27:**135-41.

199. **Rogerson, S. J., and G. V. Brown.** 1997. Chondroitin sulphate A as an adherence receptor for Plasmodium falciparum-infected erythrocytes. Parasitol Today **13:**70-5.

200. **Rothlein, R., M. L. Dustin, S. D. Marlin, and T. A. Springer.** 1986. A human intercellular adhesion molecule (ICAM-1) distinct from LFA-1. J Immunol **137:**1270-4.

201. **Rowe, J. A., J. M. Moulds, C. I. Newbold, and L. H. Miller.** 1997. P. falciparum rosetting mediated by a parasite-variant erythrocyte membrane protein and complement-receptor 1. Nature **388:**292-5.

202. **Rowe, J. A., S. J. Rogerson, A. Raza, J. M. Moulds, M. D. Kazatchkine, K. Marsh, C. I. Newbold, J. P. Atkinson, and L. H. Miller.** 2000. Mapping of the region of complement receptor (CR) 1 required for Plasmodium falciparum rosetting and demonstration of the importance of CR1 in rosetting in field isolates. J Immunol **165:**6341-6.

203. **Russell, D. G., and R. G. Burns.** 1984. The polar ring of coccidian sporozoites: a unique microtubule-organizing centre. J Cell Sci **65:**193-207.

204. **Ryter, S. W., and R. M. Tyrrell.** 2000. The heme synthesis and degradation pathways: role in oxidant sensitivity. Heme oxygenase has both pro- and antioxidant properties. Free Radic Biol Med **28:**289-309.

205. **Sabchareon, A., T. Burnouf, D. Ouattara, P. Attanath, H. Bouharoun-Tayoun, P. Chantavanich, C. Foucault, T. Chongsuphajaisiddhi, and P. Druilhe.** 1991. Parasitologic and clinical human response to immunoglobulin administration in falciparum malaria. Am J Trop Med Hyg **45:**297-308.

206. **Salmon, B. L., A. Oksman, and D. E. Goldberg.** 2001. Malaria parasite exit from the host erythrocyte: a two-step process requiring extraerythrocytic proteolysis. Proc Natl Acad Sci U S A **98:**271-6.

207. **Sam-Yellowe, T. Y.** 1996. Rhoptry organelles of the apicomplexa: Their role in host cell invasion and intracellular survival. Parasitol Today **12:**308-16.

208. **Sam-Yellowe, T. Y., H. Fujioka, M. Aikawa, and D. G. Messineo.** 1995. Plasmodium falciparum rhoptry proteins of 140/130/110 kd (Rhop-H) are located in an electron lucent compartment in the neck of the rhoptries. J Eukaryot Microbiol **42:**224-31.

209. **Sam-Yellowe, T. Y., and M. E. Perkins.** 1991. Interaction of the 140/130/110 kDa rhoptry protein complex of Plasmodium falciparum with the erythrocyte membrane and liposomes. Exp Parasitol **73:**161-71.

210. **Scherf, A., B. Pouvelle, P. A. Buffet, and J. Gysin.** 2001. Molecular mechanisms of Plasmodium falciparum placental adhesion. Cell Microbiol **3:**125-31.

211. **Serghides, L., T. G. Smith, S. N. Patel, and K. C. Kain.** 2003. CD36 and malaria: friends or foes? Trends Parasitol **19:**461-9.

212. **Sherman, I.** 1998. Malaria: Parasite Biology, Pathogenesis and Protection. ASM Press, Washington DC.

213. **Sherman, I. W., S. Eda, and E. Winograd.** 2003. Cytoadherence and sequestration in Plasmodium falciparum: defining the ties that bind. Microbes Infect **5:**897-909.

214. **Shin, S. C., J. P. Vanderberg, and J. A. Terzakis.** 1982. Direct infection of hepatocytes by sporozoites of Plasmodium berghei. J Protozool **29:**448-54.

215. **Siddiqui, W. A., L. Q. Tam, K. J. Kramer, G. S. Hui, S. E. Case, K. M. Yamaga, S. P. Chang, E. B. Chan, and S. C. Kan.** 1987. Merozoite surface coat precursor protein completely protects Aotus monkeys against Plasmodium falciparum malaria. Proc Natl Acad Sci U S A **84:**3014-8.

216. **Sim, B. K., C. E. Chitnis, K. Wasniowska, T. J. Hadley, and L. H. Miller.** 1994. Receptor and ligand domains for invasion of erythrocytes by Plasmodium falciparum. Science **264:**1941-4.

217. **Sim, B. K., P. A. Orlandi, J. D. Haynes, F. W. Klotz, J. M. Carter, D. Camus, M. E. Zegans, and J. D. Chulay.** 1990. Primary structure of the 175K Plasmodium falciparum erythrocyte binding antigen and identification of a peptide which elicits antibodies that inhibit malaria merozoite invasion. J Cell Biol **111:**1877-84.

218. **Singh, S. K., R. Hora, H. Belrhali, C. E. Chitnis, and A. Sharma.** 2006. Structural basis for Duffy recognition by the malaria parasite Duffy-binding-like domain. Nature **439:**741-4.

219. **Smith, C. W., R. Rothlein, B. J. Hughes, M. M. Mariscalco, H. E. Rudloff, F. C. Schmalstieg, and D. C. Anderson.** 1988.

Recognition of an endothelial determinant for CD 18-dependent human neutrophil adherence and transendothelial migration. J Clin Invest **82:**1746-56.

220. **Smith, J. D., C. E. Chitnis, A. G. Craig, D. J. Roberts, D. E. Hudson-Taylor, D. S. Peterson, R. Pinches, C. I. Newbold, and L. H. Miller.** 1995. Switches in expression of Plasmodium falciparum var genes correlate with changes in antigenic and cytoadherent phenotypes of infected erythrocytes. Cell **82:**101-10.

221. **Smith, J. D., A. G. Craig, N. Kriek, D. Hudson-Taylor, S. Kyes, T. Fagen, R. Pinches, D. I. Baruch, C. I. Newbold, and L. H. Miller.** 2000a. Identification of a Plasmodium falciparum intercellular adhesion molecule-1 binding domain: a parasite adhesion trait implicated in cerebral malaria. Proc Natl Acad Sci U S A **97:**1766-71.

222. **Smith, J. D., B. Gamain, D. I. Baruch, and S. Kyes.** 2001. Decoding the language of var genes and Plasmodium falciparum sequestration. Trends Parasitol **17:**538-45.

223. **Smith, J. D., S. Kyes, A. G. Craig, T. Fagan, D. Hudson-Taylor, L. H. Miller, D. I. Baruch, and C. I. Newbold.** 1998. Analysis of adhesive domains from the A4VAR Plasmodium falciparum erythrocyte membrane protein-1 identifies a CD36 binding domain. Mol Biochem Parasitol **97:**133-48.

224. **Smith, J. D., G. Subramanian, B. Gamain, D. I. Baruch, and L. H. Miller.** 2000b. Classification of adhesive domains in the Plasmodium falciparum erythrocyte membrane protein 1 family. Mol Biochem Parasitol **110:**293-310.

225. **Snow, R. W., C. A. Guerra, A. M. Noor, H. Y. Myint, and S. I. Hay.** 2005. The global distribution of clinical episodes of Plasmodium falciparum malaria. Nature **434:**214-7.

226. **Stahl, H. D., A. E. Bianco, P. E. Crewther, R. F. Anders, A. P. Kyne, R. L. Coppel, G. F. Mitchell, D. J. Kemp, and G. V. Brown.** 1986. Sorting large numbers of clones expressing Plasmodium falciparum antigens in Escherichia coli by

differential antibody screening. Mol Biol Med **3:**351-68.

227. **Stern, M., J. Savill, and C. Haslett.** 1996. Human monocyte-derived macrophage phagocytosis of senescent eosinophils undergoing apoptosis. Mediation by alpha v beta 3/CD36/thrombospondin recognition mechanism and lack of phlogistic response. Am J Pathol **149:**911-21.

228. **Stubbs, J., K. M. Simpson, T. Triglia, D. Plouffe, C. J. Tonkin, M. T. Duraisingh, A. G. Maier, E. A. Winzeler, and A. F. Cowman.** 2005. Molecular mechanism for switching of P. falciparum invasion pathways into human erythrocytes. Science **309:**1384-7.

229. **Su, X. Z., V. M. Heatwole, S. P. Wertheimer, F. Guinet, J. A. Herrfeldt, D. S. Peterson, J. A. Ravetch, and T. E. Wellems.** 1995. The large diverse gene family var encodes proteins involved in cytoadherence and antigenic variation of Plasmodium falciparum-infected erythrocytes. Cell **82:**89-100.

230. **Suguitan, A. L., Jr., R. G. Leke, G. Fouda, A. Zhou, L. Thuita, S. Metenou, J. Fogako, R. Megnekou, and D. W. Taylor.** 2003. Changes in the levels of chemokines and cytokines in the placentas of women with Plasmodium falciparum malaria. J Infect Dis **188:**1074-82.

231. **Sullivan, D. J., Jr., I. Y. Gluzman, and D. E. Goldberg.** 1996. Plasmodium hemozoin formation mediated by histidine-rich proteins. Science **271:**219-22.

232. **Taylor, H. M., T. Triglia, J. Thompson, M. Sajid, R. Fowler, M. E. Wickham, A. F. Cowman, and A. A. Holder.** 2001. Plasmodium falciparum homologue of the genes for Plasmodium vivax and Plasmodium yoelii adhesive proteins, which is transcribed but not translated. Infect Immun **69:**3635-45.

233. **Taylor, T. E., W. J. Fu, R. A. Carr, R. O. Whitten, J. S. Mueller, N. G. Fosiko, S. Lewallen, N. G. Liomba, and M. E. Molyneux.** 2004. Differentiating the pathologies of cerebral malaria by postmortem parasite counts. Nat Med **10:**143-5.

234. **Tolia, N. H., E. J. Enemark, B. K. Sim, and L. Joshua-Tor.** 2005. Structural basis for the EBA-175 erythrocyte invasion pathway of the malaria parasite Plasmodium falciparum. Cell **122:**183-93.

235. **Tordai, H., L. Banyai, and L. Patthy.** 1999. The PAN module: the N-terminal domains of plasminogen and hepatocyte growth factor are homologous with the apple domains of the prekallikrein family and with a novel domain found in numerous nematode proteins. FEBS Lett **461:**63-7.

236. **Torii, M., J. H. Adams, L. H. Miller, and M. Aikawa.** 1989. Release of merozoite dense granules during erythrocyte invasion by Plasmodium knowlesi. Infect Immun **57:**3230-3.

237. **Toye, B., G. M. Zhong, R. Peeling, and R. C. Brunham.** 1990. Immunologic characterization of a cloned fragment containing the species-specific epitope from the major outer membrane protein of Chlamydia trachomatis. Infect Immun **58:**3909-13.

238. **Trager, W., C. Rozario, H. Shio, J. Williams, and M. E. Perkins.** 1992. Transfer of a dense granule protein of Plasmodium falciparum to the membrane of ring stages and isolation of dense granules. Infect Immun **60:**4656-61.

239. **Treeck, M., N. S. Struck, S. Haase, C. Langer, S. Herrmann, J. Healer, A. F. Cowman, and T. W. Gilberger.** 2006. A conserved region in the EBL proteins is implicated in microneme targeting of the malaria parasite Plasmodium falciparum. J Biol Chem **281:**31995-2003.

240. **Triglia, T., J. Thompson, S. R. Caruana, M. Delorenzi, T. Speed, and A. F. Cowman.** 2001. Identification of proteins from Plasmodium falciparum that are homologous to reticulocyte binding proteins in Plasmodium vivax. Infect Immun **69:**1084-92.

241. **Trucco, C., D. Fernandez-Reyes, S. Howell, W. H. Stafford, T. J. Scott-Finnigan, M. Grainger, S. A. Ogun, W. R. Taylor, and A. A. Holder.** 2001. The merozoite surface

protein 6 gene codes for a 36 kDa protein associated with the Plasmodium falciparum merozoite surface protein-1 complex. Mol Biochem Parasitol **112:**91-101.

242. **Udomsangpetch, R., P. H. Reinhardt, T. Schollaardt, J. F. Elliott, P. Kubes, and M. Ho.** 1997. Promiscuity of clinical Plasmodium falciparum isolates for multiple adhesion molecules under flow conditions. J Immunol **158:**4358-64.
243. **Van den Ende, J., G. Coppens, T. Verstraeten, T. Van Haegenborgh, K. Depraetere, A. Van Gompel, E. Van den Enden, J. Clerinx, R. Colebunders, W. E. Peetermans, and W. Schroyens.** 1998. Recurrence of blackwater fever: triggering of relapses by different antimalarials. Trop Med Int Health **3:**632-9.
244. **VanBuskirk, K. M., E. Sevova, and J. H. Adams.** 2004. Conserved residues in the Plasmodium vivax Duffy-binding protein ligand domain are critical for erythrocyte receptor recognition. Proc Natl Acad Sci U S A **101:**15754-9.
245. **Vogt, A. M., A. Barragan, Q. Chen, F. Kironde, D. Spillmann, and M. Wahlgren.** 2003. Heparan sulfate on endothelial cells mediates the binding of Plasmodium falciparum-infected erythrocytes via the DBL1alpha domain of PfEMP1. Blood **101:**2405-11.
246. **Walter, P. R., Y. Garin, and P. Blot.** 1982. Placental pathologic changes in malaria. A histologic and ultrastructural study. Am J Pathol **109:**330-42.
247. **Weber, J. L.** 1988a. Interspersed repetitive DNA from Plasmodium falciparum. Mol Biochem Parasitol **29:**117-24.
248. **Weber, J. L., J. A. Lyon, R. H. Wolff, T. Hall, G. H. Lowell, and J. D. Chulay.** 1988b. Primary structure of a Plasmodium falciparum malaria antigen located at the merozoite surface and within the parasitophorous vacuole. J Biol Chem **263:**11421-5.
249. **Wickham, M. E., J. G. Culvenor, and A. F. Cowman.** 2003. Selective inhibition of a two-step egress of malaria parasites

from the host erythrocyte. J Biol Chem **278:**37658-63.

250. **Xainli, J., J. H. Adams, and C. L. King.** 2000. The erythrocyte binding motif of plasmodium vivax duffy binding protein is highly polymorphic and functionally conserved in isolates from Papua New Guinea. Mol Biochem Parasitol **111:**253-60.

251. **Yipp, B. G., S. Anand, T. Schollaardt, K. D. Patel, S. Looareesuwan, and M. Ho.** 2000. Synergism of multiple adhesion molecules in mediating cytoadherence of Plasmodium falciparum-infected erythrocytes to microvascular endothelial cells under flow. Blood **96:**2292-8.

252. **Zav'yalov, V. P., T. V. Chernovskaya, D. A. Chapman, A. V. Karlyshev, S. MacIntyre, A. V. Zavialov, A. M. Vasiliev, A. I. Denesyuk, G. A. Zav'yalova, I. V. Dudich, T. Korpela, and V. M. Abramov.** 1997. Influence of the conserved disulphide bond, exposed to the putative binding pocket, on the structure and function of the immunoglobulin-like molecular chaperone Caf1M of Yersinia pestis. Biochem J **324 (Pt 2):**571-8.